# REMOTE SENSING AND REGIONALIZATION FOR INTEGRATED WATER RESOURCES MODELING IN UPPER AND MIDDLE AWASH RIVER BASIN, ETHIOPIA

HABTE GEBEYEHU LIKASA
February, 2013

SUPERVISORS:
DR. ING. T.H.M. (TOM) RIENTJES
DR. IR. C. (CHRISTIAAN) VAN DER TOL

REMOTE SENSING AND REGIONALIZATION FOR INTEGRATED WATER RESOURCES MODELING IN UPPER AND MIDDLE AWASH RIVER BASIN, ETHIOPIA

HABTE GEBEYEHU LIKASA
Enschede, the Netherlands, [February, 2013]

Thesis submitted to the Faculty of Geo-Information Science and Earth Observation of the University of Twente in partial fulfillment of the requirements for the degree of Master of Science in Geo-information Science and Earth Observation.
Specialization: [Water Resources and Environmental Management)]

SUPERVISORS:
DR. ING. T.H.M. (TOM) RIENTJES
DR. IR. C. (CHRISTIAAN) VAN DER TOL

THESIS ASSESSMENT BOARD:
Dr. ir. C.M.M. (Chris) Mannaerts (Chair)
Dr. Paolo Reggiani (External Examiner, Deltares Delft, The Netherlands)
Etc

ABSTRACT

Water resources have an enormous impact on the economic development and environmental protection. Water resources available in different forms and can be obtained from different sources. However mostly, water resources assessment and management relies on available stream flow measurements. But, in developing country like Ethiopia most of river basins are ungauged. Therefore, applying remote sensing and regionalization for integrated water resources modeling in poorly gauged river basin is crucial. The available in-situ and online data of different satellite derived products, such as Climate Prediction Centre (CPC) and morphing technique (CMORPH), Tropical rainfall measurement mission (TRMM) Multi-satellite precipitation Analysis (TMPA-3B42) and Famine Early Warning System Network Global Potential Evapotranspiration (FEWS NET PET) and gauged rainfall data were used to force the semi-distributed conceptual hydrological model (HBV -96); and the results were compared with observed discharge of gauged catchments at their respective outlets. To minimize the errors of input variables, bias correction was applied for satellite products before using them as input for HBV-96 model to simulate the stream flows. To optimize model parameter for gauged catchments model calibration was performed manually by trial and error until the observed stream flow and simulated stream flow matches for 2005 - 2008, and the model was validated for 2009-2010. To have better understanding of model parameter performance the sensitivity analysis of eight model parameters was performed and the evaluation shows limit for evapotranspiration (LP), Percolation (Perc), Recession coefficient of upper reservoir zone (Khq) and Field capacity (FC) are sensitive. The stream flow simulated with the two satellite rainfall products before and after bias correction was compared to select better performing satellite products. According to the comparison CMORPH is performing better than TMPA 3B42, as it is shown on Hombole catchment outlet with NSE =0.752 and RVE=-6.92 during model calibration period and NSE= 0.72 and RVE=-8.594 during model validation period. Furthermore, the regionalization was applied using regional model and sub basin mean methods, the result showed that the regional model outperforms as moderate performing model with NSE = 0.64 and RVE= 1.96%. According to the result from model calibration of four catchments the objective function NSE >0.8 for three catchments and NSE=0.69 for Akaki catchment was obtained.

Keyword: HBV-96, Stream flow simulation, Regionalization, Satellite products, hydrological modeling, Water Resources

ACKNOWLEDGEMENTS

TABLE OF CONTENTS

LIST OF FIGURES

LIST OF TABLES

LIST OF ANNEXES

LIST OF ABBREVIATIONS AND ACRONOMYS

NMA	Meteorological Agency
EMoWE	Ethiopian Ministry of Water and Energy
HBV-96	Hydrologiska Byråns Vattenbalansavdelning (96)
IHMS	Integrated Hydrological Modeling System
NSEs	Nash–Sutcliffe efficiencies
RVE	Relative volume error
RMSE	Root Mean Square Error
R2	Regression coefficient
NOAA	National Oceanic and Atmospheric Administration
WMO	World Meteorological Organization
DEM	Digital elevation model
TRMM	Tropical rainfall measurement mission
TMPA	Multi-satellite Precipitation Analysis
CMORPH	Climate Prediction Centre (CPC) morphing technique
Rn	Net radiation
MP	Model Parameter
PCC	Physical Catchment Characteristics
Qq	Quick runoff
SM	Simulated Soil Moisture content
Q_{obs}	Measured stream flow at gauged station
Q_{sim}	Simulated stream flow at gauged station
HB	Hit Bias
MB	Missed Rainfall Bias
FB	False Rainfall Bias
UZ	Upper zone storage for quick runoff
LZ	Lower Zone Storage reservoir
IN	Infiltration
PET	Potential evapotranspiration
FEWS NET	Famine Early Warning System Network
Qs	Delayed/ base flow
WMO	World Meteorological Organization
MSG	Meteosat Second Generation
GIS	Geo-information science
C_{FLUX}	Correction value for Capillary fringe
ETo	Reference Evapotranspiration
ITCZ	Inter tropical Convergence Zone
FAO	Food and Agricultural Organization
CSM	commission on Sustainable development Meeting
ISOD	In-Situ Online Data
SPSS	Statistical Package for the Social Science

1. INTRODUCTION

1.1. Background

Among other natural resources, water resources occupy the most special place in environmental stability and sustainable economic development. To increase food security and to reduce energy crises, coupling integrated water resources modeling for development industries such as agriculture, hydropower and water supply are most important. On the 13th meeting of the commission on sustainable development (CSM-13) SIWI (2005) put forward five important messages. The first message says "improved water supply and sanitation and water resources management boosts countries economic growth and contributes greatly to poverty reduction". However, because of unwise use of water resources and climate changes, these goals have been challenged in the developing countries. Hence, water resources modeling play a critical role in social and economic developments, mainly in developing countries where there is often little understanding of the environment and water resources.

Ethiopia is one of East African countries, which have a number of perennial and non-perennial rivers and lakes. These Rivers and Lakes are supposed to be used for different developmental activities like water supply, Irrigation and Hydropower generation to satisfy the basic needs of the current more than 80 million Ethiopian people and that expected to increase to more than 91 million Ethiopian people in 2015 (Awulachew et al., 2007). Hence, to ensure food security increasing productivity is the country's main program. As a result, the government gives high attention to water resources development, even though it is not on a place as expected because river discharge data are hardly available since most of catchments are ungauged.

Ethiopia has about 560 river gauging stations, of which 454 are operational for both lake and rives (MoWE, 2012). Awash River is part of these rivers that originates from Ethiopian highlands and extends to the lower region of Ethiopia crossing different climatic zones and geological formations. Hence, it divided into three sub-basins; upper, middle and lower Awash River Basin. However, the basin is one of the largest Ethiopian rift valley basin, it has only few functional gauging stations (MoWE, 2012). Therefore, estimating stream flow of ungauged streams based on gauged streams by regionalization is crucial.

For poorly gauged river basins, often-integrated water resources modeling using regionalization and remote sensing is advocated. As discussed above, Awash River Basin has many ungauged catchments and therefore quantification of stream flow must rely on regionalization. Rientjes et al. (2011) performed regionalization for lake level simulation on Lake Tana, Ethiopia where stream gauges are scarce using a semi-distributed HBV-96 model. For model parameter estimation of ungauged catchments the physical catchment characteristics similarity techniques have been applied. They came up with good performing models for the ungauged streams that assisted to get stream flow hydrograph of ungauged catchments.

HBV-96 is a semi-distributed conceptual hydrological model for continuous runoff simulation, which was originally developed by SMHI in the early 70´s to assist hydropower operations (SMHI, 2008). Its main aim was to create a conceptual hydrological model with reasonable demands on computer facilities and calibration data. In addition, it also proved to be flexible and robust in solving water resource problems and applications. Furthermore, HBV-96 needs only few input variables such as precipitation; potential evapotranspiration and elevation zone data to simulate the river flow.

In scarcely monitored catchments, getting reliable data required for water resources modeling is pretty hard. However, now a day the satellite-retrieved data is easily available. For water resources modeling the required input variables such as precipitation, potential evapotranspiration, digital elevation and fraction of land cover are the main and mostly freely downloadable data sets. For precipitation retrieval satellite products such as Meteosat Second Generation (MSG), Tropical rainfall measurement mission (TRMM) Multi-satellite Precipitation Analysis (TMPA 3B42) and Climate Prediction Centre (CPC) morphing technique (CMORPH) can be used. In the same way potential evapotranspiration, estimated using Penman-Monteith formula by FEWS NET is easily retrieved using ISOD Toolbox in ILWIS. These data sets are tested and validated by different researchers. For example Wang et al. (2010) validated the Tropical Rainfall Measurement Mission (TRMM) using ground rain gauge data in Melbourne, Florida and showed correlation 0.93 for daily interval and 0.6 for 5 minute interval. Therefore, it is possible to substitute the rain gauge on daily base if the gauges are scarce.

1.2. Statement of Research Problem

As discussed in section 1.1, most of Ethiopian river basins are poorly gauged. Hence, the inflow and outflow of most catchments are not precisely quantified. On other hand, water resources planning and management require information of inflows from each catchment and total outflow from the basin. However, still no system was developed to solve this problem for Awash River Basin. Some researchers used regionalization to overcome such problem. For example (Deckers et al., 2010) perform Catchment Variability and Parameter Estimation in Multi-Objective Regionalisation of a Rainfall–Runoff Model in UK using HBV model and finally comeup with satifactory results. Therefore, it is possible to solve such problem using regionalization, which will be addressed in this research.

Awash River Basin is intensively used for irrigation and other developmental activities. However, there are only few researches available, which well discussed on Awash River Water Resources. These research includes, hydrological modeling as a tool for sustainable water resources management (Edossa et al., 2011; Tessema, 2011), Application of Artificial Neural Network Based Stream flow Forecasting Model for Agricultural Water resources Management (Edossa et al., 2011), Remote sensing based hydrological modeling for flood early warning in the upper and middle Awash river basin (Koriche, 2012). However, none of them performed stream flow simulation for ungauged catchments of Awash River Basin. Therefore, remote sensing and regionalization for integrated water resources modeling based on semi-distributed conceptual hydrological HBV-96 model will solve this problem.

1.3. Thesis Objective

1.3.1. Main Objective
➢ The main objective of this research is to simulate the stream flow of Upper and Middle Awash River Basin by combining remote sensing derived products with regionalization and a semi-distributed conceptual hydrological model (HBV-96).

1.3.2. Specific Objectives
❖ To evaluate satellite remote sensing products applicable for Awash River Basin stream flow simulation.
❖ To simulate the stream flow using HBV-96 on daily time interval
❖ To conduct regionalization for stream flow estimation of ungauged catchments

1.3.3. Research Questions
❖ Which remote sensing products are applicable for Awash River Basin Water Resources modeling?

❖ What calibration approach is suitable to optimize model parameters for water resources modeling of Awash River Basin at daily time steps using HBV-96?

❖ Which regionalization technique is most suitable to simulate stream flow of ungauged catchments in Awash River Basin?

1.4. Outline Of The Thesis

This research has seven chapters. Chapter 1 deals with the Introduction, which contains the background, statement of the problem and thesis objective. Chapter 2 deals Literature Review, which describes water resources modeling, Satellite rainfall products, Evapotranspiration, Previous work on regionalization, HBV-96 model and ISOD tool box. Chapter 3 deals with Study Area and Material used which contains the study area and Data sets used. Chapter 4 deals with the Hydrological Modeling. Chapter 5 deals with Research Methods. Chapter 6 deals with Result and Discussion and Finally Chapter 7 deals with Conclusion and Recommendation

2. LITERATURE REVIEW

2.1. Water Resources Modeling

In poorly gauged river basin, water resource modeling is an essential task, for making developmental plans and managing water resources. There are different modeling approaches for water resources modeling. The major categories are distributed physically based and lumped conceptually hydrological models. Both of them are quite different in need of input data. Hence, in poorly gauged basins issues of model complexity in terms of input data requirement is most important. However, this issue may be minimized if data from real-time meteorological observations provided by satellites and/or automatic meteorological station network are used. For example Shrestha et al. (2004) conducted water resources modeling in poorly gauged catchment by using satellite data from MODIS/TERRA and LandSatTM to assess water resources availability. In the same way, García et al. (2008) used HEC-HMS for surface water resources modeling in scarcely gauged basins in the north of Spain. They were able to optimize model parameters for further study and identify that water availability for some catchments is not sufficient and concluded that the water resources of each catchment have to be interconnected to satisfy the water demand. Similarly, hydrological modeling and forecasting using HBV-96 model in Liao river delta, China was done by Jia et al. (2012) and showed the ability of identifying the low and high flow seasons and years of the study area. Hence, water resources modeling using satellite based remote sensing coupled with HBV-96 model will enable to understand water resources potential of river basins.

2.2. Satellite Rainfall Products

Satellite based rainfall estimation is decisive in stream flow simulation which is a major concern of hydrological modeling. In particular in developing countries where stream gauging stations and meteorological stations are poor, hydrological modeling using satellite products is a novelty. Many researches carry on a satellite derived product as a gift to overcome problem of gauged data scarcity. For example Su et al. (2008) evaluate TRMM Multi-satellite Precipitation Analysis (TMPA 3B42) and its utility in hydrologic prediction in the La Plata Basin, South America and come up with evaluation indicator of R^2 0.56 to 0.81 for daily average precipitation measurement and 0.90 to 0.99 for monthly average precipitation measurement on basin level. With these data finally they were able to simulate stream flow of La Plata Basin. Haile et al. (2012) performed an evaluation of the climate prediction center (CPC) morphing technique (CMORPH) rainfall product on hourly time steps over the source of the Blue Nile River Gilgel Abbay, Ethiopia, and showed applicability of satellite based precipitation estimation in an area with few rain gauges. In addition Rojas-Gonzalez et al. (2009) conducted Performance Evaluation of MPE Rainfall Product at hourly and daily temporal resolution within a hydro-estimator pixel and showed that the bias is high for hourly base evaluation and relatively low for daily base evaluation. Hence, these researches show that it is possible to use satellite products for stream flow estimation after validating with available data sets at rain gauge stations.

2.3. Evapotranspiration

Evapotranspiration is one of the major components of the hydrological cycle. Evapotranspiration is a combination of two words, evaporation and transpiration. Evaporation refers to water converted to vapor from open water, bare soil and pant surface, whereas transpiration refers to the amount of water converted to vapor in the process of metabolic activity by plants. Even though they are two different terms it is difficult to investigate both processes separately. The evapotranspiration can be categorized as reference evapotranspiration, actual evapotranspiration and potential evapotranspiration. These evapotranspiration can be calculated from ground based measurement or satellite based estimated. For

example Li et al. (2009) evaluated the evapotranspiration mapping on regional scale or global scale to compose the temporal spatial coverage of evapotranspiration and they concluded that the satellite based estimated evapotranspiration have to be evaluated with ground based measured evapotranspiration. Generally, Evapotranspiration is classified as reference evapotranspiration, potential evapotranspiration and actual evapotranspiration.

Reference Evapotranspiration: it is the evapotranspiration from hypothetical reference surface of grass that are well irrigated, healthy and completely shading the surface having albedo of 0.23, surface resistance of 70s/m and crop height of 0.12m (FAO-56, 2007). Since it refers to well irrigated grass surface it is assumed that no water stress occurs

Potential Evapotranspiration: Is the evapotranspiration that occurs when there is sufficient amount of water is available. That is the amount of evaporation needed to saturate the surrounding air by supplying adequate amount of vapor for evaporation demand.

Actual Evapotranspiration: Is the actual amount of water that evaporates from the surfaces and transpired by vegetation in constrained available water in soil moisture. As soil moisture decrease the actual evapotranspiration decreases. Since a long term mean of potential evapotranspiration used to calculate the actual evapotranspiration, it depends more on the soil moisture conditions than on the inter-annual potential evaporation variations (SMHI, 2008 manual version 6.2).

2.4.   HBV-96 Model

Integrated water resources models are representations of a given watershed and similar to the natural hydrologic process with certain degree of uncertainty. The HBV-96 model is a semi-distributed conceptual hydrologic model and robust in data requirements. In water resources modeling reducing model complexity is most important especially when data availability is poor. Hence, input data have to be kept as simple as possible. Normally, HBV-96 requires daily mean-values of temperature, mean monthly potential evapotranspiration and precipitation as input (SMHI, 2008 manual version 6.2). Despite its simplicity, its simulation performance is commendable, and the original use for hydrological forecasting has expanded to applications such as filling gaps in measured time series, simulation of stream-flow in ungauged rivers, design floods and water supply quality studies input data. The flexible structure of the HBV-96/IHMS system allows the model to make necessary sub-divisions with respect to different climate zones, land-use, density of the hydro-meteorological network etc. Different researchers used it in different countries. For example Wale et al. (2009) used HBV-96 model to determine the inflow from ungauged catchments by transferring calibrated model parameters of gauged catchments to ungauged catchments in Lake Tana Basin, Ethiopia. In the same way, Booij (2005) developed the relationships between key parameters and river basin characteristics (e.g. land use, soil type) to estimate the parameter values for the ungauged sub-basins using HBV-96 model for 118 sub-basins using four gauged stream data of the basin. Therefore, using HBV-96 in scarcely gauged river basin is recommendable.

2.5.   Previous Work on Regionalization

As it was discussed in sections 1.1 and 1.2, most of Ethiopian rivers are ungauged. Therefore, regionalization is the key tool to solve this problem. For example, Rientjes et al. (2011) and Wale et al. (2009), performed model calibration in Lake Tana Basin to get optimized parameters for gauged catchments and   used the advantage of physical catchment characteristics similarity to transfer the optimized parameter to ungauged catchments.   Also Bao et al. (2012) did comparison of physical catchment characteristics similarity and regression methods to improve capability of   stream flow estimation of ungauged catchments in China and they finally concluded that the physical catchment

characteristics outperform than regression method. Therefore, from these results it can be concluded that the Physical catchment similarity is considered as the most valuable for regionalization in poorly gauged river basins.

2.6. In-situ and Online Data (ISOD)

In-situ and online data is globally available in time series data of various sources from a network of satellites via internet online. It is basically based on high quality data distribution system which provides a wide range of satellite products and services available to user community. Climate Prediction Center (CPC) and Morphing (CMORPH), Tropical Rainfall Measurement Mission (TRMM) Multi-satellite Precipitation Analysis (TMPA 3B42), FEWS NET Global potential Evapotranspiration (FEWS NET PET) and Digital Elevation Model (DEM) are some of the products users can easily get if there is an intranet connection. Since in-situ and online data provide adequate information of land surface variables, it is critical to support developing countries, which had low economy to measure hydrological data with expensive automatic ways. The freeware ISOD Toolbox was developed as a plug-in ILWIS, to utilize data distributed online freely (after Maathuis et al., 2012). To facilitate easily importing of various satellite data products that are freely online available through archives the ISOD Toolbox were developed as plug-in of ILWIS and is offering a set of benefits with free of charge. For more information related to installation and configuration of the ISOD Toolbox consult user guide manual of ISOD Toolbox (Maathuis et al., 2012). In general the structure of ISOD Toolbox is shown as Figure 2.1
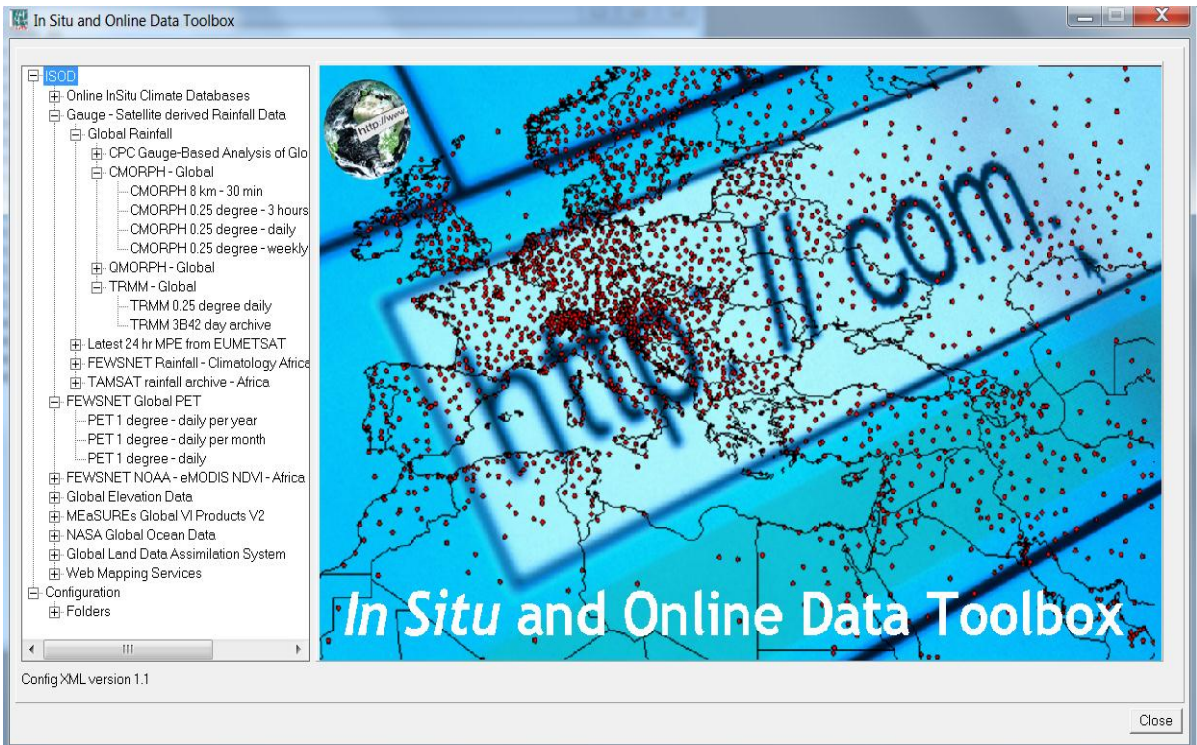
Figure 2.1 ISOD Toolbox Structure version 1.1 menu Plug-in ILWIS Software (after Maathuis et al., 2012).

3. STUDY AREA AND MATERIALS

3.1. Study Area

Awash River Basin is the most intensively utilized and the longest river basin of the Great Rift Valley in Ethiopia and located from 7^0 N to 10^0N and 38^0E to 41^0E. The River Basin covers a total area of 110, 000 km² with a total length of 1,200km along its course. Awash originate from central Ethiopian highlands, about 150 km west of Addis Ababa, at an elevation of about 3,000 m above mean sea level and flows north-eastwards, where it finally drains into Lake Abe. It has been divided into three distinct zones: Upper Basin, Middle Basin and Lower Awash Basin on the basis of various inter-related factors such as location, altitude, climate, topography etc. (MoWE, 2012). For this research the upper and some part of Middle Awash Basin covering area of 30,265km² is considered (Figure 3.1).
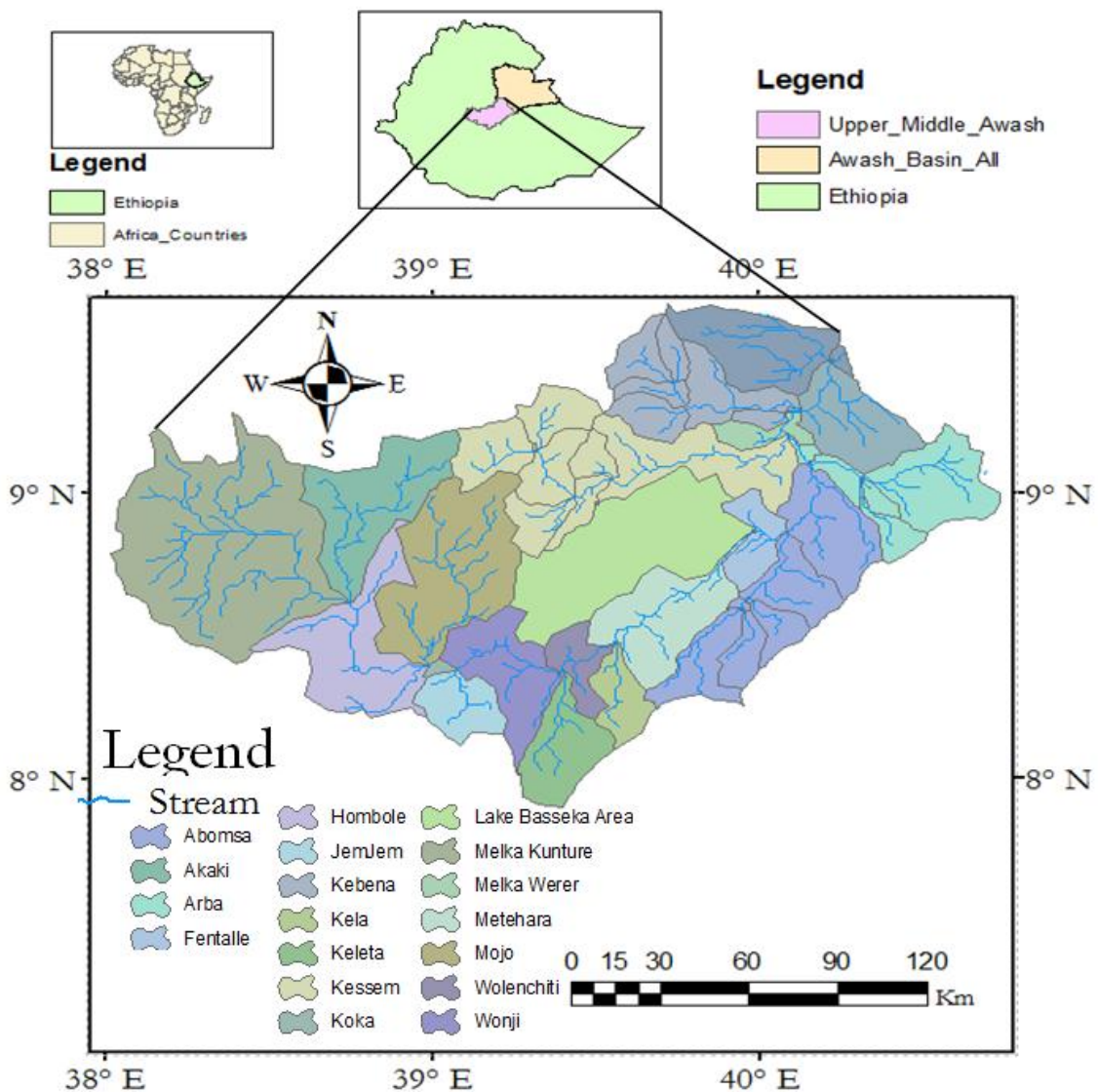
Figure 3.1 Study Area's Location

3.1.1. Climate

The Awash Basin climate comes under the Inter-Tropical Convergence Zone (ITCZ) influence, which causes rainfall distribution to vary seasonally. In March the ITCZ shifts from south of Ethiopia in general and/ or

Awash River basin in particular to north, bringing the small or spring rains. From June to July when it reaches north of Ethiopia across the basin, then there is high rainfall. It returns to southwards during August to October and brings back the low rainfall to dry airstreams that exist until the cycle repeats itself in March. In general the mean annual rainfall varies from 1,600mm at Ankober, in the north east of Addis Ababa to 160mm at Asayita on the northern limit of the Basin(MoWE, 2012). The mean annual rainfall over the entire Western Catchment is 850mm and over the headwaters of the Awash, as gauged at Melka Hombole is 1216mm. Mean annual temperatures range from 20.8^{0}C at Koka to 29^{0}C at Dubti. The highest mean monthly temperatures in June are 23.8^{0}C and 33.6^{0}C Koka and Dubti, respectively. Mean annual wind speeds at Koka is 1.2m/s. The detail explanations of all the above information is available at the web site of (MoWE, 2012).

3.1.2. Soils and Land Cover

Soils, land cover and rainfall are the major physical catchment characteristics that govern runoff generation. Mostly runoff generation depends on topography, infiltration rate, soil water holding capacity, etc. which are highly related to soil types and land cover. Awash River Basin comprises different soil types. The dominant soils in the study area are leptosoil, chromic, eutric, dystricts, vertic etc. (Figure 3.2). The land covers of the area are the natural vegetation (short grass, savannah, tree/shrubs and marshes), wasteland (desert and sand dunes), agricultural lands and lakes.
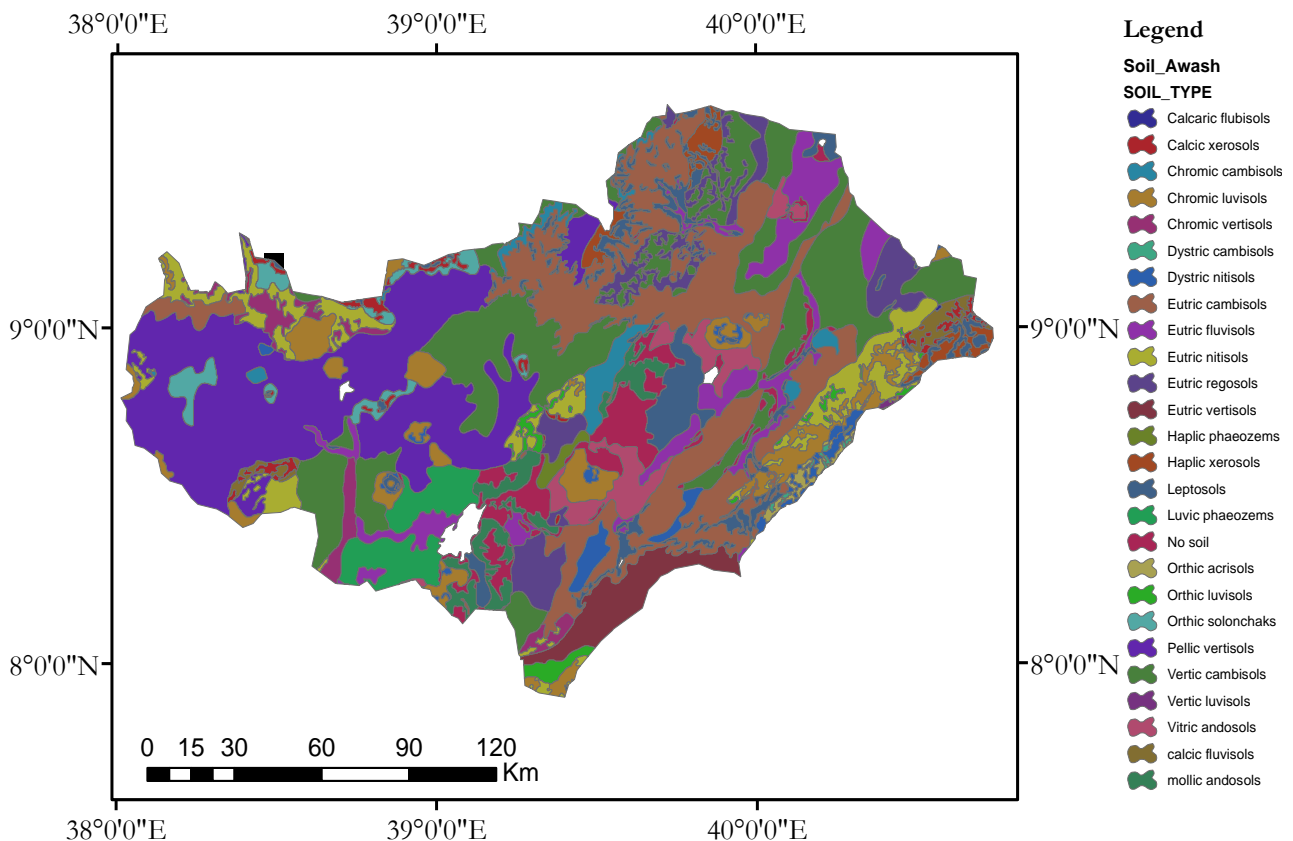
Figure 3.2 Major soil map of Awash River Basin(After Koriche, 2012).

3.1.3. Topography and Geology

Awash River Basin is one of the Great Rift Valley Rivers of Ethiopia. It arises from Ethiopian Plateau near to Ginchi at altitude of about 3000m above mean sea level where the terrain is flat the river flows through the Great Rift Valley gorges and ends up at Afar depression in Lake Abe at elevation of 250m above mean sea level. The slope of area varies from steep to medium as it extends from upper to middle Awash River Basin.

3.1.4. Contribution for Economic Value

The Awash River Basin is the most intensively utilized river basin in Ethiopia. Large irrigation schemes such as Metehara Sugar Factory, Wonji Sugar Factory, Fentalle Irrigation Project, Kessem Irrigation Project, horticulture productions sites and many more small farm irrigation projects have been functional for many years following the construction of the Koka Dam in 1960 (Behailu, 2004). As discussed in Behailu (2004) the reservoir storage capacity is reduced to 30% due to filling up of the reservoir with sediment and thus the water management of the reservoir is becoming exceedingly difficult.

3.2. Data Sets

3.2.1. Data Collected From Offices

Available meteorological data such as precipitation, temperature, specific humidity and wind speed were collected from Ethiopian National Meteorological Agency (ENMA) for 19 stations within or around the study area (Table 3.1 and Figure 3.3). Since this data is required to validate satellite data that are freely available, it is collected for a period of 2005-2010.

 In the same way the stream flow discharge in Awash River Basin were collected from the Ethiopian Ministry of Water and Energy (EMoWE) (Table 3.2). These data are required for model calibration and validation and therefore for the period of 2005 - 2010 data is collected. Furthermore, the land use, land cover and soil map are collected from Awash River Basin Authority (after Koriche, 2012). On top of data collection, during field visit Awash River Basin Authority and Ethiopian Ministry of Water and Energy (EMoWE) have been interviewed to get better background about Awash River Basin. During the interview, we discussed reliability of river gauging instruments installed. They orally explained that the gauges sometime submerge specially during peak flow and it is difficult to read. The other problem was the sediment deposition that causes the river bed channels silted up with sediments and increases the water level reading regardless of increase stream discharge. Hence, the stream flow data are not free of observation error.

Table 3.1 Available Meteorological stations (Source:-ENMA, 2012)

Station Name	Available period	Station Name	Available period
Abomsa	2005-2010	Methara	2005-2010
Addis Ababa (Obs)	2005-2010	Mojo	2005-2010
`Akaki	2005-2010	Adama	2005-2010
Ambo Agriculture	2005-2010	Nura Era	2005-2010
Asgori	2005-2010	Shola Gebeya	2005-2010
Awash Melka	2005-2010	Teji	2005-2010
Debre Berhan	2005-2010	Ziway	2005-2010
Bishoftu	2005-2010	Meiso	2005-2010
Gelemso	2005-2010	Meki	2005-2010
Kulumsa	2005-2010		
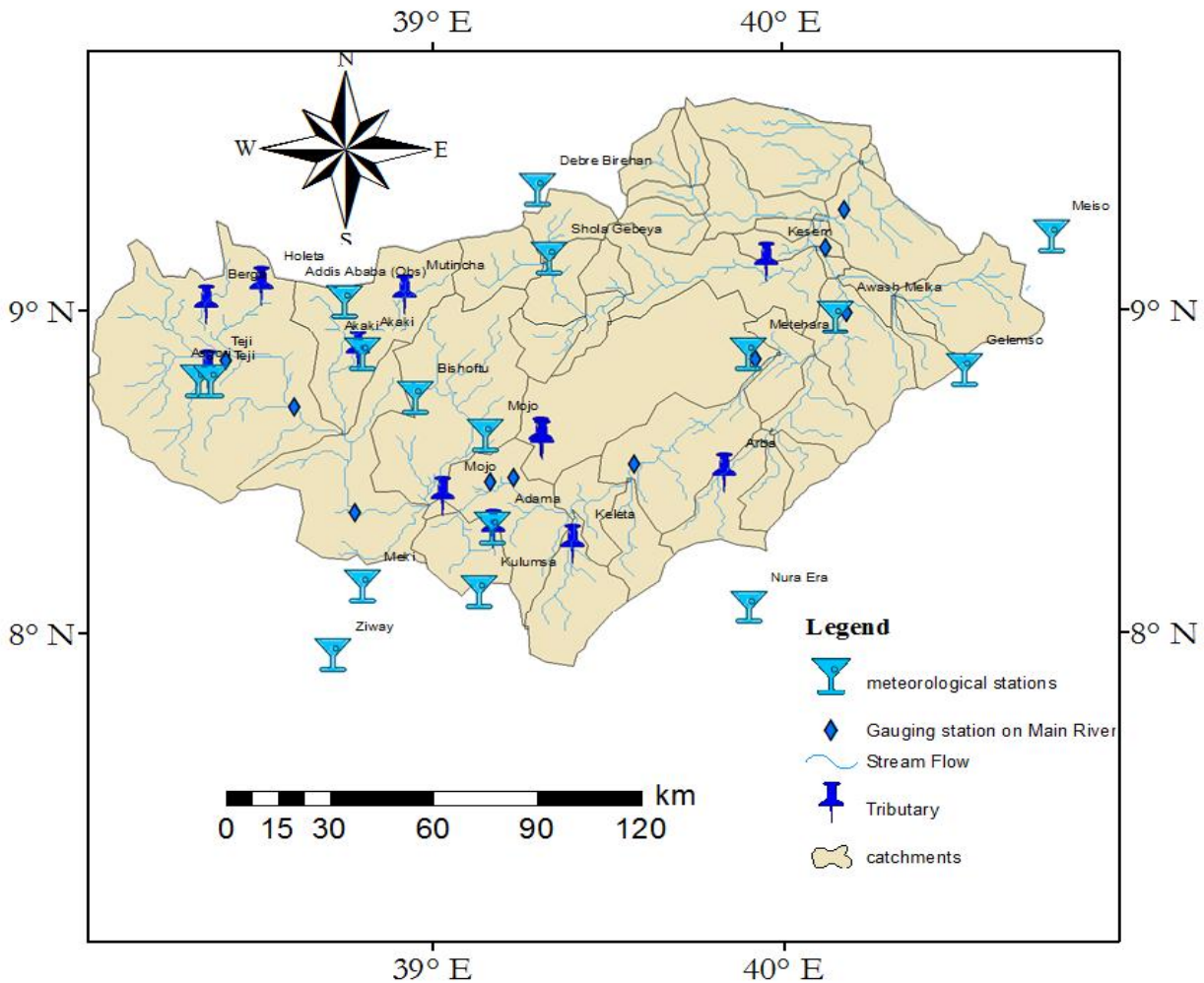
Figure 3.3 Meteorological Stations within and around Awash River Basin

Table 3.2 Available Stream Gauged Data (2005-2010)

Gauged Rivers	Berga River	Holeta River	Awash Bello	Teji River	Akaki River	Melka Kunture	Hombole	Mojo River
Latitude	9.02	9.08	8.85	8.78	8.88	8.70	8.38	8.60
Longitude	38.35	38.42	38.42	38.42	38.78	38.60	38.78	39.08

3.2.2. Satellite Remote Sensing Data Products

For this research satellite products of rainfall and potential evapotranspiration (PET) are required as input for the model.

Satellite Rainfall Products: Precipitation varies both spatially and temporally in Awash River Basin in particular and in Ethiopia in general. To represent the rainfall variability a satellite remote sensing retrieved rainfall product was used for HBV-96 model setup after comparing products with ground truth measurements (see section 5.1.1 for more detail). These satellite products include Tropical Rainfall Measuring Mission (TRMM) Multi-satellite Precipitation Analysis (TMPA 3B42), and Climate Prediction Centre (CPC) morphing technique (CMORPH) precipitation derived products. CMORPH estimated precipitation is derived from low orbiting passive microwave satellite observations and geo-stationary infrared satellite data which covers 60^0N to 60^0S of the Globe with temporal resolution of 3- hours and spatial resolution of 0.25^0 x 0.25^0 or 27.5km x

27.5km. The geo-stationary infrared satellite has high temporal and spatial coverage and low accuracy since the rainfall estimation mainly depend on cloud top brightness temperature, not on actual rain drops property. Whereas the low orbiting passive microwave satellite detects the emissivity from the rain drops with low frequency channels (10-37GHz) and from surface with high frequency channels (85 and above GHz) and they have low spatial and temporal resolution. Hence, by combining both low orbiting passive microwaves and geostationary satellite the high quality precipitation estimation CMORPH was produced using vector motion (Joyce et al., 2004). The most representative low orbiting passive microwave used are the following (After Joyce et al., 2004):

- On board of National Oceanic and Atmospheric Administration (NOAA) 15, 16, 17, and 18; Advanced Microwave Sounding Unit-B (AMSU-B);
- On board of the United States Defense Meteorological Satellite Program (DMSP) 13, 14 and 15; Special Sensor Microwave/Imager (SSM/I)
- On board of NASA's Aqua satellite; Advanced Microwave Scanning Radiometer (AMSR-E); and
- On board of NASA's Tropical Rainfall Measuring Mission (TRMM) spacecraft; TRMM Microwave Imagery (TMI) for more detail see (Joyce et al., 2004).

Similarly, TMPA 3B42 combines passive microwave and IR satellite estimated rainfall with gauge adjustment precipitation computed on global grids. The Tropical Rainfall Measuring Mission (TRMM) Multi-Satellite precipitation Analysis (TMPA) Product 3B42 based on Version 7 algorithm is provided with rainfall rates of (mm/ h) at surface level with a part of global coverage between 60^0N and 60^0S from 1998 to three month before the present time (Huffman et al., 2007). These data provided in 3-hourly temporal resolution and 0.25^0 x 0.25^0 or 27.5km x 27.5km as grid. It produced at the NASA Goddard Space Flight Centers (GSFC) using TMPA. The method combines precipitation estimates of passive microwave (PMW) sensors such as:

- TRMM Microwave Imager (TMI) on board of NASA's TRMM platform
- Special Sensor Microwave/Imager (SSM/I) on board of DMSP
- Advanced Microwave Scanning Radiometer-EOS (AMSR-E) on board of NASA's Aqua satellite
- Advanced Microwave Sounding Unit-B (AMSU-B) on board of National Oceanic and Atmospheric Administration (NOAA)

(For more detail consult; http://cics.umd.edu/~msapiano/PEHRPP/3b42rt.html)

These passive microwave estimate are calibrated by TRMM Precipitation Radar (PR) TMI combined instrument product to a high quality (HQ) microwave product. Where high quality microwave data for a certain location and time step is lacking, HQ-calibrated infrared (IR) data, referred to as "variable rain rate" (VAR), is used to fill the gap. The Climate Prediction Centre (NOAA/CPC except a Global Precipitation Climatology Project, GPCP product used prior to 2000) produces the input IR dataset. The TMPA 3B42 product is composed of calibrated high quality microwave and VAR infrared data for more detail consult (Huffman et al., 2007).

Potential Evapotranspiration (PET): Evapotranspiration is a process by which water molecules converted to vapor by transpiration from plant leaves and evaporation from soil surface. The process is driven by solar radiation and to a small extent by ambient temperature of the air. When there is difference in humidity between the surrounding air and surface the vapor continues to escape from the surface and eventually stops if the surrounding air reaches equilibrium state. Wind blows facilitate the removal of vapors from surface. Hence, net radiation, temperature, relative humidity, wind speed and sun shine hours are the main variables in computing evapotranspiration. Potential evapotranspiration shows the power of air to evaporate water from surface (demand for evaporation) when there is no water limitation. Evapotranspiration rates from a reference surface of grass with 0.12m height, 0.23albedo and 70s/m surface resistance, with no shortage of water, is reference evapotranspiration (FAO-56, 2007). In this study, the selected hydrological model (HBV-96) requires

a mean monthly potential evapotranspiration as input state variable. The potential Evapotranspiration can be calculated using net radiation (R_n) see section 5.1.2 for more detail. The variables required to compute the net radiation are long wave incoming radiation, short wave incoming radiation, Land surface temperature and albedo are obtained from Global Land data assimilation system (GLDAS) for more detail see (http://earlywarning.usgs.gov/fews/global/web/readme.php?symbol=pt) and FEWS NET Global PET is calculated using Penmann-Monteith equation. For this research the FEWS NET Global Potential evapotranspiration which originally estimated using Penmann-Monteith equation on daily bases is imported from ISOD Toolbox plugged in ILWIS from archive directory of (http://igskmncngs600.cr.usgs.gov/ftp2/bulkdailydata/global/pet/days/) (see for detailed section 5.3).

Digital elevation model (DEM): To determine the flow direction and to delineate the catchment areas of the basin according to their stream flow, elevation data is the most crucial. In hydrological modeling, setting the boundary of each catchment is the first and fundamental task. Freely available Elevation data imported using ISOD Toolbox plugged in ILWIS with 1x1km spatial resolution and $5^0 \times 5^0$ tiles from (http://srtm.csi.cgiar.org/SELECTION/inputCoord.asp). The general over all satellite data used and their sources are shown as (Table 3.3).

Table 3.3 Summary of remote sensing data used and their source

Data Sets	Spatial Resolution	Temporal Resolution	Source
Rainfall (CMORPH)	$0.25^0 \times 0.25^0$ or 27.5km x 27.5km	3-hour	ftp://ftp.cpc.ncep.noaa.gov/precip/global_CMORPH/3-hourly_025deg/ using ISOD Toolbox
Rainfall (TMPA 3B42)	$0.25^0 \times 0.25^0$ or 27.5km x 27.5km	3-hour	http://disc2.nascom.nasa.gov/opendap/TRMM_L3/TRMM_3B42/ Using ISOD Toolbox
Potential Evapotranspiration (PET)	$1^0 \times 1^0$ or 111.12km x 111.12km	daily	http://igskmncngs600.cr.usgs.gov/ftp2/bulkdailydata/global/pet/years/ Using ISOD Toolbox
Digital Elevation	1km x 1km		http://igskmncngs506.cr.usgs.gov/gmted/Global_tiles_GMTED/ Using ISOD Toolbox

4. HYDROLOGICAL MODELING

4.1.   Hydrological Process

Before performing hydrological modeling, it is important to understand hydrological processes. Various hydrological processes contribute to the formation of stream flow. Mainly, rainfall runoff generation governed by precipitation, evapotranspiration, infiltration, surface runoff and ground water flow. Generally, the stream flow is composed of quick runoff, subsurface flow and delayed flow. To estimate stream flow there are different hydrological models developed and tested in different countries with different approaches. Hence, the main idea of stream flow simulation is to estimate the stream flow by parameter optimization using one of these hydrological models.

4.2.   Hydrological Model Classification

There are many hydrological models developed to facilitate stream flow simulation. These models share many similarities since their basic assumptions are similar. Traditionally there are two types of hydrological models proposed by hydrologists, distributed physically based and lumped conceptually hydrological model. The first are distributed physically based models, in which the stream flow simulation based on complex mathematical equations to solve mass conservation and momentum equations.

The second are the lumped conceptually models, which simplify the complex physical process, and can be taken as opportunity in catchment scale hydrological modeling. These models have simple model structures of interconnected reservoirs. On top of that lumped conceptually models simplify model complexity by introducing model parameter optimization which is difficult and time consuming to measure directly in the field. Model parameters can be fine-tuned (optimized) using parameter calibration using different available hydrological modeling tools and remain constant as long as catchment property is not changed (Rientjes et al., 2011, Zeweldi et al., 2009). Therefore, since these models usually require few input data which are easily available, they are robust when data availability is limited for stream flow simulation. HBV is one of these model which was used and tested for its application in runoff modeling in more than 40 countries, including Ethiopia (SMHI, 2008).

4.3.   Selection of Model for Stream Flow Simulation

Selecting the most appropriate model for any type of hydrological modeling is most critical. The selection is mainly based on their input data requirement, computational power, simplicity, output reliability etc. The distributed physically based models are more practical if input data are adequate. Hence, such models suffer from data demand and over parameterization since measurement, scale and observation scale are different. In sparsely gauged river basins such as Awash River Basin it is ideal to use physically based distribute model. On other hand, a lumped conceptually model requires less input data and the desired output is more reliable. Hence, for stream flow simulation and regionalization in sparsely gauged River Basins lumped conceptually models are more appropriate. Depending on all above-mentioned criteria the semi distribute hydrological model HBV-96 selected for this research and more detail of this model described below.

4.4.   Mode Structure (HBV-96)

The HBV-96 is a semi-distributed conceptual hydrological model, which developed in Sweden to assist hydropower works. HBV -96 has a power to run the stream flow simulation for each sub catchment that has observed stream flow separately and sum up the simulation results. This make HBV-96 a flexible and few input variable requires to start the model (SMHI, 2008). Hence it a robust in poorly gauged river

basin like Awash River Basin. The model simulate the stream flow using different routings such as upper reservoir zone and lower reservoir zone as shown in Figure 4.1

SF: Snowfall
RF: Rainfall
EA: Actual Evapotranspiration
IN: Infiltration
EI: Evaporation from interception
FC: Maximum soil moisture storage
LP: limit for potential Evapotranspiration
SM: Soil Moisture
R: Recharge
CF: Capillary Fringe
UZ: Upper Zone Reservoir
Q_0: quick Runoff
PERC: Percolation
LZ: Lower Zone Reservoir
Q_1: Base Flow
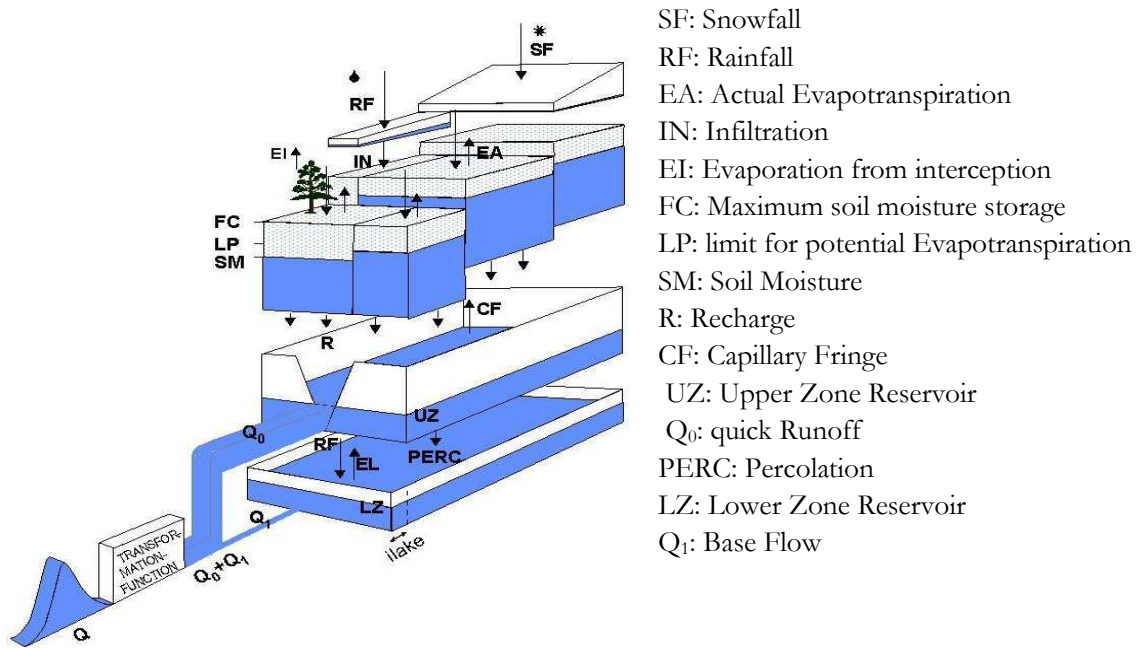
Figure 4.1 Schematic representation of the HBV-96 model for one sub-basin (Source: SMHI, 2008 manual version 6.2)

The HBV -96-model approach has four routines. These are precipitation and snow routine, soil moisture routine, quick runoff routine and delayed/base flow routine. Each of these routings discussed below in detail.

Precipitation Routine: Precipitation is the main factor in stream flow simulation using HBV-96 model. To adjust precipitation to the current altitude the lapse rate parameter pcalt, is applied (SMHI, 2008 manual version 6.2)

Soil Moisture Routine: The soil moisture routine depends on soil infiltration rate and intensity of rainfall. Depending on the relation between maximum soil moisture holding capacity (FC) and simulated soil moisture(SM), recharge will be generated. If the infiltrated rain satisfies the soil, moisture it will produce the recharge otherwise it will either seep down or evaporate. In general, the indirect runoff will be expressed as Equation 4.1.

$$R = IN * \left(\frac{SM}{FC}\right)^{\beta} \tag{4.1}$$

 Where: R is recharge(mm)**,** IN is infiltration (mm), SM is simulated Soil Moisture content (mm), FC is field capacity (mm) and β is Beta (which empirical coefficient and it is unit less)

From equation 4.1 it is clear that indirect runoff has a direct relationship with soil infiltration where simulated soil moisture inversely relates to the maximum soil moisture holding capacity of the soil.

The actual evapotranspiration (ET$_a$) depends on potential evapotranspiration (PET), soil moisture content (SM), field capacity (FC) and lower potential evapotranspiration limit (LP) and can be expressed by the following Equation 4.2.

$$ET_a = \left(\frac{SM}{FC*LP}\right) * PET \tag{4.2}$$

Quick runoff routine: The causes for quick runoff are capillary fringe/rise, percolation to ground recharge and seepage from earth surface (Figure 4.1). On other hand the capillary fringe depends on the maximum soil moisture content and simulated soil moisture content, which can be determined, using Equation 4.3.

$$C_F = C_{FLUX} * \left(\frac{FC-SM}{FC}\right) \tag{4.3}$$

Where: C$_F$ is capillary fringe and CFLUX is correction value for Capillary fringe

Soil water either rises upward as capillary rise or percolates to deep lower zone from the upper zone. In general, water that remains in excess from the deep percolation and capillary rise will produce quick runoff. This can be calculated using Equation 4.4.

$$Q_q = K_{hq} * UZ^{(1+\alpha)} \tag{4.4}$$

Where: Q$_q$ is quick runoff, K$_{hq}$ is recession coefficient, UZ is upper zone storage for quick runoff and α is Alfa (Measure for non- linearity of flow in the quick runoff)

Delayed/base flow routine: The lower reservoir zone contributes to base flow and depends on its storage depth, which can be calculated as equation 4.5.

$$Q_s = K_4 * LZ \tag{4.5}$$

Where: Q$_s$ is delayed/ base flow, K$_4$ is recession coefficient and LZ is lower zone storage depth.

From Equation 4.5 one can deduce that runoff from the lower zone (ground water) is governed by the recession coefficient and the actual lower zone storage depth.

5. RESEARCH METHOD

For this research, three specific objectives are sets. It is well understood that time is the main factor to accomplish these three objectives. Hence, to accomplish them within the period allocated the Methodology followed starting from the principal objectives are discussed blow.

5.1. Data Pre-processing

For this research, different data sets of in-situ and satellite derived are used. Most of the satellite data sets used has different spatial and temporal resolutions, format and coordinate system. Therefore, before using these data sets re-sampling each of them to a common spatial and temporal resolution to same coordinate system of Ethiopia is the primary task. To accomplish this task different resampling techniques such as bi-cubic, bilinear and nearest neighbor were used.

5.1.1. Office Collected Data Pre processing

Precipitation: precipitation data inside and around Awash River Basin for 19 stations were collected from Ethiopian national Meteorological Agency for six years (2005-2010). This time series data have few missing values. Hence, before proceeding to the next process the missing data have been filled depending on their similarities with surrounding stations provided that each station is consistent. The consistency of stations were tested using double mass curve i.e cumulative precipitations of each stations with average cumulative of precipitation of its surrounding stations for six years recoded data (Figure 5.1and Annex C). The test result shows all stations are consistent with regression coefficient (R^2>0.9) that means there is not as much disturbance of the stations. After checking the consistency, the missing data are filled using arithmetic mean method from surrounding stations. The missed data free rainfall imported to ILWIS and converted to point map. To cover the whole study area the point maps were spatially interpolated using moving average of weighted distance method of power 1 with the spatial resolution of the satellite rainfall product used i.e 0.25x0.25 degree (see Figure 6.2). The target station and its surrounding station used for the consistency check are shown as Table 5.1

Table 5.1 Target meteorological station and its respective surrounding stations used for consistency check

S. No.	Target Station	Surrounding Station
1	Addis Ababa	Akaki, Ambo Agriculture, Asgori, Debire Birehan
2	Abomsa	Adama, Kulumsa, Nura Era, Meki, Mojo
3	Akaki	Addis Ababa, Bishoftu, Teji, Shola Gebeya
4	Ambo Agriculture	Addis Ababa, Asgori, Teji
5	Asgori	Addis Ababa, Ambo Agriculture, Akaki, Teji
6	Awash Melka	Debire Birehan, Meiso, Gelemso, Abomsa, Shola Gebeya
7	Bishoftu	Akaki, Mojo, Shola Gebeya, Asgori
8	Kulumsa	Meki, Mojo, Ziway, Adama, Nura Era
9	Meiso	Metehara, Awash Melka, Gelemso
10	Meki	Adama, Kulumsa, Mojo, Teji, Ziway
11	Metehara	Awash Melka, Abomsa, Adama, Shola Gebeya
12	Mojo	Bishoftu, Adama, Meki, Kulumsa
13	Adama	Mojo, Kulumsa, Metehara, Abomsa,
14	Nura Era	Ziway, Kulumsa, Abomsa, Adama, Gelemso
15	Teji	Asgori, Abomsa, Meki, Addis Ababa
16	Ziway	Meki, Kulumsa, Nura Era , Teji
17	Shola Gebeya	Debire Birehan, Awash Melka, Addis Ababa, Bishoftu
18	Gelemso	Nura Era, Abomsa, Meki, Meiso, Metehara
19	Debire Birehan	Meki, Awash Melka, Addis Ababa, Shola Gebeya
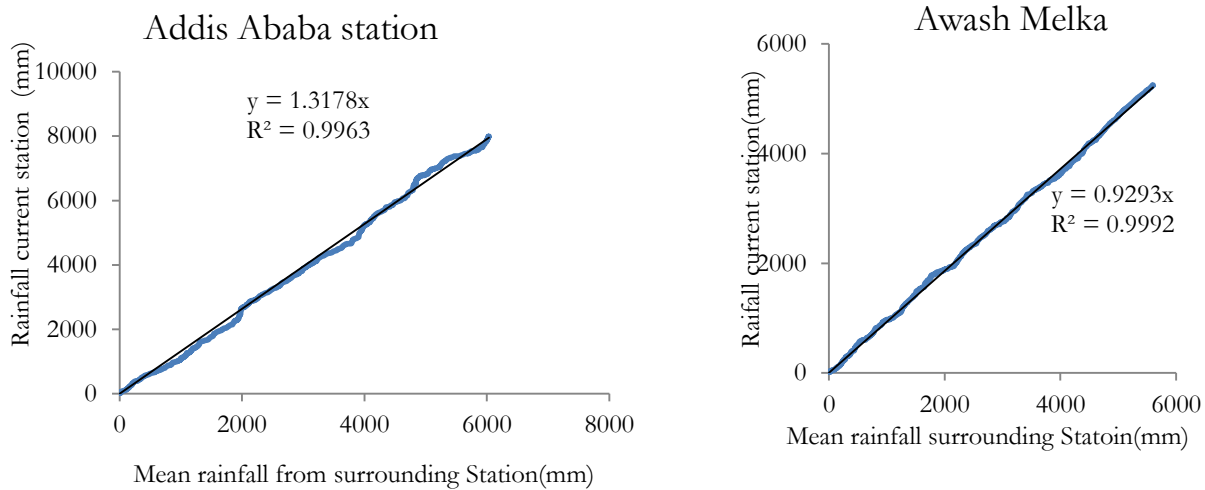
Figure 5.1 Precipitation Consistency Test Using Double Mass Curve

Maximum and Minimum Temperature, Wind speed and sunshine Hours: Maximum and minimum temperature, wind speed and sunshine hours are collected from National Meteorological Agency, Ethiopia have missing data too. Since temperature highly depends on elevation, those stations that have small elevation difference have been selected for filling the missing data. Depending on their similarities the data gap was filled using normalization (Equation 5.1) from surrounding stations (Subramanya, 2008).

$$T_X = \frac{T_{px}}{N} * \left(\frac{T_1}{T_{P_1}} + \frac{T_2}{T_{P_2}} + \cdots + \frac{T_N}{T_{PN}} \right) \tag{5.1}$$

Where: T_X is missing daily temperature at station X,

T_{px} is previous year similar season daily temperature at station X,

$T_1, T_2, \ldots, T_N$ are daily temperature records of surrounding station when there is missing at station X,

$Tp_1, Tp_2, \ldots, T_{pN}$ are the previous year similar season daily temperature records at surrounding station when T_{px} is used and

N is number of surrounding station used.

 Stream Flow data:-Stream flow data were collected from Ethiopian Ministry of Water and Energy (EMoWE). The data was screened to identify the reliable and unreliable data. For the screening a composite hydrograph of each basin with respect to rainfall was plotted on the same graph sheet (Figure 5.2). During screening it was observed that there are missing stream flow data and unexpected trends in hydrographs recession limps (see Figure 5.2 c). There is an unexpected sharp rise and fall in stream flow hydrograph without significant change in precipitation. However, it is obvious that during recession stream flow hydrographs decay exponentially. Therefore, during a recession periods the stream flow hydrographs will follow a linear decay when it is converted to natural logarithm (ln). Hence, considering this fact the missing data were filled using exponential interpolation and expressed as follows (After SWDP, 2009 HP Training Module).

$$\partial = \frac{\ln Q_{t_1} - \ln Q_{t_0}}{t_1 - t_0} \tag{5.2}$$

$$Q_t = Q_{t_0} * Exp(\partial * (t - t_0)) \tag{5.3}$$

Where: ∂ is the slope of the logarithmically transformed flow recession, Q_{t_0} is the discharge (m³/sec) before gap at time t_0, Q_{t_1} is the discharge (m³/sec) after gaps at time t_1 and Q_t is the interpolated discharge (m³/sec) at time t

Furthermore, most of river flows collected are not reliable and has a lot of missing data such as Kessem River (Figure 5.2). Hence, such river are excluded for model calibration and considered as ungauged river.
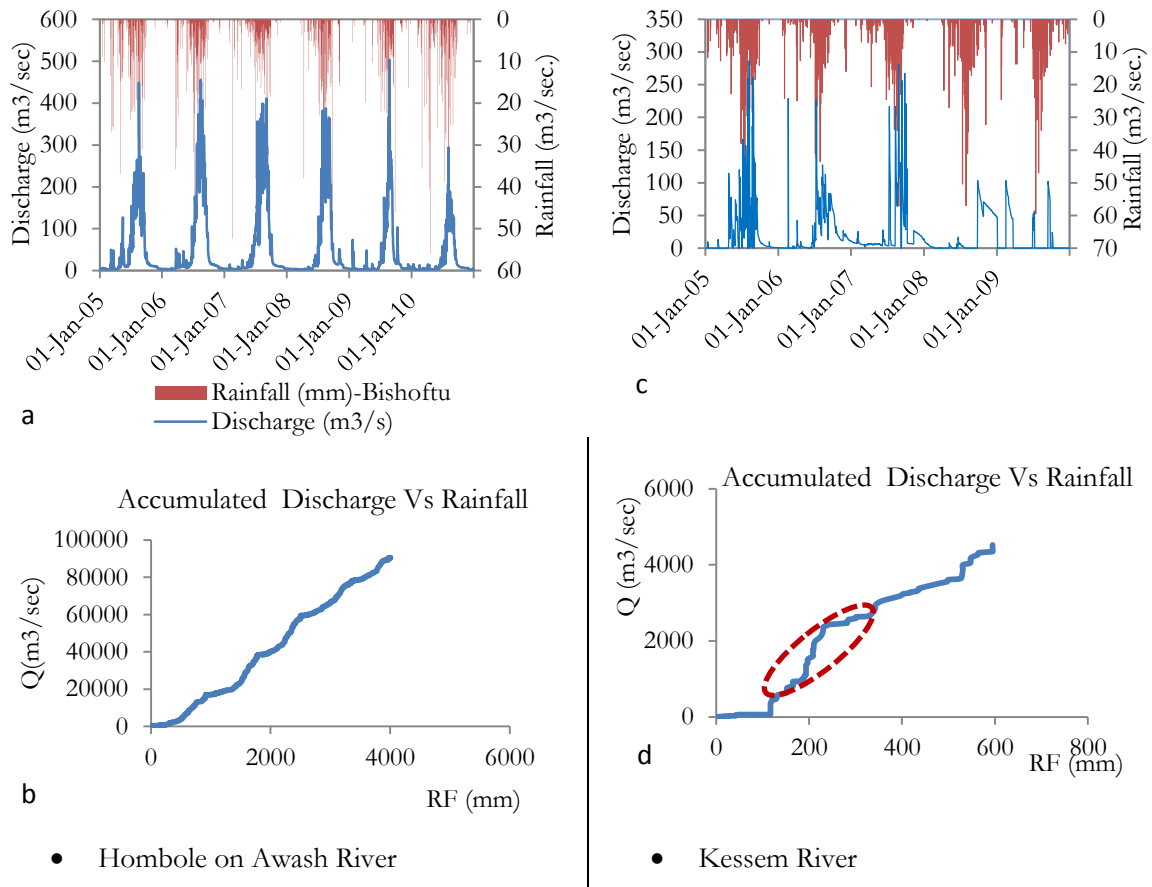
Figure 5.2 Composite hydrograph of River Flow and Rainfall

5.1.2.   Satellite Derived Precipitation Selection

In hydrological modeling, rainfall is the main input variable and can be from ground-based measurements (rain gauge, radar etc.) or from satellite remote sensing. The ground-based measurements are supposed to be reliable; although they have poor spatial coverage in most part of the world. Currently there are a number of satellite precipitation estimates products available, which are comparable with ground-based measurements. Considering this, for this research two remote sensing precipitation products notably Climate Prediction Centre (CPC) and Morphing technique (CMORPH) and Tropical Rainfall Measuring Mission (TRMM) Multi-precipitation Analysis (TMPA 3B42) are evaluated.

CMORPH and TMPA 3B42 data sets are compressed using UNIX standard compression with extension (.z) and they are imported using ISOD Toolbox plug-in ILWIS from archive directory of ftp://ftp.cpc.ncep.noaa.gov/precip/global_CMORPH/3-hourly_025deg   and http://disc2.nascom.nasa.gov/opendap/TRMM_L3/TRMM_3B42/, respectively in raster format.   The

batch file script is used for simplicity and to facilitate the importing. The general satellite data rainfall pre-processing is shown as Figure 5.3.
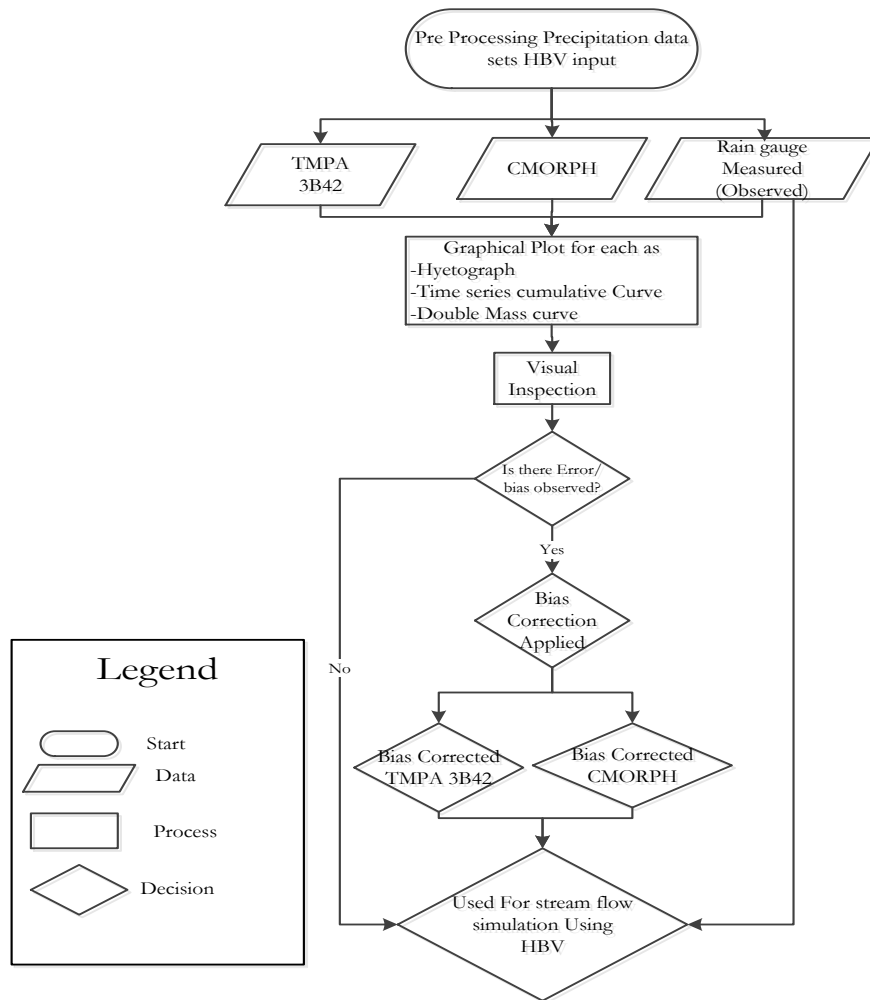
Figure 5.3 Precipitation Data pre-processing for HBV input preparation

Both remote sensing satellite rainfall products have a spatial resolution of 0.25x0.25 degree or 27.5kmx27.5km and 3-hour temporal resolution. For comparison purpose, the pixels that overlay with the respective rain gauge station were taken and to use as HBV-96 input variable the average of all pixels within the respective catchment is taken. Since measured rainfall at each station is available at daily base, the 3-hour satellite rainfall retrieved is cumulated to daily. A map list of annual rainfall of 365/366 (leap year) bands created with the create map list facility in ILWIS and the values of overlapping pixels with the rain gauge station were collected using cross section facility in ILWIS from all 365/366(leap year) map list for comparison and all pixel values within the catchment are collected then averaged to use as input for HBV-96. The daily rainfall of both satellite products and measured rainfall at each station was cumulated starting from 01-january-2005 to 31-December-2010 for comparison as graphical plots.

To evaluate the consistency of CMORPH and TRMM 3B42 a cumulative mass curve time series of the satellite retrieved rainfall and observed rainfall at each station collected from NMA, Ethiopia are plotted on the same sheet (see Figure 6.4). In addition to evaluate the effects of each deviation (error) of satellite retrieved precipitation a double mass curve was plotted using the observed cumulative precipitation as x-axis and cumulative satellite product as y-axis (See Figure 6.5). Following this each graph was visual

inspected and it was observed that there is inconsistency in satellite data sets and respective rain gauge measured precipitation.

Bias Observation: For satellite rainfall, product bias can be distinguished as hit bias, missed rainfall bias and false rainfall bias. Hit bias occurs when there is rainfall detected by both satellite and rain gauge but differ in amount. That is there is a rainfall records by the satellite as well as it also recorded by rain gauge but there is over or underestimation. On other hand, missed rainfall bias occurs when there is rainfall recoded by rain gauge but missed from satellite. Similarly, false rainfall bias occurs when there is no rainfall recorded by rain gauge but detected by satellite(Habib et al., 2009). These bias are mathematically expressed as follows (after Habib et al., 2009):

$$\text{Hit Bias} = \sum_{i=1}^{n}(P_{satellite} - P_{rain\ gauge}) \quad (\text{When } P_{satellite}>0 \text{ and } P_{rain\ gauge}>0) \tag{5.4}$$

$$\text{Missed Rainfall Bias} = \sum_{i=1}^{n} R_{rain\ gauge} \quad (\text{When } P_{satellite}=0 \text{ and } P_{rain\ gauge}>0) \tag{5.5}$$

$$\text{False Rainfall Bias} = \sum_{i=1}^{n} P_{satellite} \quad (\text{When } P_{satellite}>0 \text{ and } P_{rain\ gauge}=0) \tag{5.6}$$

Where: Hit Bias (mm), Missed Rainfall Bias (mm), False Rainfall bias (mm) $P_{satellite}$ is precipitation detected by satellite (mm/day), $P_{rain\ gauge}$ is precipitation recorded by rain gauge(mm/day), and n is sample size (days).

The biases evaluation expressed above are applied for each year separately. After applying for respective year, the mean of biases are calculated by dividing the total bias of each category by number of respective bias in days and the results are shown as Table 6.2.

Bias correction: The satellite retrieved precipitation bias correction is applied using the following equation 5.7, which is derived from equations 5.4, 5.5 and 5.6.

$$P_{satellite\ bias\ corrected} = P_{satellite} - \text{Mean of Hit Bias} + \text{Missed Rainfall} - \text{False Rainfall}. \tag{5.7}$$

Where: $P_{satellite\ bias\ corrected}$ is bias corrected satellite rainfall products (mm/day), Mean of hit bias is hit bias divided by number of hit bias occurred (days) the its unit is (mm/day), Missed rainfall is a rainfall that not detected by satellite (mm/day) and False rainfall is the rainfall that is detected by satellite but not recorded by rain gauge (mm/day)

The same bias correction was applied for satellite retrieved precipitation is used as input for HBV model set up.

5.1.3.   Potential Evapotranspiration Estimation

In-situ Reference evapotranspiration: The in-situ reference evapotranspiration were calculated based on Penman-Monteith equation(FAO-56, 2007)   using meteorological variables such as air temperature, relative humidity, wind speed, sunshine hours collected from National Meteorological Agency, Ethiopia for six years from 2005 to 2010.

$$\text{ET}_o = \frac{\Delta*(R_n-G)+\gamma*\frac{900}{T+273}*U_2*(e_s-e_a)}{\Delta+\gamma*[1+0.34*U_2]} \tag{5.8}$$

Where: - ET_o is reference Evapotranspiration (mm/day), T is air temperature [°C], e_s is saturated Vapor Pressure (kpa), e_a is actual Vapor Pressure (kpa), γ is psychometric constant (Kpa/⁰C), Δ is slope of Vapor pressure curve, U_2 is Wind speed at 2m height (m/sec)

To compute the reference evapotranspiration there are still unknown variables to be estimated. These variables includes psychometric constant (γ) , saturation vapor pressure (e_s), Actual vapor pressure (e_a) and Slope of vapor pressure curve (Δ) which will be solved step by step as shown blow. The psychometric constant estimated from air pressure using Equation 5.9

$$\gamma = 0.665 * 10^{-3} * P \tag{5.9}$$

Where: P is air pressure (kpa)

The saturated vapor pressure is related to air temperature (T); hence, it may be determined using air temperature as Equation 5.10.

$$e^o(T) = 0.6108 * \exp\left[\frac{17.27*T}{T+237.3}\right] \tag{5.10}$$

Where: e° (T) is saturation vapor pressure at air temperature T [kPa], and T is air temperature [°C]
Since temperature varies temporally, the saturation vapor pressure will be calculated for mean values. Therefore, the mean saturated vapor pressure according to (FAO-56, 2007) is given below in equation 5.11 and the actual vapor pressure which depends on saturation vapor pressure and relative humidity can be calculated using equation 5.12.

$$e_s = \frac{e^o(T_{max})-e^o(T_{min})}{2} \tag{5.11}$$

$$e_a = e_s * \frac{RH_{mean}}{100} \tag{5.12}$$

Where: RH_{mean} is mean of relative humidity (%)
Finally, the slope of vapor pressure curve calculated as equation 5.12.

$$\Delta = \frac{4098*\left[0.6108*\exp\left(\frac{17.27*T}{T+237.3}\right)\right]}{(T+237.3)^2} \tag{5.12}$$

Where: T is mean air temperature [°C]

FEWS NET Global PET: The hydrological model selected for this research requires as input the mean monthly potential evapotranspiration (PET). Hence, PET data obtained from FEWS NET Global PET, which can be freely retrieved using ISOD Toolbox plug-in ILWIS free ware. FEWS NET Global potential evapotranspiration is calculated using climate data extracted from Global Data Assimilation System (GDAS) such as air temperature; atmospheric pressure, relative humidity, and solar radiation using penman-Monteith equation (see http://earlywarning.usgs.gov/fews/global/web/readme.php?symbol=pt for more detail). After the data imported as raster format in ILWIS, the required data that cover the study area masked to simplify processing. Following this map list of these, raster's created in ILWIS and the overlapping pixel of FEWS NET with respective meteorological station was collected using cross section facility in ILWIS.

Evaluation for Biases: A FEWS NET Global PET extracted was evaluated against the estimated reference evapotranspiration using bias indictors (Equation 5.13 to 5.16). To have better understanding the progressive effects of accumulated error of FEWS NET Global PET a double mass curve of FEWS NET falling in respective meteorological stations is used and visually inspected. Furthermore, to observe the deviation from mean value of calculated reference evapotranspiration the time series plot on the same sheet for both calculated ET_O and FEWS NET retrieved PET is used (Figure 5.3). After visual inspection of the plots, it was understood that there is deviation between the Evapotranspiration estimates. Hence, using some evaluator indicators such as mean bias, relative bias (%), absolute bias (%) and root mean square error (RMSE) a simple statistics was applied. Mean Bias is used to evaluate the total mean bias of the time series in the entire study period. On the other hand the relative bias shows the measure of total volume differences between two time series. The relative bias between FEWS NET PET and ET_O was determined by Equation 5.14, however this bias do not show the actual difference when there are overestimation or underestimation in time series. Hence, the absolute relative bias is applied to show the measure of the timing gaps between the time series regardless of the volume gaps. That is if there is over or underestimation in time series one cannot cancel the other (Equation 5.15). The root mean square error is applied to evaluate the total mean error of the time series (equation 5.16). For more detail regarding theses bias evaluator indicators consult (Liu et al., 2011). The evaluator indicators are mathematically expressed as:

$$\text{Mean Bias(MB)} \quad = \frac{\sum_{i=1}^{n} \text{FEWS NET PET} - \sum_{i=1}^{n} ET_0}{N} \tag{5.13}$$

$$\text{Relative Bias(RB)(\%)} \quad = \frac{\sum_{i=1}^{n} \text{FEWS NET PET} - \sum_{i=1}^{n} ET_0}{\sum_{i=1}^{n} ET_0} \tag{5.14}$$

$$\text{Absolute Relative Bias(ARB)(\%)} \quad = \frac{\sum_{i=1}^{n} |(\text{FEWS NET PET} - ET_0)|}{\sum_{i=1}^{n} ET_0} \tag{5.15}$$

$$\text{Root Mean Square Error(RMSE)} \quad = \sqrt{\frac{\sum_{i=1}^{n} (\text{FEWS NET PET} - ET_0)^2}{N}} \tag{5.16}$$

While applying evaluation it was found that there is error/bias. Since HBV-96 requires a monthly mean of Potential evapotranspiration, the error/ bias of FEWS NET PET have to be minimized as much as possible before using it for the model setup. The bias correction is applied using the concept of mean value ratio that means if the bias is removed the mean ratio of both data sets (ET_O and FEWS NET PET) will be unity(Haddeland et al., 2011). The method is expressed mathematically as follows:

$$\text{PET}_{\text{bias corrected}} \quad = \text{FEWS NET PET} * \frac{\overline{ET_0}}{\overline{\text{FEWS NET PET}}} \tag{5.17}$$

Where: $\text{PET}_{\text{bias corrected}}$ is a bias corrected potential evapotranspiration.

After applying bias correction (equations 5.17), a PET that has the least error is used as input for HBV -96 model set up. In general, the overall procedures followed are shown as flow chart in
Figure 5.4
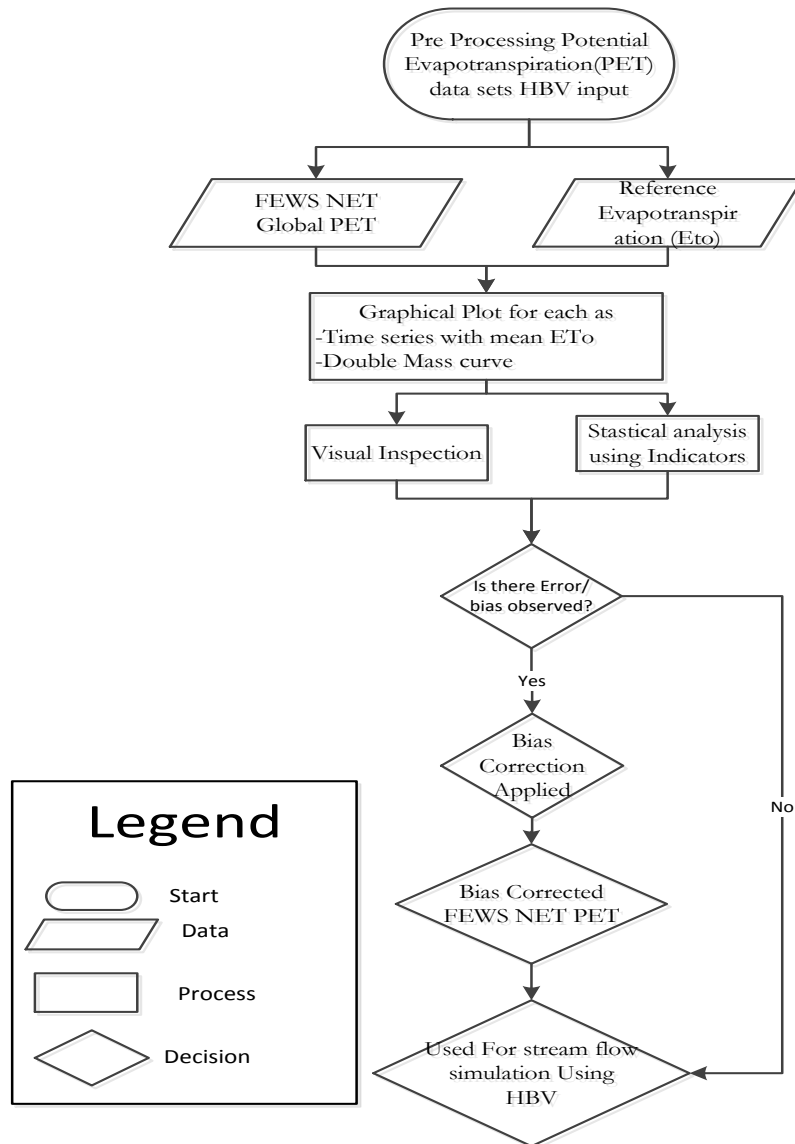
Figure 5.4 Potential Evapotranspiration pre-processing to prepare for HBV-96 input Variable

5.1.4. Meteorological Forcing Data Processing For HBV-96

For this research, meteorological forcing such as rainfall and potential evapotranspiration derived from satellite and in-situ measured data sets are used. The in-situ measured rainfall is based on rain gauge measurements, which are point data. To cover the entire area the point data are imported to ILWIS GIS free software and spatially interpolated using inverse distance method with the default weighted exponent of 1 and spatial resolution of 0.25 x 0.25 degree or 27.5km x 27.5km (see Figure 6.2). Then, from the spatially interpolated rainfall, value of all respective pixels falling within the catchment are collected and averaged before using it as input for HBV-96. Similarly, the rainfall from all pixels of CMORPH and TMPA 3B42 that are within the respective catchment are collected and averaged. Before using, these data sets as input for HBV-96 bias corrections are applied following the same procedure as described in section 5.1.2. On the other hand, the meteorological forcing potential evapotranspiration obtained from FEWS NET Global PET. In the same way as that of rainfall, the value of pixels of FEWS NET PET within the catchment is collected and bias correction is applied with the same procedure as described under section 5.1.3. The bias corrected PET is used as input for HBV-96 model setup.

5.1.5.   Catchment Extraction and Flow Direction

For this research a digital elevation model (DEM) is imported using ISOD Toolbox plugged in ILWIS 1.3 for easiest way of processing from (http://srtm.csi.cgiar.org/SELECTION/inputCoord.asp) having spatial resolution of 1kmx1km. The imported DEM has some undefined values especially for low laying elementary depression area. This issue is resolved using sink/fill operation in ILWIS. However, since the elevation is in metric unit system, before making sink/fill operation the coordinate system has to be converted to metric unit system using coordinate transformation system (UTM in this case). In ILWIS kriging operation was used, which is similar to moving average, to resolve the undefined and the local peaks and depression of 8 surrounding pixel removed using sink/ fill operations. The next step is to extract flow direction maps and extraction catchments. Depending on topography the minimum thresh hold (number of pixel to be considered) is provided to extract the catchments. The extracted catchments are either dense or scarce when compared to the actual drainage of the field (see Figure 5.5 a). Therefore, another crucial work done is to merge the short flow lines and narrow drainage to match the catchments with natural drainage areas (see Figure 5.5 b). At the last using screen digitizing the catchment of Awash River Basin extracted.

a. Catchment extracted using threshhold number of Pixel =500

b. Catchment extracted using as threshhold number of Pixel =1000
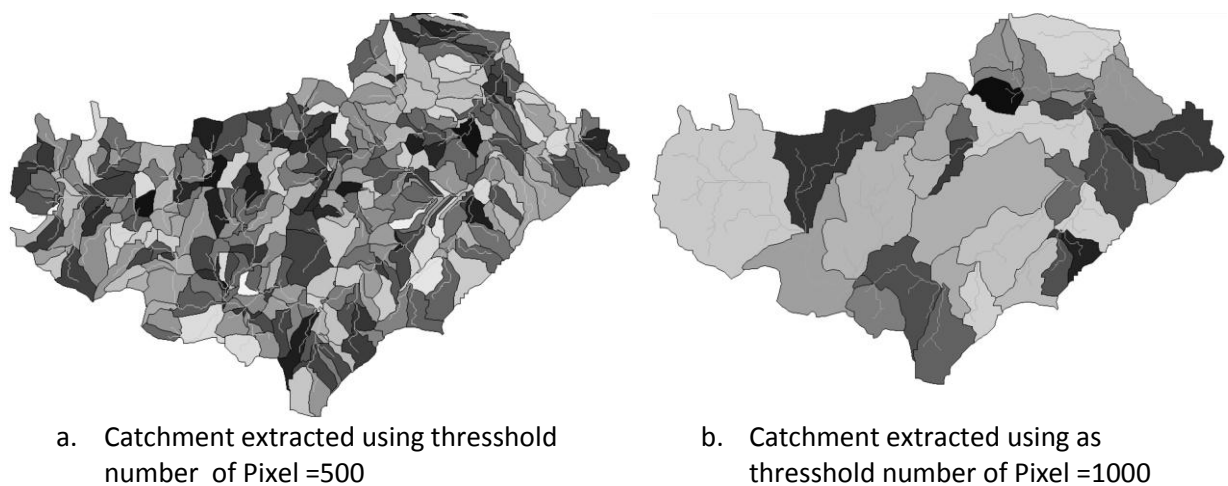
Figure 5.5 Catchment extraction using different number of pixels has to be considered as threshold

5.1.6.   Elevation Zone Preparation

The land cover map collected from Awash River Basin Authority is used. First, the raster map of extracted catchment and the Digital Elevation Model (DEM) were crossed to determine elevation Zone of each catchment. The land cover raster map was resampled to the spatial resolution of digital elevation model and crossed with the raster map of elevation zone created by crossing the DEM and the extracted catchment raster map. Finally the fraction of land cover per elevation zone is determined which can be used as input for the HBV. This is needed to estimate the soil moisture in HBV model correcting effects of elevation and land cover. Hence, depending on information from the actual evapotranspiration and the soil moisture obtained by the model, the stream flow hydrograph of the basin will be obtained with optimized parameters.
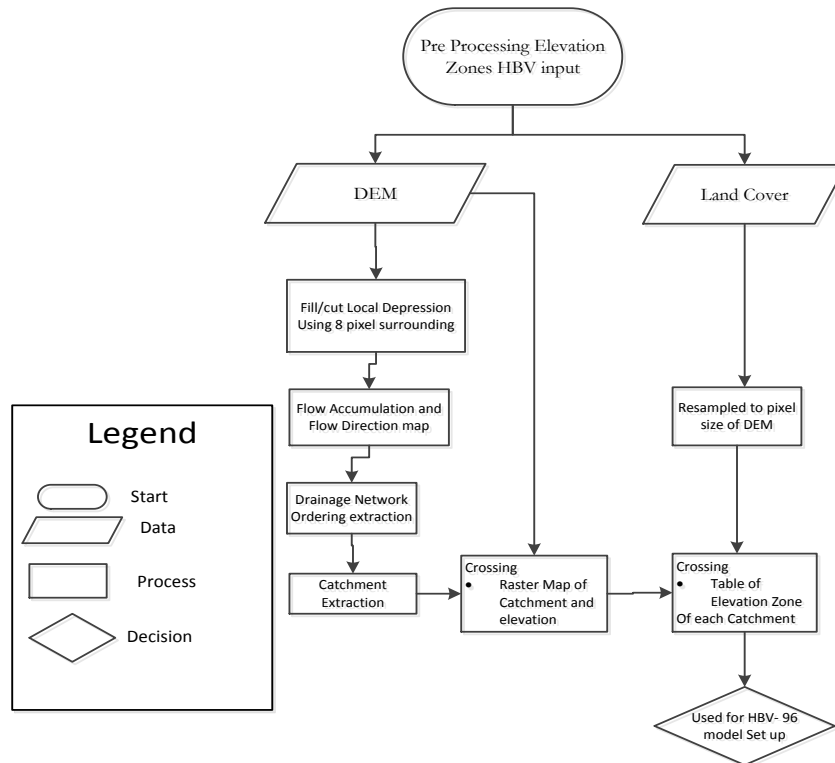
Figure 5.6 Catchment Extraction and Elevation Zone data preparation for HBV model setup

5.2. Model Calibration and Validation

5.2.1. Model Calibration

The model parameter optimization usually depends on matching observed and simulated discharge at the outlet of a catchment. Similarly, HBV-96 is a semi-distributed conceptual hydrological model that requires a number of model parameter has to be optimized to minimize parameter error offsets depending on observed and simulated discharge at the catchment outlet. Some of the model parameters to be optimized include field capacity (FC), limit for Evapotranspiration (LP), Recession coefficient of lower reservoir K4, Recession coefficient of Upper reservoir Khq, Empirical coefficient (Beta), non-linearity response (Alfa) and percolation (Perc).

At the begging, when model calibration start with default model parameters the simulated and observed stream flow most probably will not fit. Hence, the main idea of model parameter optimization is to maximize the stream flow estimation minimizing model uncertainty that is the observed and simulated stream flow hydrograph will fits. The model parameter calibration was performed manually until the model simulated stream flow match with observed stream flow. Since there are different factors such as model structure, boundary condition, initial condition of model parameters and meteorological forcing that are not free of error, including model complexity, models are always uncertain.

Calibration requires multiple statistics, each covering a different aspect of the hydrograph (Moriasi et al., 2007). According to Moriasi et al. (2007) there are different objective functions for model evaluation in stream flow simulating. The objective functions like Nash-Sutcliffe coefficient of efficiency (NSE) and Relative Volumetric Error (RVE) are most widely used in hydrological uncertainty evaluation. NSE is the best objective function reflects an overall fit of a hydrograph simulated with observed and it can be $-\infty$ to 1. The value 1 indicates the model is perfect fit, whereas the $-\infty$ indicates the totally disagreement. The

model is considered as good performing model when NSE is 0.8 to 0.9 and fair to good performing model when NSE is 0.6 to 0.8. RVE represents variation between simulated and observed discharge as relative volume. RVE ranges -∞ to +∞ , where the good model RVE is -5% to 5% while the value -10% to -5% and 5% to 10% are considered as reasonably well performing model. In general, these objective functions mathematically can be expressed as:

$$RVE = \left[\frac{\sum_{i=1}^{n} Q_{sim} - \sum_{i=1}^{n} Q_{obs}}{\sum_{i=1}^{n} Q_{obs}} \right] \qquad (5.18)$$

$$NSE = 1 - \left[\frac{\sum_{i=1}^{n}(Q_{obs} - Q_{sim})^2}{\sum_{i=1}^{n}(Q_{obs} - \overline{Q_{obs}})^2} \right] \qquad (5.29)$$

Where: n is number of observations, Q_{obs} is observed stream flow at gauged station (m³/sec), $\overline{Q_{obs}}$ is mean of observed stream flow at gauged station (m³/sec), Q_{sim} is simulated stream flow at gauged station (m³/sec), NSE is Nash-Sutcliffe coefficient of efficiency, RVE is Relative Volumetric Error(%) .

The calibration period most of the time covers 2/3 of the available time series and the remaining 1/3 of time series is required for model validation purposes. Hence, for this thesis, the calibration was performed for periods of 2005-2008 and the general procedures are shown as Figure 5.7.
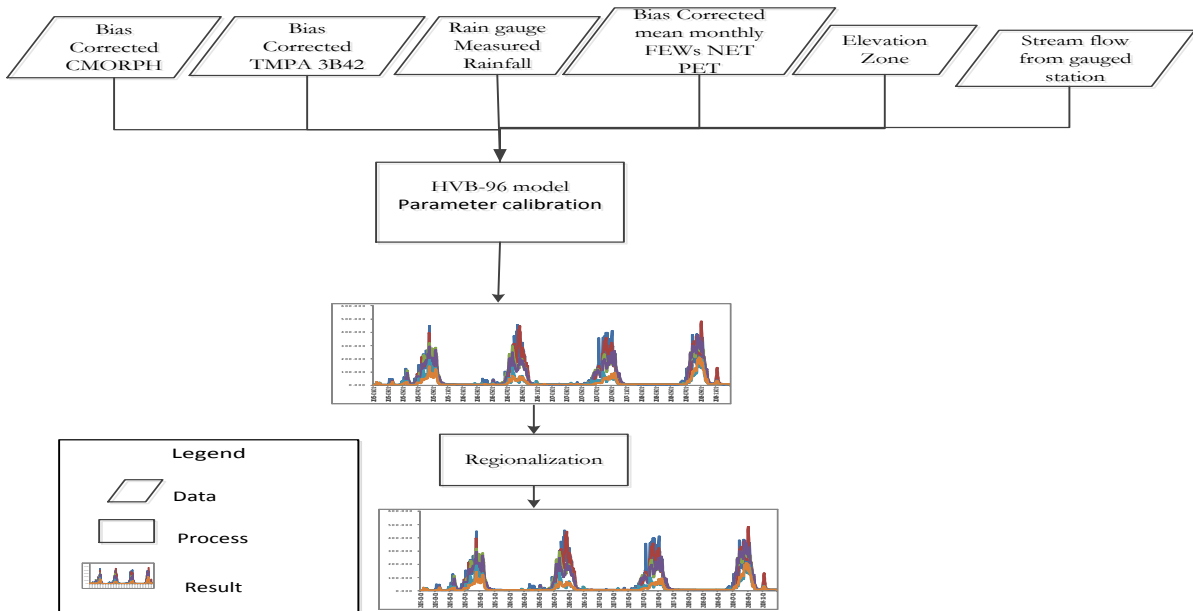
Figure 5.7 HBV- 96 Model parameter optimization procedures

5.2.2. Model Validation

After model calibration applied there may be over or underestimation of model parameter. So applicability estimated model parameters have to be re-evaluated by changing external forcing variables. Hence, model validation is essential part of modeling, for acceptances and usage of model parameters that support future short-term or long-term decision making/forecasting. Model Validation is performed to ensure:

- ❖ Whether the model parameters values adopted are performing well when external forcing is changed
- ❖ The conceptual and boundary condition for algorithms development have been implemented properly

❖ The model errors remain minimum

Model validation for Upper and Middle Awash River Basin was carried out for two years (2009-2010). The performance indicator discussed under section 5.2.1 applied to evaluate the model validity. When parameters are not valid as the external forcing changed the model recalibrated until the performance indicators fall within an acceptable range as discussed in section 5.2.1 (See Table 6.4) and the model is validated. Hence, the optimized model parameters are representative for the area as long as the catchment not changed.

5.3. Regionalization

Stream flow modeling at catchment scale is a process by which stream flow is simulated using different modeling criteria. Similarly, this is true for HBV-96 too. The stream flow simulation needs a model parameter optimization for gauged catchments by fitting the observed (measured) and simulated stream flows. However, for ungauged catchments it is difficult to determine model parameters using HBV-96. Hence, in such catchment it is vital to use regionalization. Using regionalization, information can be transferred from gauged catchments to area of interest-ungauged catchment. This method were used by different researchers in different countries using different techniques (Islam et al., 2005; Rientjes et al., 2011; Wale et al., 2009; Kim et al., 2008; Wagener et al., 2006, Booij, 2005).

As discussed in sub-section 5.2.1 about eight model parameters require optimization for gauged streams. These parameters should be determined for ungauged catchment too. However, it is difficult to determine for ungauged catchment by model calibration since observed stream flows are not available. Therefore, as discussed in section 2.5 different researchers' used regionalization to solve such problem using available techniques such as linking physical catchment characteristics(PCCs) with model parameters (MPs), spatial proximity, regression, Area ratio conversion, sub basin mean etc. To use spatial proximity it is assumed that, if catchments are spatially proximate most probably they have similar hydrological responses since meteorological forcing and catchment properties vary smoothly (Rientjes et al., 2011). Hence, these parameters have to be optimized for gauged catchments and then after identifying the spatial proximity of gauged and ungauged catchments the model parameters transfer to ungauged catchment will takes place. However, in Awash River Basin most of gauged catchments are located at upstream, while ungauged catchments are located downstream. The sub-basin means assume that the catchments will have collectively average similar properties, and then the mean of MPs will represent the area. Hence, for this research linking PCCs and MPs (Rientjes et al., 2011, Deckers et al., 2010, Wale et al., 2009) and sub basin mean are selected.

Hydrological response is highly related to physical catchment characteristics. Hence, linking PCCs and MPs depending on simple and multiple regressions is fundamental. Using stepwise regression in SPSS software the most significant PCCs are selected and less significant PCCs are removed, finally the regression equation for a particular model parameter is established. Note that the regression equation established alone is no grantee; hence the physical meaning of each PCC with respect to model parameter must be considered. After evaluating the PCCs statistical significance and hydrological applicability the regression equation is established.

In general, considering these facts first model parameters have to be optimized for gauged catchments and transferred to ungauged catchments. After model parameters are estimated, their performance on stream flow simulation will be evaluated for their consistency taking the downstream gauged catchments. This will help us to determine applicability of determined parameters of ungauged catchments for the whole basins.

5.4.   Physical Catchment Charactestics (PCCs) Selection

Runoff generation is governed by catchment physical characteristics (PCCs)(Rientjes et al., 2011). The PCCs mainly related to land uses, Soil type, climate and topography. The main challenge is to evaluate the relation between model parameters (MPs) and PCCs, since one MPs may be affected by more than one PCCs(Deckers et al., 2010). For example, the maximum water holding capacity (FC) is mainly related with soil texture and land uses. That is soil water holding capacity is related to soil pore space, which is highly affected by soil types and land use. In other word, the soil pore space may be modified by external factors such as water ponding for a long time, which is related to drainage density. Similarly, the imperial coefficient Beta (β) and non-linearity response Alfa (α) related with geography and geo-physiography and runoff coefficient. The runoff coefficient mostly is determined by climate, soil type and land uses, especially when empirical equations are used, it can be determined from standard tables using soil type and land uses values as main indicators (Raghunath, 2009). However, to solve this main challenging in this research the relation between PCCs and MPs are established using simple and multiple regressions.

During DEM processing in ILWIS PCCs such as, catchment area (km²), longest flow path (km), maximum, minimum and mean elevation (m) of each catchment, which is named after this geography and physiology, are collected. The PCCs related with soil and land cover are collected from soil map and land cover maps, while PCCs that related to climate data such as precipitation and PET are collected from climatic data sets all of them are shown in

Table 5.2. The PCC selection for this research is based on related researches (Rientjes et al., 2011, Wale et al., 2009, Perera, 2009) on Lake Tana Basin, Ethiopia.

Table 5.2 Physical Catchment Characteristics (PCCs)

Group	Parameter	Physical Catchment characteristics and Unit
Physiology and Geography	AREA	Catchment area (Km²)
	EL	Elongation(-)
	DD	Drainage Density(m/km²)
	SHAPE	Catchment Shape(-)
	CI	Circularity INDEX(-)
	HI	Hypsometric Integrity(-)
	AV.SLOPE	Average Slope (%)
	LFP	Longest Flow Path(km)
	MDEM	Mean Digital Elevation(m)
Soil type	CHR	Chromic soil Area (%)
	EUTR	Eutric soil Area (%)
	LUV	Luvic Soil Area (%)
	LEPT	Leptosoil Area (%)
	VERT	Vertisol Area (%)
Land Use	DCROP	Dominantly Cropped (%)
	MCROP	Moderately Cropped (%)
	URBAN	Urban (%)
	FOREST	Forest (%)
	GRASS	Grass land (%)
Climate	SAMR	Standard Annual Mean Rainfall (mm)
	MPWET	Mean Rainfall of Wet season (mm)
	MPDRY	Mean Rainfall of dry season (mm)
	MPET	Mean potential Evapotranspiration (mm)

5.5.   The Regional Model

Simple Regression method: The relation between model parameter and physical catchment characteristics is determined based on simple linear regression. The simple linear regression tries to fit two variables, dependent and independent variables. Most of the time linear regression is expressed by correlation coefficient. The correlation coefficient of two variable is between – 1 and 1. It can be determined using the following equation (Field, 2009):

$$t_{cor} = |r| * \frac{\sqrt{n-2}}{\sqrt{1-r^2}} \qquad\qquad (5.20)$$

The hypothesis is made to test whether the relation exist between MPs and PCCs. The hypothesis is given as follows:

H_o: The correlation between MPs and PCCs is null, $\rho = 0$

H_1: The correlation between MPs and PCCs is not null, $\rho \neq 0$

The confidence level interval of $\alpha = 0.1$ and two-tailed test with degree of freedom of n-2 are used for this research to determine the t_{cr} at which the significance of the correlation is tested. Using n=4, df =2 and α=0.1 from statistics table of t-critical (After Nikolopoulos, 2004) t_{cr}=2.92 is found. Using equation 5.20, the correlation coefficients(r) greater than or equal to 0.90 or less than or equal to -0.90 are result as statistically significant for rejecting or accepting the hypothesis. The correlation coefficient of each model parameter and physical catchment characteristics determined using excel; data analysis facility and using as input range data list of MPs and PCCs.

Multiple Regressions: Multiple regressions are used to select the independent variable(s), which can efficiently determine the dependent variable(s). Dependent variables are whose value are to be determined and independent variables are those having fixed value or already determined. In our case, the dependent variables are MPs and the independent variables are PCCs. To select the best independent variables stepwise multiple regressions is used in SPSS version 21. To establish the regression equation, each independent variable (PCCs) should not be correlated (i.e $R_i^2 \approx 0$) for more detail procedures how to use SPSS consult (Field, 2009). The PCCs co-linearity is tested using tolerance level and variance inflection factor (VIF) which are expressed as follows.

$$\text{Tolerance } = 1 - R_i^2 \qquad\qquad (5.21)$$

$$\text{VIF} \quad = \frac{1}{\text{Tolerance}} \qquad\qquad (5.22)$$

Where: R_i^2 is coefficient of determination and VIF is variance inflection factor.

Stepwise multiple regression start with no predictors (empty model). Hence, the independent variables are forced to the model till the VIF value or tolerance level is reached. The best value for tolerance and VIF is 1, while the trouble values are approximately 0 and greater than 10, respectively (Meyers et al., 2007 and O'Brien, 2007). The independent variables fulfilling this condition will be selected for regression equation. The general regression equation is given as follow:

$$MP_i = \beta_o + \sum_{i=1}^n \beta_i \, PCC_i + \varepsilon_i \qquad\qquad (5.23)$$

Where: MP_i are model parameters, PCC_i are physical catchment characteristics, β_o is regression constant, β_i are regression coefficients and ε_i is an error associated with predicators.

6. RESULTS AND DISCUSSION

6.1. Precipitation Data Analysis And Comparison

As discussed in section 5.1.2 the satellite rainfall products of TMPA 3B42 and CMORPH since (2005-2010) were retrieved and compared with rain gauge observed at 19 stations inside and around the study area. The main objective of this comparison is to select the most reliable satellite rainfall product(s) for stream flow simulation. The comparison is based on the mean annual cumulative histogram, a cumulative mass curve plot on daily time steps, double mass curve plot, biases and root mean square error (Figure 6.1, Figure 6.3, Figure 6.4 ,Figure 6.5, Table 6.1, Annex A, Annex B and Annex F).
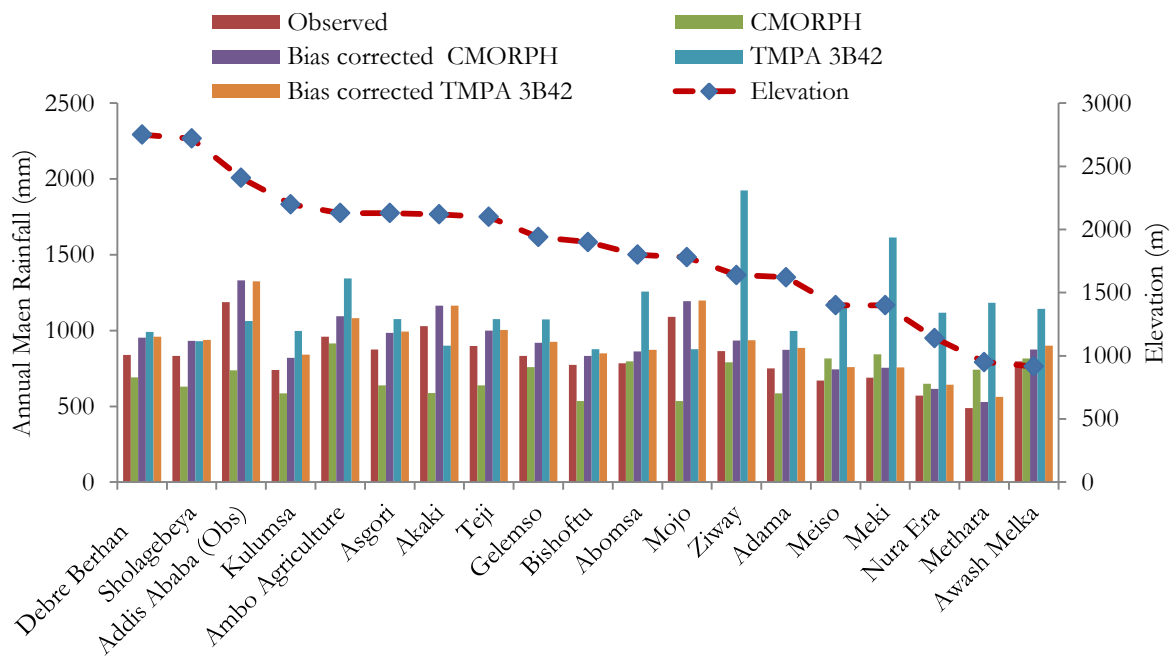
Figure 6.1 Comparisons of mean annual rainfall of CMORPH, TMPA 3B42, bias corrected TMPA 3B42, bias corrected CMORPH and observed rainfall

Figure 6.2 Shows that rainfall varies spatially with highest rainfall in the western region and lowest rainfall in the Eastern region. Similarly, from Figure 6.1 and Annex F it can be deduced that maximum and minimum precipitation are 916mm at Ambo Agriculture and 535mm at Mojo Stations for CMORPHH, while 1924mm at Ziway and 877mm at Bishoftu for TMPA 3B42, respectively. After bias correction the maximum and minimum precipitation are 1188mm and 488mm for observed, 1324mm and 562mm for bias corrected TMPA 3B42, while 1332mm and 529mm for bias corrected CMORPH all at Addis Ababa and Metehara, respectively. The analysis also shows that the precipitation estimate of remote sensing satellite depends on areas climatic condition. CMORPH under estimates precipitation at all stations except at Meiso, Meki, Awash Melka and Metehara stations where the temperature is relatively high and elevation is low. The over and underestimation is related to convective rainfall which is quite common in Ethiopia. When there is convective, rainfall within one pixel of satellite, there may be differences in rainfall intensity at each corner of the pixel. Hence, since the satellite gives an average value for the pixel it overestimates in areas of low rainfall intensity and underestimates in areas of high rainfall intensity, provided that the rain gauge stations are well organized for their areal representativeness. The result is the agrees with what Zeweldi et al. (2009); Koriche (2012) and Romilly et al. (2010) get in their analysis. TMPA 3B42 overestimates at all stations except at Addis Ababa, Akaki and Mojo stations where rainfall is higher than

at other stations (Figure 6.1). This result similar withIslam et al. (2005), who performed the TMPA 3B42 evaluation with rain gauge over Bangladesh. They concluded that TMPA 3B42 underestimates rainfall at stations having heavy rainfall. Even though it is difficult to generalize it is always the case the underestimation of TMPA 3B42 observed in this research is at the area of high rainfall relative to other stations too.
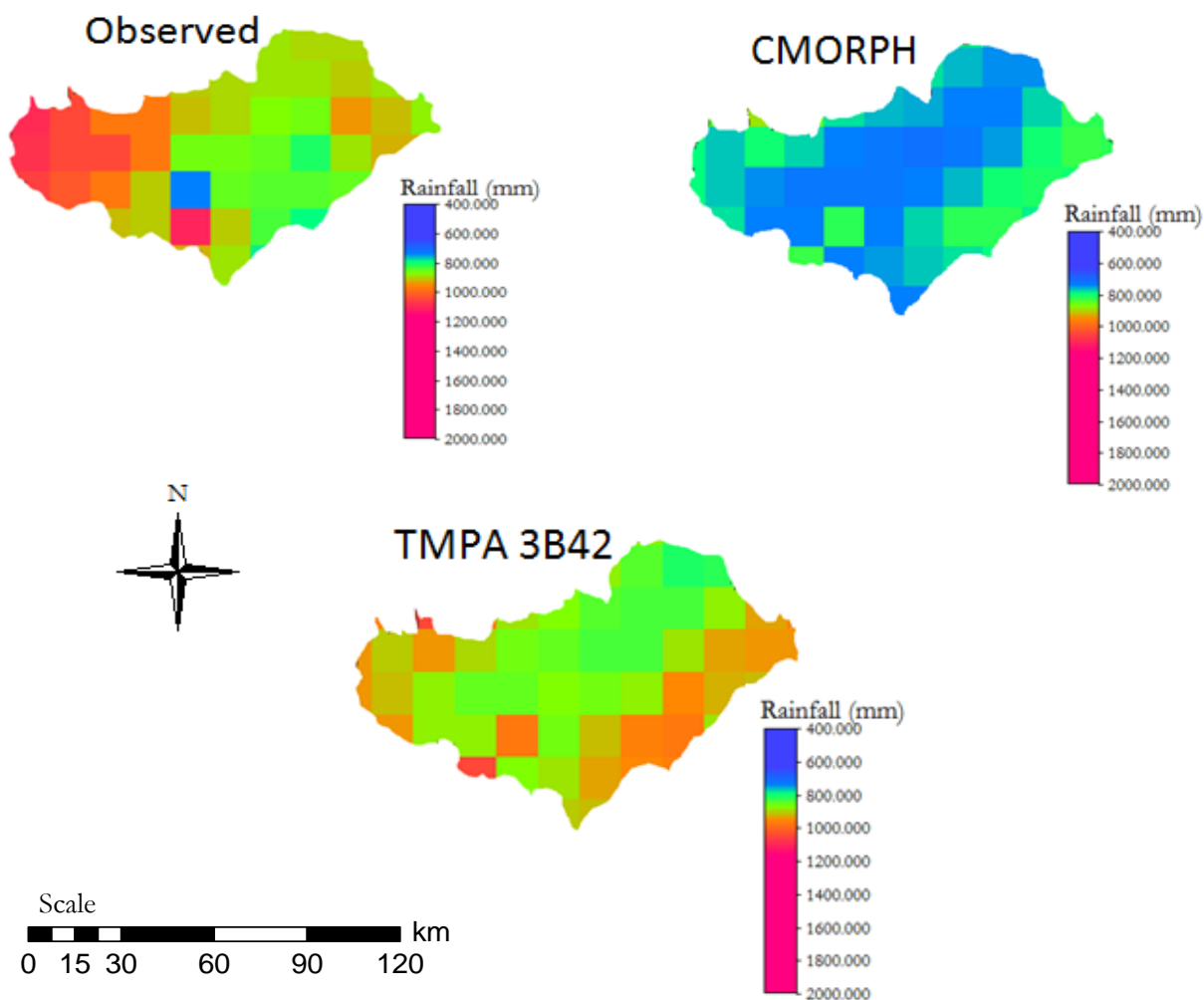
Figure 6.2 Annual Mean Rainfall of Observed, CMORPH and TMPA 3B42 in Upper and Middle Awash River Basin

If there is no error/ deviation between satellite-retrieved rainfall and the gauged rainfall, the accumulated rainfall mass curve will exactly match (Figure 6.5 and Annex B). However, since there is always uncertainty in remote sensing rainfall detection the exact match is not expected. This case is clearly shown in Figure 6.4, Figure 6.5, Annex A and Annex B. Figure 6.4 and Annex A shows accumulated mass curve of the satellite-retrieved rainfalls before and after bias correction and gauged rainfall for 2005-2010. These curves clearly indicate that due to accumulated deviation between the satellite-retrieved rainfall and gauged rainfall the gaps are high at the end of year 2010. Figure 6.5 and Annex B shows the double mass curves of satellite-retrieved rainfall before and after bias correction is applied. These curves also show that the offsets of accumulated deviation between satellites retrieved rainfall and gauged rainfall. Therefore, these two curves show that there is deviation between satellites retrieved rainfall products and gauged rainfall. Hence, to minimize errors bias correction applied.

Table 6.1 comparison of daily TMPA 3B42 and CMORPH with rain gauge measured rainfall using RMSE for 19 stations

Station Name	RMSE(mm/day)	
	CMORPH	TM PA 3B42
Debre Berhan	5.49	6.32
Shola Gebeya	5.38	6.57
Addis Ababa	8.36	8.34
Kulumsa	5.24	6.42
Ambo Agriculture	5.81	7.24
Asgori	5.41	7.13
Akaki	7.08	7.97
Teji	5.42	7.17
Gelemso	7.24	7.58
Bishoftu	5.63	7.24
Abomsa	6.56	7.95
Mojo	8.12	8.85
Ziway	7.39	8.25
Adama	6.99	7.86
Meiso	6.02	7.53
Meki	6.57	7.96
Nura Era	6.55	8.24
Metehara	5.54	7.1
Awash Melka	6.69	7.9
Mean	**6.39**	**7.56**

Furthermore, to assess deviations a root mean square error is applied (Table 6.1). Accordingly, the maximum RMSE are observed at Mojo as 8.85mm/day and at Addis Ababa 8.36mm/day for TMPA-3B42 and CMORPH, respectively. Similarly, the minimum RMSE are observed as 6.32mm/day at Debire Birehan and 5.24mm/day at Kulumsa for TMPA-3B42 and CMORPH, respectively. Generally, the RMSE is higher for TMPA-3B42 at all stations. That is TMPA 3B42 agrees less with rain gauge measured rainfall with mean RMSE of 7.56mm/day, Whereas CMORPH agree more with rain gauge measured than TMPA 3B42 with a mean RMSE of 6.39 (Table 6.1). In addition, CMORPH under estimate (2006-2010) and overestimate 2005 as compared to measured rainfall at Ambo Agriculture, whereas TMPA 3B42 overestimates over the entire study period (2005-2010) (Figure 6.4). On the other hand, both CMORPH and TMPA 3B42 overestimates rainfall at Meiso station and both underestimate rainfall at Addis Ababa station over the entire study period (2005-2010). For the remaining 15 stations, the result is shown as Annex A.

Bias Correction: Using different technique for error determination, the disagreements between observed and satellite rainfall data were assessed (see section 5.1.2). Prior to use a satellite derived rainfall data for stream flow simulation, bias correction has been applied. Three bias correction methods are applied for precipitation. These are hit, missed rain and false rain bias corrections (see section 5.1.2).

Hit bias correction (see Equation 5.4) is applied when there is rainfall recorded by rain gauge that also detected by satellite. Figure 6.3 shows that hit bias is negative for CMORPH at all stations showing that it under estimates rainfall when both detect rainfall. The maximum and minimum, men hit bias for CMORPH are -6.00mm at Mojo and -0.65mm at Metehara (Table 6.2), respectively. Similarly, the hit bias is positive for TMPA 3B42 at all stations except for Addis Ababa, Akaki, Mojo, Adama and Meki stations (Figure 6.3). This implies that TMPA 3B42 overestimates rainfall at those stations having positive hit bias and underestimates at stations having negative hit bias when both satellite and rain gauge record rainfall. Over all, the mean maximum hit bias is -3.36mm at Mojo and the minimum mean hit bias is -0.08mm at Debire Birehan for TMPA 3B42 (Table 6.2). The hit bias corrections are applied to fill gaps in satellite data sets using Equation 5.4.

The second bias correction applied is missed rainfall bias (see Equation 5.5). This bias occurs when there are rainfall records by rain gauge but not detected by satellite. The maximum mean missed rain biases are 10.31mm at Mojo and 10.82mm at Meki for TMPA 3B42 and CMORPH, respectively. While, the minimum mean missed rainfall biases are 3.38mm at Shola Gebeya and 1.37mm at Debire Birehan for

TMPA 3B42 and CMORPH, respectively (Figure 6.3 and Table 6.2). Since these data are missed from satellite data sets they are filled in back when bias correction applied.

The third and last bias correction applied is the false rainfall bias (see Equation 5.6), occurs when there are rainfalls records observed by the satellite but not really recorded by the rain gauges, hence they are false. The maximum and minimum false rain observed are 7.19mm at Nura Era and 1.67mm at Addis Ababa for TMPA 3B42, and 4.62mm at Awash Melka and 1.37mm at Debire Birehan for CMORPH, Respectively. The false bias is higher for TMPA 3B42 at all 19 stations (Table 6.2 and Figure 6.3). Since, these biases are falsely detected due to some algorithms by satellites they are excluded from satellite data sets when bias correction is applied.

In general after bias correction is applied the satellite retrieved rainfall shows good agreement with rain gauge recorded rainfall when observed as time series accumulated mass curve plot (Figure 6.4 and Annex A) and Double mass curve plot (Figure 6.5 and Annex B). These plots show consistent agreements of bias corrected satellite retrieved and observed rainfall data. However, since it is very difficult to remove all biases still there is small overestimation of satellite data sets as it can be seen from Figure 6.1 and Annex F.

Table 6.2 Mean Biases determined for satellite rainfall for 19 stations (2005-2010) within and around the study area

Station Name	Mean Hit Bias TMPA 3B42 (mm/day)	Mean Missed Rainfall Bias TMPA 3B42 (mm/day)	Mean False Rainfall Bias TMPA 3B42 (mm/day)	Mean Hit Bias CMORPH (mm/day)	Mean Missed Rainfall Bias CMORPH (mm/day)	Mean Missed Rainfall Bias CMORPH (mm/day)
Ambo Agriculture	1.13	4.88	2.93	-1.95	4.58	2.71
Asgori	1.19	5.46	3.85	-2.96	4.28	2.28
Teji	0.78	4.86	4.62	-3.38	3.60	3.02
Addis Ababa	-2.06	6.43	1.67	-3.98	6.06	1.40
Akaki	-0.64	8.04	4.35	-5.11	6.86	2.49
Bishoftu	0.88	4.84	5.48	-2.83	4.42	1.86
Mojo	-3.36	10.31	5.11	-8.41	7.60	2.20
Adama	-1.85	6.98	3.81	-5.09	6.50	2.44
Kulumsa	1.13	4.49	2.81	-1.97	3.89	1.79
Meki	-3.03	9.66	4.27	-6.00	10.82	2.89
Ziway	0.68	6.59	4.64	-3.07	5.69	2.63
Meiso	0.51	7.83	5.81	-1.92	8.12	3.60
Gelemso	0.37	3.90	6.69	-1.99	4.14	4.35
Awash Melka	0.75	5.45	5.54	-2.24	4.65	4.62
Metehara	2.99	5.30	4.67	-0.65	3.02	3.06
Abomsa	0.48	4.03	3.32	-2.30	4.61	2.22
Nura Era	1.28	8.13	7.19	-2.90	8.01	3.95
Debre Berhan	0.08	3.84	1.71	-2.46	2.78	1.37
Shola Gebeya	0.39	3.38	3.01	-2.46	2.53	1.76
Maximum	**-3.36**	**10.31**	**7.19**	**-6.00**	**10.82**	**4.62**
Minimum	**0.08**	**3.38**	**1.67**	**-0.65**	**2.53**	**1.37**
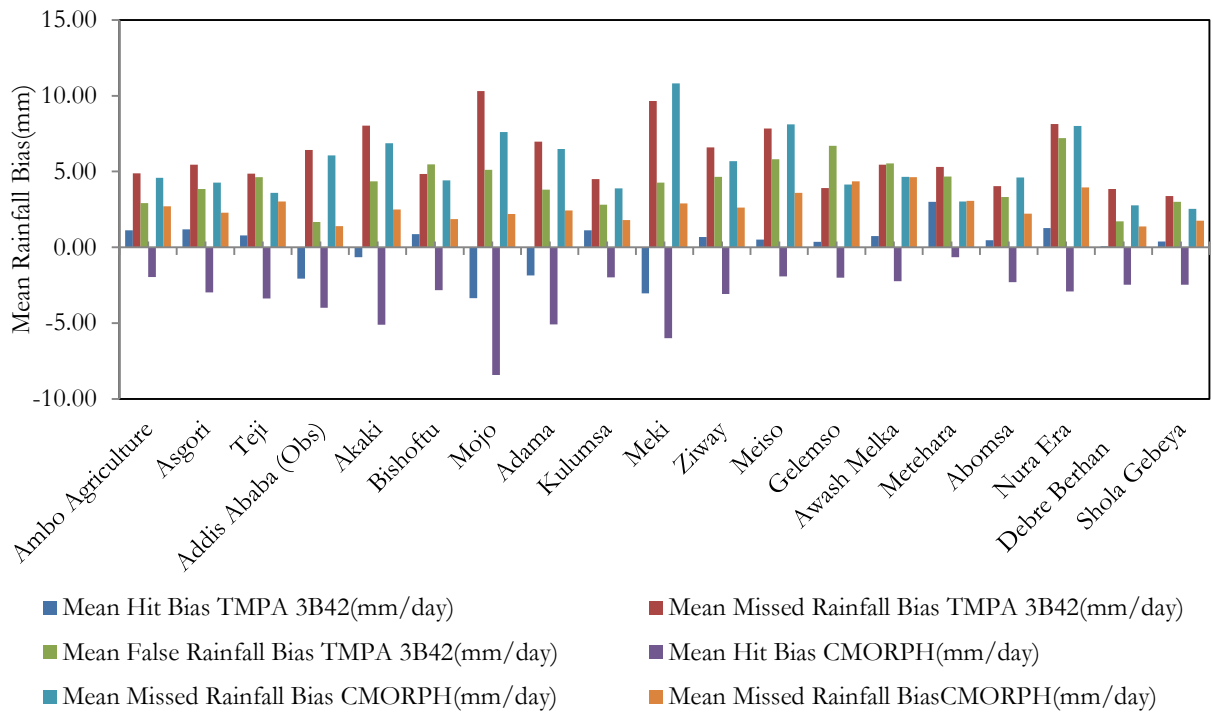
Figure 6.3 Mean Biases determined for TMPA 3B42 and CMORPH rainfall for 19 stations since 2005-2010 on daily bases.
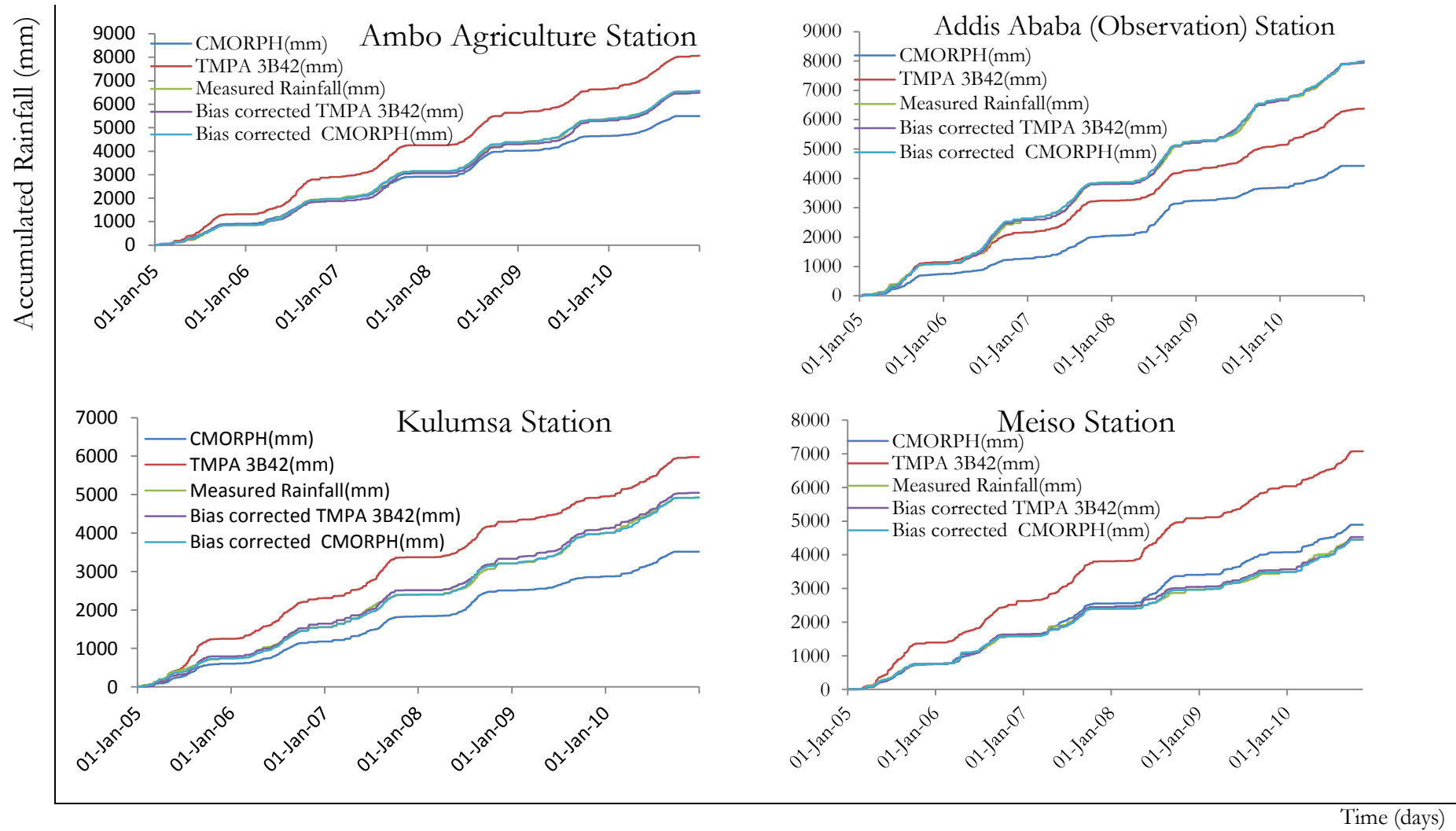
Figure 6.4 Cumulative mass curve of CMORPH, TMPA 3B42, Bias corrected CMORPH, Bias corrected TMPA 3B42 and measured rainfall.
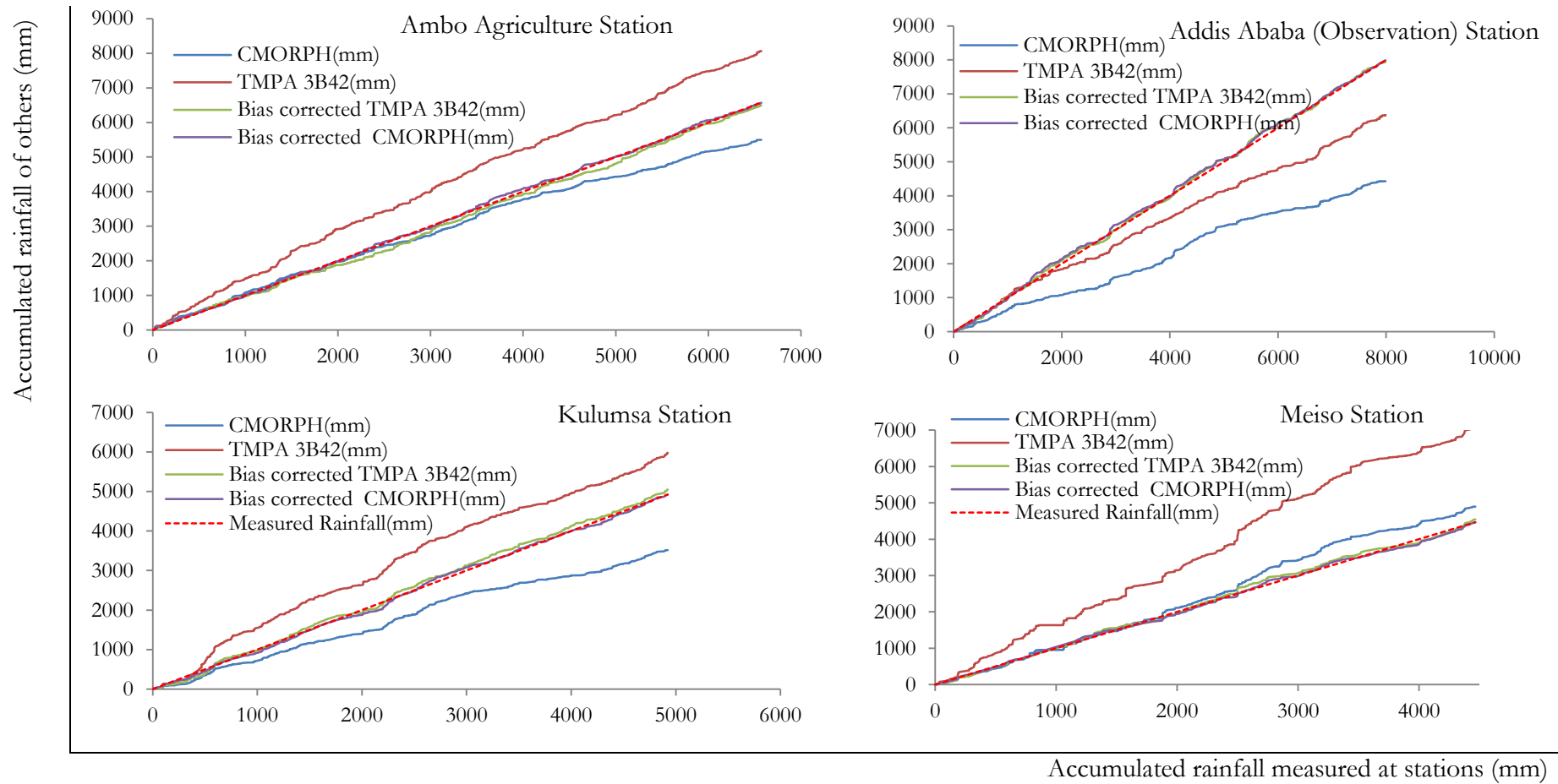
Figure 6.5 Double mass curve of CMORPH, TMPA 3B42, Bias corrected CMORPH, B ias corrected TMPA 3B42 and measured rainfall

6.2. Evapotranspiration (ET) Analysis

The potential evapotranspiration (PET) calculated based on Penman-Monteith formula is required as input variable for HBV-96 model set up (Lindström et al., 1997) is obtained from FEWS NET Global PET. However, before using it was evaluated for errors. As described in sub section 5.1.3 the daily FEWS NET retrieved PET is compared with daily in-situ evapotranspiration calculated using meteorological data collected from NMA, Ethiopia. The comparison was based on a daily time series plot of ETO and FEWS NET Global PET with respect to the mean of ETO (Figure 6.6 and Annex D) and double mass curve (Figure 6.7 and Annex E). Furthermore, its consistency was evaluated using root mean square error (RMSE), Mean Bias, Relative Bias and Relative Absolute Bias (Table 6.3). Accordingly, the Maximum and minimum RMSE are 2.15mm/day and 1.09mm/day at Adama and Akaki stations, respectively. Similarly, Maximum and minimum values of mean bias -1.80mm/day at Adama and -0.2mm/day at Meiso, Relative bias -39.87% at Adama and -5.43% at Ambo Agriculture and absolute relative bias is 41.07% at Adama and 22.80% at Akaki stations, respectively (Table 6.3).   In general the overall mean are 1.50mm/day, -0.47mm/day, -10.21% and 29.76% for RMSE, mean bias, relative bias and absolute relative biases, respectively. From these indicators and the graph (Figure 6.6, Figure 6.7, Annex D and Annex E) it can be concluded that there are gaps or differences between in-situ and FEWS NET estimated Evapotranspiration, hence bias correction is applied.

For bias correction, the concept of mean ratio is applied (Equation 5.17). That means if both data sets are giving the same result, their mean ratio will be unity. Using this concept, the FEWS NET PET is multiplied by mean ratios of in-situ ETO and FEWS NET PET. After bias correction the error offsets are minimized as expected (Figure 6.6 and Figure 6.7). The double mass curve (Figure 6.7 Annex E) shows a linear pattern with slope of unity and the daily time series plot also shows the FEWS NET retrieved PET is undulating around mean values of ET_O as similar as ET_O (Figure 6.6 and Annex D), which clearly indicates that biases are minimized. Hence, the bias corrected FEWS NET PET estimate is used as input for the HBV model.

Table 6.3 RMSE, Mean Bias, Relative Bias (%) and Absolute Relative Bias (%) for Evapotranspiration consistency evaluation

Station Name	RMSE (mm/day)	Mean Bias(mm/day)	Relative Bias (%)	Absolute Relative Bias (%)
Abomsa	1.66	-0.86	-21.78	33.47
Akaki	1.09	0.50	13.22	22.80
AMBO Agriculture center	1.11	-0.20	-5.43	23.02
Kulumsa	1.47	-0.88	-24.58	33.34
Meiso	1.24	0.34	8.00	22.95
Methara	1.36	-0.52	-10.81	21.81
Adama	2.15	-1.80	-39.87	41.07
Nura Era	2.13	-1.55	-33.40	37.71
Addis Ababa	1.32	0.78	22.75	31.65
Mean	**1.50**	**-0.47**	**-10.21**	**29.76**
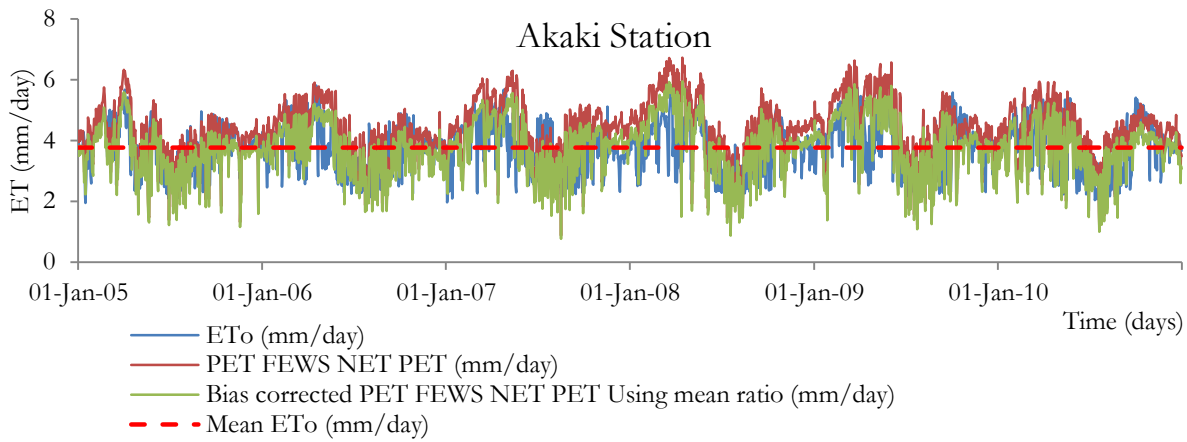
Figure 6.6   Time Series Plot of ET$_O$, FEWS NET PET, and Bias corrected FEWS NET PET
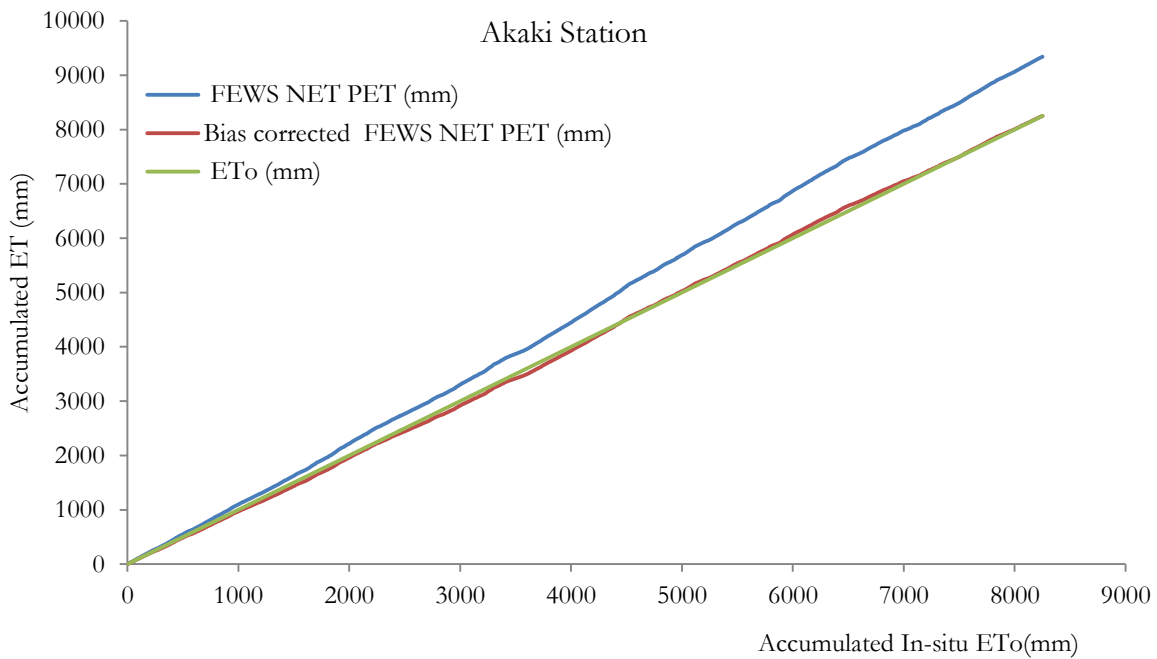
Figure 6.7   Double mass curve of ET$_O$, FEWS NET PET and Bias corrected FEWS NET PET

6.3.   HBV Model Calibration Result

After warming up the model for the year 2005, the model calibration for the period of 2005-2008 is performed manually by trial and error changing one model parameter at a time. To evaluate the model performance visual inspection of hydrograph fits between the observed and the simulated stream flow with combination of the objective functions NSE and RVE are used. Visual inspection helps to assess whether the simulated and observed hydrographs are matching. As discussed under section 5.2 the NSE is used to evaluate the overall fit between simulated and observed discharge at the catchment outlet and the model parameter optimization is stopped when higher NSE value is reached, i.e no more increment of NSE value when MP value increased or decreased rather decreases (see Figure 6.9). Finally the sets of parameters that are performing best are adopted.   The model parameters for higher NSE of four calibrated catchments are shown as Table 6.4.

Table 6.4 Prior model parameter range, default model parameter and optimized model parameter of Upper and Middle Awash River Basin after model calibration.

Model Parameters	Prior Model Parameter range		Optimized model parameter			
	Lake Tana Basin, Ethiopia	Scandinavian Countries	Melka Kunture	Akaki	Hombole	Mojo
α(Alfa)	0.1 - 3	0 - 1.5	0.672	0.005	0.144	0.008
β (Beta)	1-4	1-4	1.377	1.6	1.8	1.6
Cflux	0 - 2	0 - 2	0.5555	0.12	1	0.7
FC	100 - 800	100 - 1500	948	510	120	888
K4	0.0005 - 0.15	0.001 - 0.1	0.00004	0.0005	0.000005	0.00002
Khq	0.0005 - 0.15	0.005 - 0.5	0.08	0.044	0.22	0.09
LP	0.1 - 1	<=1	0.8	0.5	1	0.73
perc	0.1 - 2.5	0.01 - 6	1.55	2.35	0.01	0.9
NSE			**0.852**	**0.689**	**0.897**	**0.858**

Note: The prior model parameter range are taken from Rientjes et al. (2011) and Perera (2009) for Lake Tana Basin, Ethiopia and from SMHI (2008) manual version 6.2 for Scandinavian Countries.

As shown in Table 6.4 some of optimized model parameter for Upper and Middle Awash River Basin are not within a parameter space of Lake Tana Basin, Ethiopia. For example, Alfa prior model parameter space is 0.1 to 3, but the optimized Alfa for Upper and Middle Awash river Basin shows 0.005 and 0.008 for Akaki and Mojo catchments, respectively. Similarly, FC is out of range for Melka Kunture and Mojo and Perc is out of range for Hombole Catchment. On the same way, K4 which controls the base flow is lower than the minimum model parameter of both Lake Tana Basin and Scandinavian countries for all of the catchments except Akaki. This is may be due to the base flow is very low (see Figure 6.8) and furthermore, Since Awash River Basin and Lake Tana Basin has their own physical catchment characteristics, these model parameters space variations are expected. On other hand even though it is hardly possible to compare model parameter space of catchments in different countries that are far apart, the optimized model parameters which are out of range as compared to Lake Tana Basin are within parameter space of Scandinavian Countries except K4. Hence, the model parameters space for Upper and Meddle Awash rive could be determined using more detailed analysis and it is difficult to handle in this research due to time constraint.

6.4.   Comparison of Stream Flow Simulated

The model parameters are optimized using rain gauge measured data as input for HBV-96. That is the model is first calibrated using rain gauge measured rainfall to establish model parameters. Second, the bias corrected satellite retrieved rainfall data are used. To have better understanding thirdly, satellite data without bias correction is used as input to HBV-96. The results of stream flow simulated with all and observed stream flow results are shown as Figure 6.8 for comparison. The main objective of the comparison is to assess, the satellite rainfall which is better for stream flow simulation in Upper and Middle Awash River Basin.

First the stream flow simulation result using rain gauge measured rainfall data set is discussed. As shown in a model calibration using observed rainfall result in NSE greater than 0.8 for the three catchments, except at Akaki catchment with a NSE equal to 0.69. In addition, Figure 6.8 clearly indicates that the

hydrograph shapes of the simulated and the observed stream flow at the outlet of Hombole catchment is matching. The recession and base flow are well represented, but the peak flow is not. Particularly the deviation is clearly visible for 2007. The deviation may be the result of observation error during measurements or from model uncertainty (see section 5.2.1). Such errors are difficult to correct unless the observer him/herself correct it. Hence, there is no any correction applied for these errors. Effects of this error however, are relatively negligible.

The second discussion focuses on inter comparison of stream flow simulation using three rainfall data sets. From Table 6.5 and Figure 6.8 it is clear that the stream flow simulation using bias corrected satellite retrieved rainfall perform resemble to stream flow simulation using rain gauge measured rainfall. The stream flow simulation using the rain gauge measured rainfall outperforms well which can be considered as best model since NSE is 0.8 to 0.9 and RVE is -5% to 5% (Table 6.5). Whereas, the stream flow simulation using bias corrected TMPA 3B42 and CMORPH perform well, they are considered as moderate performing model since NSE is 0.6 to 0.8 (Table 6.5). While comparing capability of both bias corrected satellite retrieved rainfall the CMORPH outperforms TMPA 3B42 with NSE of 0.752 during models calibration and 0.72 during model validation, whereas bias corrected TMPA 3B42 has NSE of 0.735 during model calibration and 0.671 during model validation. The RVE of both bias corrected TMPA 3B42 and CMORPH are -7.621% and -6.293% during model calibration and -9.50% and -8.59% during model validation, respectively. Hence, the results indicate a moderately performing model after proper model calibration is performed. On the other hand, the original TMPA 3B42 and CMORPH show poor capability of stream flow simulation (Table 6.5 and Figure 6.8)

Table 6.5 Model Calibration results using different rainfall data sets for stream flow simulation at Hombole catchment

Activity	Objective Function	Rain gauge	Bias corrected TMPA 3B42	Bias corrected CMORPH	TMPA 3B42	CMORPH
Calibration	RVE (%)	-1.78	-7.62	-6.29	-47.38	-51.34
	NSE	0.897	0.735	0.752	0.385	0.391
Validation	RVE (%)	2.08	-9.50	-8.594	-53.17	-56.81
	NSE	0.876	0.671	0.720	0.2044	0.2981
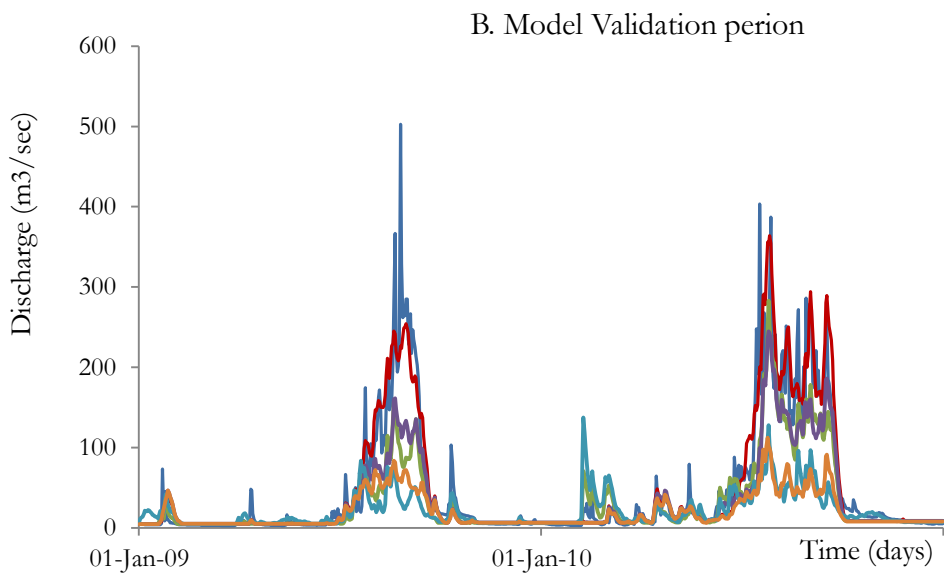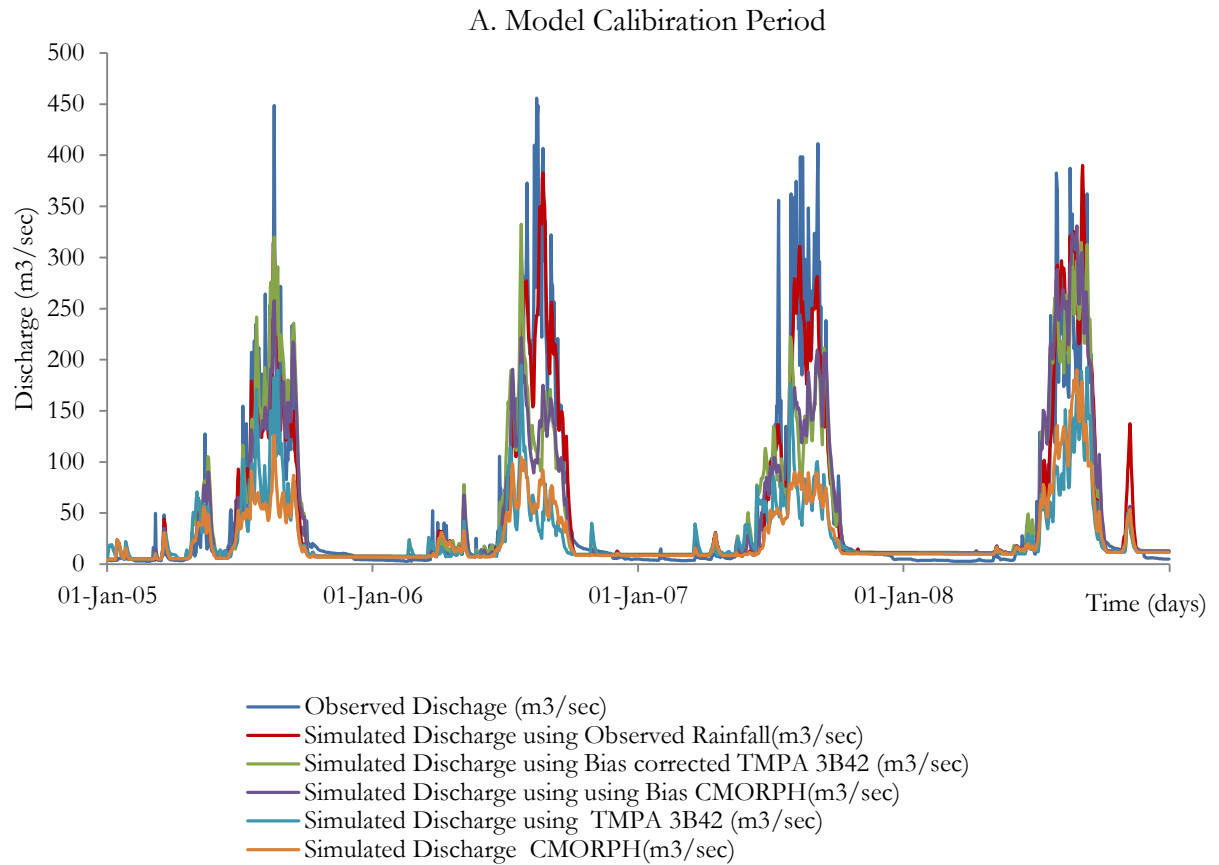
Figure 6.8 Stream flow simulated using observed rainfall, CMORPH and TMPA 3B42 and bias corrected CMORPH and TMPA 3B42 at Hombole outlet.

6.5.   Sensitivity Analysis

To have better understanding on the effect of each model parameter, a sensitivity analysis was applied during model calibration. The sensitivity analysis were applied by changing the values of one model parameter at a time (Aghakouchak et al., 2012). That is the value of each model parameter is increased and decreased up to 60% by 20% interval. For the first 20% model parameter increment and decrement the

NSE value change is within tolerable range (Figure 6.9). Hence the Model parameter space can be established by adding 20% to the highest respective model parameter and deducting 20% from the minimum respective model parameter. The effect of each model parameter was analyzed based on objective functions NSE and RVE using graphical plot for visualization and the results are shown as Figure 6.9. The main idea of sensitivity analysis is to select the most effective model parameter for model calibration. Those model parameters having steep slope are considered as most sensitive while those having moderate to gentile slope are considered as less sensitive. The most sensitive model parameters are FC, Perc, Beta, LP and Khq, while the less sensitive model parameters are Alfa, K4 and Cflux (see Figure 6.9), similarly Perera (2009) found FC, Beta, KF and LP as sensitive model parameter, Badilla, 2008 also found FC and Khq as sensitive model parameter and Abebe et al., 2010 also showed FC, Beta, LP and Perc are sensitive HBV model parameter.

Field capacity (FC) has an effect on partitioning precipitation into soil moisture and runoff. As shown in Equation 4.1 when FC increase the recharge (R) decreases. When recharge increases the upper reservoir zone storage depth (UZ) increases, which results in quick runoff increases (Equation 4.4). Therefore, when FC increased the soil storage will increases; hence the amount of water available for quick runoff generation is decreased. Figure 6.9 also shows as field capacity increases the RVE become more negative showing that the volume of simulated runoff is decreasing and when it decreases RVE become more positive showing the volume of simulated runoff is increasing.

Similarly, Beta controls the response function of (ΔQ/ΔP or R/IN) which is normally called runoff coefficient or an increase of soil moisture (1- R/IN)(SMHI, 2008). Equation 4.1 shows as Beta increases the soil moisture increase and the reverses are true when decreased which results decrease in simulated stream flow volume. The effect of Beta on simulated stream flow is shown as Figure 6.9. Figure 6.9 shows that as Beta increases the RVE become more negative and as Beta decreases RVE become more positive. Hence, the peak flow may be well represented with low value of Beta and the base flow will be less since much runoff is generated and less water will be stored during rainy seasons.

On other hand, Equation 4.3 shows the relation between limit for potential evapotranspiration (LP) and actual evapotranspiration. As LP increases the amount of water depleted as evaporation decreases and the volume of simulated stream flow will increases. This effect is clearly shown in Figure 6.9 that shows as LP increases the RVE increase and vice versa, showing that they are positively related. Hence, the LP has positive impact on simulated stream flow volume.

The recession coefficient for upper zone reservoir (Khq) control the recession during peak flow from the upper reservoir zone with Alfa, whereas the recession coefficient for lower reservoir(K4) control the recession during low flow from the lower reservoir zone (Equations 4.4 and 4.5). Alfa control shape of the hydrograph. Figure 6.9 shows that, RVE increases as Khq increases showing that it has positive impact on volume of stream flow generated. The increase in Alfa and K4 shows no significant change on NSE and RVE which indicate that they are less sensitive. At last, Perc and Cflux show the percolation to lower zone reservoir and capillary rise coefficient from lower zone reservoir, respectively. Perc will result in an increase in delayed runoff and decreases the peak flows, since it controls the flow from the upper zone reservoir to the lower zone reservoir storage. Hence, the lower reservoir will contain more water and release it during the low flow season, whereas the Cflux represents a rise of water from lower zone (Equation 4.5), hence it affects the base flows.
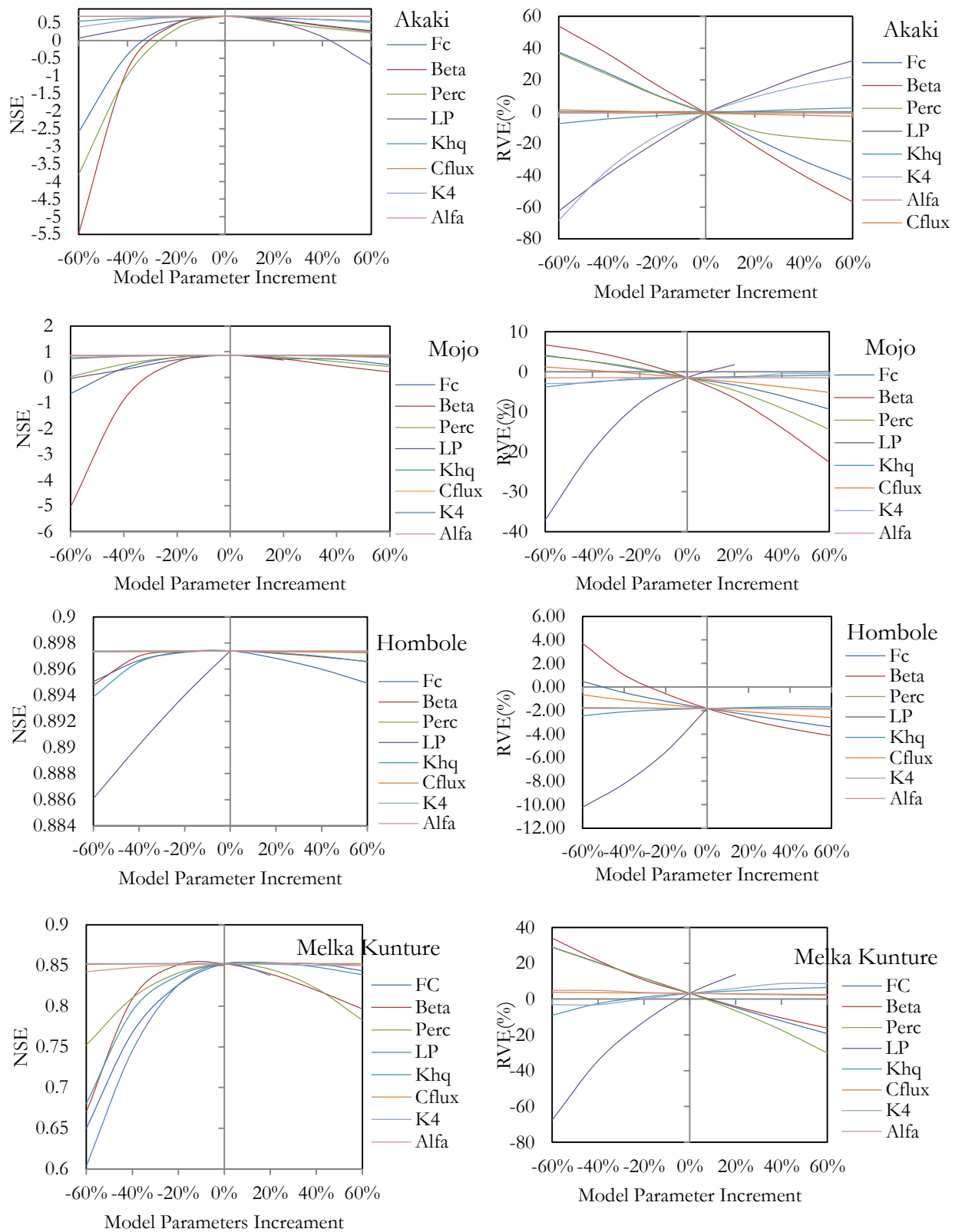
Figure 6.9 Model Parameter sensitivity analysis plots

6.6. Regionalization Model Results

Simple regression results:

As it was described in section 5.5 the correlation coefficients (r) greater than 0.90 or less than -0.90 are considered statistically significant and the results are shown as (Table 6.6) in bold. The core idea of why simple regression applied is to see the relation between model parameter and physical catchment characteristics. The optimized MPs (Table 6.4) and PCCs (Annex G) of gauged catchments are used to determine the correlations. Accordingly, the simple regression showed that the correlation between PCCs and MPs is found for 23 out of 184 relations (Table 6.6). As shown in (Table 6.6) Field capacity (FC) has negatively correlated with circularity index (CI) which is calculated as catchment perimeter square divided by catchment area. In addition, LP is positively correlated with LUV and negatively correlated with SHAPE which is calculated as maximum elevation minus minimum elevation divided by square root of catchment area. The recession coefficient (K4) shows positive correlation with GRASS, MCROP, URBAN, AV. SLOPE and EL, while negative correlation with LUV, LFP and DCROP. Khq positively correlated with CI and negatively correlated with PET and SHAPE. Similarly, the correlation of others is shown in (Table 6.6)

Table 6.6 Correlation values of model parameter and physical catchment characteristics with statistically significant values shown as bolded

PCCs	FC	LP	K4	Khq	Perc	Alfa	Beta	C$_{flux}$
CHR	0.16	-0.80	0.88	-0.74	**0.94**	0.10	-0.46	**-0.94**
EUTR	0.13	-0.51	0.64	-0.55	0.79	0.46	-0.56	-0.74
LEPT	0.44	-0.85	0.76	-0.89	**0.99**	0.20	-0.67	**-0.96**
LUV	-0.22	**0.92**	**-0.92**	0.82	**-0.97**	0.08	0.42	**0.99**
VERT	-0.23	0.40	-0.49	0.52	-0.73	-0.62	0.67	0.65
DCROP	0.30	0.77	**-0.99**	0.46	-0.69	0.48	-0.13	0.80
FOREST	-0.38	0.62	-0.61	0.72	-0.88	-0.48	0.73	0.81
GRASS	-0.24	-0.74	**0.97**	-0.50	0.77	-0.24	-0.03	-0.84
MCROP	-0.15	-0.84	**1.00**	-0.59	0.80	-0.36	-0.04	-0.89
URBAN	-0.13	-0.88	**0.99**	-0.60	0.77	-0.50	0.03	-0.87
SAAR	0.17	-0.15	0.27	-0.31	0.53	0.77	-0.63	-0.43
MPWET	0.41	-0.27	0.26	-0.50	0.63	0.79	-0.80	-0.52
MPDRY	-0.53	0.48	-0.06	0.49	-0.18	0.53	0.09	0.21
PET	0.63	-0.89	0.53	**-0.90**	0.73	-0.33	-0.43	-0.74
AREA	0.58	0.15	-0.30	-0.24	0.22	**0.98**	**-0.93**	-0.05
LFP	0.25	0.67	**-0.93**	0.45	-0.75	0.12	0.08	0.81
MDEM	0.48	-0.53	0.48	-0.71	0.83	0.60	-0.82	-0.74
HI	-0.67	0.44	0.04	0.53	-0.19	0.37	0.24	0.19
AV.SLOPE	-0.35	-0.68	**0.96**	-0.39	0.69	-0.30	0.08	-0.77
SHAPE	0.52	**-0.98**	0.73	**-0.94**	0.88	-0.28	-0.45	**-0.90**
CI	**-0.92**	0.69	-0.26	**0.93**	-0.75	-0.27	**0.92**	0.66
EL	0.04	-0.80	**0.92**	-0.68	**0.91**	0.00	-0.34	**-0.93**
DD	-0.43	0.64	-0.60	0.76	**-0.90**	-0.47	0.76	0.83

Multiple Regression Result: Multiple regressions applied here to establish the regional model using MPs of gauged catchment (Table 6.4) and PCCs of gauged catchments (see Annex G). It is applied using a stepwise regression method, entering one MP and all expected PCCs to the model. As described in sub

section 5.5 depending up on the tolerance and VIF values the PCCs are selected to establish the regression equation. Each model parameter in relation with regression analysis is shown in Table 6.6 and discussed:

Field Capacity (FC): According to the multiple regressions, FC got best co-linearity with circularity index (CI) and moderately cropped (MCROP) (Table 6.7). The result shows that the tolerance level is 0.94 and VIF 1.06, which are approximately 1. Hence, the stepwise regression stopped and the regression equation is established. The other important issue is hydrological relation of FC, CI and MCROP are also considered as hydrologically meaning full and affect the hydrological responses. However, FC got high correlation coefficient with HI in (Rientjes et al., 2011) and with Arable and HIGHP in (Deckers et al., 2010) who apply regionalization in Lake Tana, Ethiopia and Wale Basin, UK basins, respectively.

Limit for Potential Evapotranspiration (LP): The limit for evapotranspiration shows high co-linearity with SHAPE. So no more PCCs is required to improve the co-linearity hence the stepwise regression stopped and the regression equation is established for LP using SHAPE with tolerance of 1.00 and VIF of 1.00. However, the hydrological relation of SHAPE with LP is questioned, the regression equation is established provided that MPs may have indirect relation.

Beta: The multiple regressions showed that the empirical coefficient model parameter Beta has best co-linearity with circularity index (CI) and catchment area (AREA) with a tolerance 0.80 and VIF 1.26. From hydrological point of view, Beta will be affected largely by geography and geomorphology. Hence, the PCCs co-linearity found here are feasible and the regression equation is derived

Alfa: The regression analysis shows the non-linearity response Alfa showed best co-linearity with catchment area (AREA) and circularity index (CI). Alfa is a response function for quick runoff. Hence, the statically found PCCs are hydrologically acceptable, i.e the larger the area and more circular high quick responses. The regression shows tolerance of 0.80 and VIF of 1.26. Therefore, the regression is accepted and the regression equation is established.

K4: The K4 is a recession coefficient response for delayed runoff. The regression statistics show high co-linearity with moderately cropped (MCROP) with tolerance of 1.00 and VIF of 1.00. Hence, the regression equation is established using MCROP.

Khq: is a recession response during peak flow. It is highly dependent on geo-physiology and geography. According to multiple regression analysis, Khq showed best co-linearity with SHAPE and AREA with a tolerance 0.99 and VIF 1.01. Hence, the regression result accepted and its equation is established.

Percolation (Perc): The rainfall infiltrated either depleted as quick runoff or deep percolate. However, this mainly depends on soil texture and structure. If the soil infiltration rate is less than the rainfall intensity the some part of rainfall will cause the direct runoff. The infiltrated rainfall also depends on vertical and horizontal hydraulic conductivity. In general, term the water movement in soil governed by soil texture. The regression result also shows that Perc is best co-linear with Leptosoil (LEPT) with tolerance of 1.00 and VIF 1.00. Therefore, the regression result accepted and its regression equation is established.

Capillary Rise coefficient (C_{flux}): The C_{flux} is a model parameter, which used to correct water rise in the form of capillary through soil matrix. Therefore, the main deriving forces for capillary rise are soil structure and available film of water on soil matrix. According to the regression analysis, the C_{flux} showed

best co-linearity with Luvicsoil (LUV) with a tolerance of 1.00 and VIF of 1.00. The regression result is accepted and its regression equation is established.

Table 6.7 The regional model for MPs and PCCs links.

	Coefficients		t-stat	Sig.	90.0% Confidence Interval		Co-linearity Statistics	
	β	Std. Error			Lower Bound	Upper Bound	Tolerance	VIF
FC = βo+β1*CI+β2*MCROP								
β0	1908.815	1.534	1244.70	0.001	1899.132384	1918.50		
β1	-36.699	0.043	-860.65	0.001	-36.96795347	-36.43	0.94	1.06
β2	-122.473	0.364	-336.30	0.002	-124.7721316	-120.17	0.94	1.06
LP= β0+β1*SHAPE								
β0	1.1700594	0.063	18.54	0.003	0.898571783	1.44		
β1	-0.0174897	0.002	-7.10	0.019	-0.028083066	-0.01	1.00	1.00
Beta= β0+β1*CI+β2*AREA								
β0	1.41302	0.040	35.01	0.018	1.1581716	1.667859		
β1	0.01000	0.001	10.84	0.059	0.0041770	0.015822	0.80	1.26
β2	-0.00006	0.000	-9.74	0.065	-0.0000982	-0.000021	0.80	1.26
Alfa= β0+β1*AREA+β2*CI								
β0	-0.53693	0.005	-118.91	0.005	-0.5943029	-0.479555		
β1	0.00021	0.000	310.73	0.002	0.0002040	0.000221	0.80	1.26
β2	0.00654	0.000	63.43	0.010	0.0052331	0.007855	0.80	1.26
K4= β0+β1*MCROP								
β0	0.00001	0.000	1.68	0.235	-0.0000146	0.000033		
β1	0.00021	0.000	47.63	0.000	0.0001890	0.000227	1.00	1.00
Khq= β0+β1*SHAPE+β2*AREA								
β0	0.30068	0.006	49.90	0.013	0.2241233	0.377246		
β1	-0.00649	0.000	-35.01	0.018	-0.0088443	-0.004134	0.99	1.01
β2	-0.00002	0.000	-11.80	0.054	-0.0000327	0.000001	0.99	1.01
Perc= β0+β1*LEPT								
β0	-0.57716	0.203	-2.85	0.104	-1.4489614	0.294634		
β1	0.14475	0.015	9.73	0.010	0.0807637	0.208730	1.00	1.00
Cflux = β0+β1*LUV								
β0	0.10429	0.053	1.95	0.190	-0.0515779	0.260156		
β1	0.03130	0.003	10.90	0.008	0.0229183	0.039689	1.00	1.00

6.7. Regional Model Validation

The main idea of regionalization is to estimate the stream flow of ungauged catchments. Two regionalization approaches are used to establish model parameter of ungauged catchments. These are the sub basin mean and physical catchment characteristics similarity (regional model). The model parameter estimated using regional model is shown as Table 6.8 and the catchment with its sub-catchment code is shown as Figure 6.11. Before using the established model parameters have to be evaluated for their predicting capability using independent gauged stream flow. For this research one gauging station at Melka

Werer which includes all the ungauged catchments and located at the end of downstream of the study area is used. According to the regionalization validation result shown in Figure 6.10 the stream flow estimated based on model parameter determined based on regional model validation result shows the peak runoff is over estimated and recession part of the hydrograph is well represented. Furthermore, the evaluator indicators NSE = 0.64 and RVE = 1.96% are obtained, which shows that the model is moderately performing and the positive sign of RVE indicates the simulated stream flow is overestimated. The peak flows are overestimated due to the fact that during rainy season water is harvested and stored by series of hydraulic structures. The result shows the model is performing moderate due to the base flow is much affected during dry season since the head regulators at Metehara, Kessem Irrigation Project and Koka Dam releases the stored water during rainy season and the simulated stream base flow is under estimated. Therefore, the regional model is validated as moderate performing model. While the validation result from sub basins mean shows that it has less predicting capability with NSE = 0.25 and RVE =-53.81%. The sub basin mean method is not successful due to the fact that the ungauged catchments are located at downstream whereas the gauged catchments are located at upstream. Hence, the sub basins mean approach is not effective for Awash River Basin stream flow simulation of ungauged catchments.
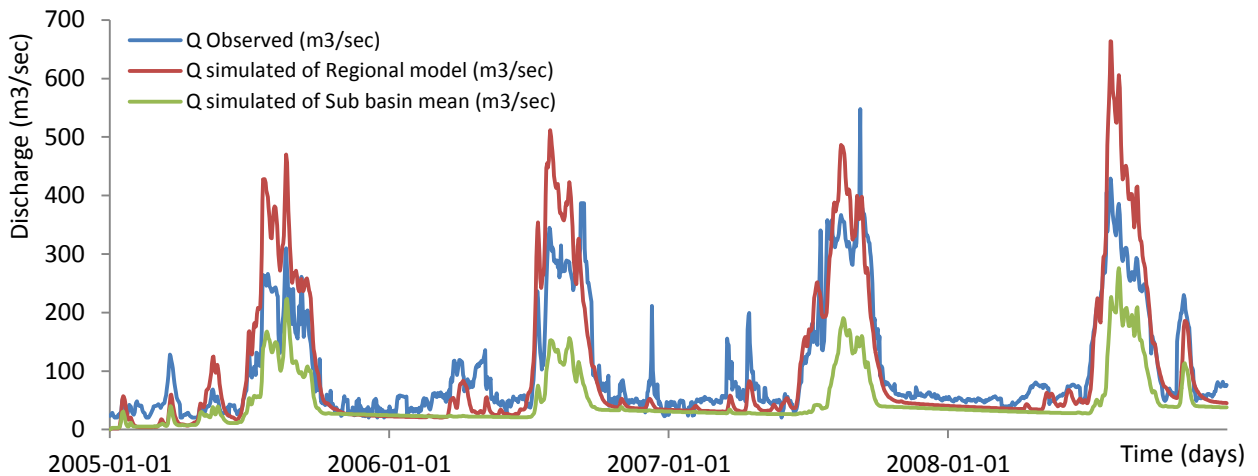

Figure 6.10 Regionalization model Validation Result.
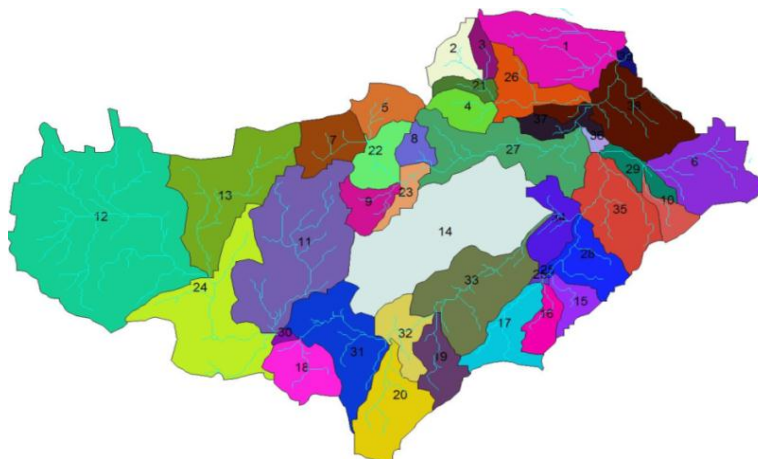
Figure 6.11 Upper and Middle Awash River Basin Catchments Code used

Table 6.8. Model parameter estimated for ungauged catchments using regional Model

Catchments	Sub-Catchment Code[1]	Model Parameters							
		α(Alfa)	β (Beta)	C_{flux}	FC	K4	Khq	LP	perc
Jimjams	18	0.22	1.51	1.02	963.91	0.00001	0.0710	0.67	3.61
Wonji	31	0.10	1.61	0.81	749.60	0.00001	0.0544	0.59	0.10
Keleta	20	0.10	1.52	0.10	1027.26	0.00001	0.0083	0.48	2.51
Kela	32	0.10	1.66	0.10	587.97	0.00001	0.1000	0.71	1.65
Wolenchiti	19	0.10	1.57	0.49	861.50	0.00001	0.0749	0.65	1.87
Metehara	33	0.12	1.40	0.10	120.00	0.00213	0.0606	0.63	2.61
Abomsa	17	0.12	1.68	0.10	520.44	0.00001	0.1020	0.72	1.55
	16	0.10	1.54	0.10	588.74	0.00066	0.0500	0.59	2.07
	15	0.15	1.55	0.10	267.03	0.00108	0.1500	0.86	1.82
	25	0.15	1.54	0.10	182.22	0.00126	0.1637	0.90	2.21
	28	0.15	2.24	0.10	250.00	0.00191	0.0800	0.60	0.78
	35	0.12	1.49	0.10	1030.89	0.00012	0.1200	0.79	1.24
Fentale	34	0.08	2.17	0.10	120.00	0.00611	0.1895	0.89	0.01
Arba	10	0.10	1.66	0.10	597.93	0.00001	0.1012	0.71	0.65
	29	0.10	1.80	0.10	115.00	0.00009	0.1012	0.70	2.71
	6	0.01	1.52	0.10	172.83	0.00159	0.0115	0.47	2.16
	36	0.01	1.55	0.10	1011.46	0.00001	0.2012	0.98	1.11
Melka Werer	37	1.11	1.45	0.10	317.94	0.00011	0.0318	0.72	1.12
	38	1.12	1.38	0.10	125.30	0.00077	0.0575	0.80	1.01
Kebena	26	1.01	1.42	0.10	325.24	0.00258	0.0800	0.83	1.83
	3	0.03	1.56	0.10	333.36	0.00110	0.1200	0.76	0.97
	2	0.12	1.56	0.10	127.35	0.00127	0.1200	0.78	1.43
	21	0.12	1.59	0.10	160.98	0.00107	0.0125	0.48	2.12
	4	0.01	1.48	0.10	130.20	0.00185	0.1250	0.78	1.64
Kessem	5	0.13	1.47	0.10	992.34	0.00026	0.1250	0.80	1.22
	7	0.12	1.46	0.10	1024.83	0.00026	0.1250	0.80	0.92
	22	0.12	1.51	0.99	871.94	0.00026	0.1250	0.80	1.24
	9	0.01	1.57	0.10	952.30	0.00001	0.1833	0.93	1.25
	23	1.25	1.38	0.10	213.11	0.00045	0.0800	0.29	1.25
	8	1.25	1.17	0.10	234.81	0.00151	0.0800	0.61	1.25
	27	0.03	1.55	0.10	125.04	0.00149	0.1100	0.74	1.12

---

[1] See Figure 6.11

7. CONCLUSION AND RECOMMENDATION

7.1. Conclusion

The main objective of this research is to simulate the stream flow of Upper and Middle Awash River Basin by combining remote sensing derived products with regionalization and a semi-distributed conceptual hydrological model (HBV-96) for the period of 2005-2010. The freely available in-situ online data (ISOD) from Famine Early Warning System Network (FEWS NET), Climate Prediction Centre (CPC) and Morphing technique (CMORPH), Tropical Rainfall Measurement Mission (TRMM) Multi satellite Precipitation Analysis (TMPA 3B42) and in-situ measurements were used for model set up. The sensitivity analysis was applied during calibration period to have better understanding the effects of model parameter change on stream flow simulation. The HBV-96 model was calibrated for period of 2005-2008 and validated for a period of 2009-2010. The Satellite rainfall estimates and gauged rainfall were compared using cumulative mass curve for 2005-2010, double mass curve and evaluated using bias indicators, finally bias correction applied. Similarly the potential evapotranspiration estimates from satellite based and in-situ based ET_O estimate, both which are basically estimated based on Penman-Monteith method were compared using double mass curve, time series plot and bias evaluators indicators, and finally bias correction applied to minimize the errors. The effect of in-situ based and satellite based rainfall estimate on the stream flow simulation using HBV-96 was investigated too. Regionalization was applied using regional model and sub basin mean to estimate stream flow of ungauged catchments.

The sensitivity of eight HBV-96 model parameters was evaluated. According to the sensitivity analysis, the FC, Perc, Beta, LP and Khq are sensitive model parameters. When FC increased the simulated stream flow volume decreases, since it is related inversely to the recharge to upper zone reservoir in the model. Similarly, as Beta increase the simulated stream flow volume decreases showing the fact that soil moisture is less than the maximum water holding capacity (FC) (See Figure 6.9) and when it decreased the reverse is true. On other hand, the increase of model parameter Perc will result in an increase in delayed runoff and decreases the peak flows, since it controls the flow from the upper zone reservoir to the lower zone reservoir storage. When there is high percolation (high perc) to the lower zone reservoir storage from the upper zone reservoir storage, water available for quick flow and direct runoff decreases which causes to decease in peak flow during rainy season and increases the base flow. Whereas, when the evaporation limit (LP) increased the actual evapotranspiration decreases, which result in increasing of simulated stream flow volume (Equation 4.2 and Figure 6.9). The increases in recession coefficient (Khq) which controls the peak flow result in an increase simulated stream flow volume and the reverse is true when decreased. Since they are less sensitive, the remaining model parameter such as Alfa, K4 and C_{flux} have less effect on simulated stream flow hydrograph.

After warming-up the model for one year 2005, the model was calibrated by trial and error changing one model parameter at a time manually using the stream flow observed for the period of 2005 - 2008 and validated since 2009 and 2010, using the gauged rainfall and FEWS NET PET. The final calibration and validation result showed that in 2005- 2009 the simulated peak flow is lower than the observed peak flow and the whereas, in 2010 the simulated peak flow is higher than the observed peak flows, the cause of this variation may be resulted from observation error which is difficult to identify. The objective functions NSE = 0.897and RVE = -1.78% during calibration periods and NSE = 0.876 and RVE = 2.08% during validation period were obtained using gauged rainfall as meteorological forcing variable at Hombole station. Furthermore, the evaluation with other meteorological forcing variable was accessed and showed that bias corrected satellite rainfall estimate can perform stream flow resemble to gauged rainfall. The objective function obtained are NSE =0.752 and RVE = -6.29% during calibration period, whereas NSE = 0.720 and RVE = -8.59% during validation period for bias corrected CMORPH, While NSE= 0.735

and RVE = -7.62% during calibration period, whereas NSE = 0.671 and RVE = -9.50% for bias corrected TMPA 3B42 during validation period. Finally, it can be concluded that CNORPH is better performing than TMPA 3B42 for stream flow simulation of Upper and Middle Awash River Basin.

For regionalization the physical catchment characteristics similarity to establish the regional model and sub basin mean are used. Multiple regressions are applied to establish the regression equation to determine the model parameter of ungauged catchment (Table 6.7). The regional model was validated using observed discharge at Melka Werer at most downstream of Upper and Middle Awash River Basin that includes all ungauged catchments. The validation result shows that NSE = 0.64 and RVE =1.96% using regional model which can be considered as moderately performing model, whereas the sub basin mean showed poor model result with NSE = 0.24 and RVE = -53.81% hence it not successful for Upper and Middle Awash River Basin Stream flow simulation.

The satellite rainfall estimate rainfall of CMORPH and TMPA 3B42 for the period of 2005-2010 were evaluated with gauged rainfall. The comparison shows that CMORPH underestimates at all station except at Meiso, Meki, Awash Melka and Metehara stations where the temperature is relatively high and lower elevation. Whereas, TMPA 3B42 overestimate rainfall at station except Addis Ababa, Akaki and Mojo stations where rainfall is relatively higher as compared to other stations. Furthermore the evaluation using root mean square shows that TMPA 3B42 less agree with gauged rainfall with mean RMSE of 7.56mm, whereas CMORPH agrees more with mean RMSE of 6.39mm (Table 6.1). In addition, the evaluation using different bias shows that CMORPH got negative hit bias at all station showing that it underestimate rainfall when satellite detect rainfall and the rain gauge also record rainfall, whereas hit bias is positive for TMPA 3B42 at all stations except, for Addis Ababa, Akaki, Mojo, Adama and Meki stations (Figure 6.3).

The FEWS NET PET estimates using Global Data Assimilation System meteorological variables by Penman-Monteith method were compared with ET_O estimates using in-situ measured meteorological variables. According to the comparison based on different bias evaluation indicators and RMSE FEWS NET PET has on average RMSE =1.50mm/day, Mean bias -0.47mm/day, Relative volume bias = -10.21% and Absolute Relative Bias = 29.76% (Table 6.3). The bias correction is applied to minimize the error of sets and the resulting bias corrected is shown as figure 6.7 which shows the bias is minimized as expected. The bias corrected PET is used as input for HBV-96 model set up.

7.2. Recommendations

➢ For this study due to availability of limited reliable gauged stream flow data only four gauged catchments that found within the Upper and Middle Awash River Basin are calibrated using HBV -96. However, to establish a best performing regional model for ungauged catchments a model parameter has to be calibrated for more gauged catchments. Hence, for next study it is recommended if more gauged catchments from other basin adjacent to Awash River Basins are used.

➢ As discussed in section 2.2, there are a number of Irrigation projects and other hydraulic structures in Awash River Basin. Getting such data within a few days during field data collection period is difficult, therefore they are not considered in this study. However, it is recommended if water abstraction for different activities is considered in stream flow simulations of Awash River Basin.

➢ For this study only two satellite-based rainfall estimated are evaluated. To indicate the best satellite based rainfall estimate used for stream flow simulation of Upper and Middle Awash Basin the evaluation has to be applied for more satellite based rainfall estimates. Furthermore, the evaluation of the satellite based rainfall estimate with the gauge measured rainfall was done only for 19 stations. Hence, the spatially interpolated using inverse distance method is not free of error. Therefore, to further minimize the errors, using more rain gauge stations is advocated.

➢ Application of HBV-96 for stream flow simulation in Upper and Middle Awash River basin is robust since it require few input variables to set up the model.

LIST OF REFERENCES

Abebe, N. A., Ogden, F. L., andPradhan, N. R. (2010). Sensitivity and uncertainty analysis of the conceptual HBV rainfall–runoff model: Implications for parameter estimation. *Journal of Hydrology, 389*(3–4), 301-310. doi: http://dx.doi.org/10.1016/j.jhydrol.2010.06.007

Aghakouchak, A., Nakhjiri, N., andHabib, E. (2012). An educational model for ensemble streamflow simulation and uncertainty analysis. *Hydrology and Earth System Sciences Discussions, 9*(6), 7297-7315. doi: 10.5194/hessd-9-7297-2012

Awulachew, S. B., Yilma, A. D., Loulseged, M., Loiskandl, W., Ayana, M., andAlamirew, T. (2007). Water Resources and Irrigation Development in Ethiopia. (pp. 78). Colombo, Sri Lanka: International Water Management Institute.

Badilla, R. A. (2008). *Flood modelling in Pasig - Marikina river basin.* ITC, Enschede. Retrieved from http://www.itc.nl/library/papers_2008/msc/wrem/badilla.pdf

Bao, Z., Zhang, J., Liu, J., Fu, G., Wang, G., He, R., Yan, X., Jin, J., andLiu, H. (2012). Comparison of regionalization approaches based on regression and similarity for predictions in ungauged catchments under multiple hydro-climatic conditions. *Journal of Hydrology, 466–467*(0), 37-46. doi: http://dx.doi.org/10.1016/j.jhydrol.2012.07.048

Behailu, S. (2004). STREAM FLOW SIMULATION FOR THE UPPER AWASH BASIN. [Unpublished MSc. Thesis, Addis Ababa University, Addis Ababa, Ethiopia.]. 1-81.

Booij, M. J. (2005). Impact of climate change on river flooding assessed with different spatial model resolutions. *Journal of Hydrology, 303*(1–4), 176-198. doi: 10.1016/j.jhydrol.2004.07.013

Deckers, D., Booij, M., Rientjes, T., andKrol, M. (2010). Catchment Variability and Parameter Estimation in Multi-Objective Regionalisation of a Rainfall–Runoff Model. *Water Resources Management, 24*(14), 3961-3985. doi: 10.1007/s11269-010-9642-8

Edossa, D. C., andBabel, M. S. (2011). Application of ANN-Based Streamflow Forecasting Model for Agricultural Water Management in the Awash River Basin, Ethiopia. [Article]. *Water Resources Management, 25*(6), 1759-1773. doi: 10.1007/s11269-010-9773-y

FAO-56. (2007). FAO Irrigation and Drainage Paper No. 56. Retrieved 17-Aug-2012, 2012, from http://www.kimberly.uidaho.edu/ref-et/fao56.pdf

Field, A. P. (2009). *Discovering statistics using SPSS : (and sex and drugs and rock 'n' roll).* Los Angeles [i.e. Thousand Oaks, Calif.]; London: SAGE Publications.

García, A., Sainz, A., Revilla, J. A., Álvarez, C., Juanes, J. A., andPuente, A. (2008). Surface water resources assessment in scarcely gauged basins in the north of Spain. *Journal of Hydrology, 356*(3–4), 312-326. doi: 10.1016/j.jhydrol.2008.04.019

Habib, E., Larson, B. F., andGraschel, J. (2009). Validation of NEXRAD multisensor precipitation estimates using an experimental dense rain gauge network in south Louisiana. *Journal of Hydrology, 373*(3–4), 463-478. doi: http://dx.doi.org/10.1016/j.jhydrol.2009.05.010

Haddeland, I., Heinke, J., Vo, F., Eisner, S., Chen, C., Hagemann, S., andLudwig, F. (2011). Effects of climate model radiation, humidity and wind estimates on hydrological simulations. *Hydrology and Earth System Sciences Discussions, 8*(4), 7919-7945. doi: 10.5194/hessd-8-7919-2011

Haile, A. T., Emad, H., andRientjes, T. H. M. (2012). Evaluation of the climate prediction center (CPC) morphing technique (CMORPH) rainfall product on hourly time scales over the source of the Blue Nile River. *HYDROLOGICAL PROCESSES*, 1-11. doi: 10.1002/hyp.9330

Huffman, G. J., Adler, R. F., Bolvin, D. T., Gu, G., Nelkin, E. J., Bowman, K. P., Hong, Y., Stocker, E. F., andWolff, D. B. (2007). The TRMM Multisatellite Precipitation Analysis (TMPA): Quasi-global, multiyear, combined-sensor precipitation estimates at fine scales. *Journal of Hydrometeorology, 8*(1), 38-55. doi: 10.1175/jhm560.1

Islam, M. N., Uyeda, H., andIeee. (2005). *Comparison of TRMM 3B42 products with surface rainfall over Bangladesh.*

Jia, Q. Y., andSun, F. H. (2012). Modeling and forecasting process using the HBV model in Liao river delta. *Procedia Environmental Sciences, 13*(0), 122-128. doi: 10.1016/j.proenv.2012.01.012

Joyce, R. J., Janowiak, J. E., Arkin, P. A., andXie, P. P. (2004). CMORPH: A method that produces global precipitation estimates from passive microwave and infrared data at high spatial and temporal resolution. [Article]. *Journal of Hydrometeorology, 5*(3), 487-503. doi: 10.1175/1525-7541(2004)005<0487:camtpg>2.0.co;2

Koriche, S. A. (2012). *Remote sensing based hydrological modelling for flood early warning in the upper and middle Awash river basin.* University of Twente Faculty of Geo-Information and Earth Observation (ITC), Enschede. Retrieved from http://www.itc.nl/library/papers_2012/msc/wrem/koriche.pdf

Li, Z. L., Tang, R. L., Wan, Z. M., Bi, Y. Y., Zhou, C. H., Tang, B. H., Yan, G. J., andZhang, X. Y. (2009). A Review of Current Methodologies for Regional Evapotranspiration Estimation from Remotely Sensed Data. *Sensors, 9*(5), 3801-3853. doi: 10.3390/s90503801

Lindström, G., Johansson, B., Persson, M., Gardelin, M., andBergström, S. (1997). Development and test of the distributed HBV-96 hydrological model. *Journal of Hydrology, 201*(1–4), 272-288. doi: 10.1016/s0022-1694(97)00041-3

Liu, W. J., Hong, Y., Khan, S., Huang, M. B., Grout, T., andAdhikari, P. (2011). Evaluation of Global Daily Reference ET Using Oklahoma's Environmental Monitoring Network-MESONET. *Water Resources Management, 25*(6), 1601-1613. doi: 10.1007/s11269-010-9763-0

Maathuis, B., Mannaerts, C., Schouwenburg, M., Retsios, B., andLemmens, R. (2012). In Situ and Online Data ToolboxInstallation, Configuration and User Guide. [Teaching Material].

Meyers, L. S., Guarino, A. J., andGamst, G. (2007). *Applied multivariate research : design and interpretation.* Thousand Oaks [u.a.]: Sage.

Moriasi, D. N., Arnold, J. G., Van Liew, M. W., Bingner, R. L., Harmel, R. D., andVeith, T. L. (2007). MODEL EVALUATION GUIDELINES FOR SYSTEMATIC QUANTIFICATION OF ACCURACY IN WATERSHED SIMULATIONS. *Hydrology*, 885-900.

MoWE. (2012, Nov.04, 2010). Awash River Basin - Back ground. *Federal democratic republic of Ethiopia, MINISTRY OF WATER AND ENERGY* Retrieved 23-Aug-2012, 2012, from http://www.mowr.gov.et/index.php?pagenum=3.3&pagehgt=1000px

Nikolopoulos, K. (2004). Introduction to econometrics: Christopher Dougherty (2nd edition), Oxford University Press, 2002, Paperback, 424 pages. ISBN: 0198776438, £27.99. *International Journal of Forecasting, 20*(1), 139. doi: http://dx.doi.org/10.1016/j.ijforecast.2003.11.008

NMA. (2012). Meteorological Station Information Retrieved 14-August-2012, 2012, from http://www.ethiomet.gov.et/stations/information

O'Brien, R. M. (2007). A caution regarding rules of thumb for variance inflation factors. *Quality & Quantity, 41*(5), 673-690. doi: 10.1007/s11135-006-9018-6

Perera, B. U. J. (2009). *Ungauged catchment hydrology : the case of Lake Tana basin.* ITC, Enschede. Retrieved from http://www.itc.nl/library/papers_2009/msc/wrem/perera.pdf

Raghunath, H. M. (2009). *Hydrology : principles, analysis, and design.* New Delhi: New Age International.

Rientjes , T. H. M., Haile, A. T., Gieske, A. S. M., andMaathuis, B. H. P. (2011). Satellite based cloud detection and rainfall estimation in the upper blue Nile basin. *In: Nile River Basin : Hydrology, Climate and Water Use : e-book / editor A.M. Melesse. - Dordrecht : Springer, 2011. - 419 p. ISBN 978-94-007-0689-7. pp. 93-107.*

Rientjes, T. H. M., Perera, B. U. J., Haile, A. T., Reggiani, P., andMuthuwatta, L. P. (2011). Regionalisation for lake level simulation : the case of lake Tana in the upper blue Nile, Ethiopia. *JournalHydrology and earth system sciences (HESS) : open access, 15*(4), 1167-1183.

Rojas-Gonzalez, A. M., Harmsen, E. W., andPol, S. C. (2009). Performance evaluation of MPE rainfall product at hourly and daily temporal resolution within a Hydro-Estimator pixel. *WSEAS Transactions on Environment and Development, 5*(7), 478-487.

Romilly, T. G., andGebremichael, M. (2010). Evaluation of satellite rainfall estimates over Ethiopian river basins. *Hydrology and Earth System Sciences Discussions, 7*(5), 7669-7694. doi: 10.5194/hessd-7-7669-2010

Shrestha, R., Takara, K., Tachikawa, Y., andJha, R. N. (2004). Water resources assessment in a poorly gauged mountainous catchment using a geographical information system and remote sensing. *Hydrological Processes, 18*(16), 3061-3079. doi: 10.1002/hyp.5749

SIWI. (2005). M AKING WATER A PART OF ECONOM IC DEVELO PM ENT The Economic Benefits, from http://www.who.int/water_sanitation_health/waterandmacroecon.pdf

SMHI. (2008). Integrated Hydrological Modelling System. *Manual, Version 6*, 1-120.

Su, F., Hong, Y., andLettenmaier, D. P. (2008). Evaluation of TRMM multisatellite precipitation analysis (TMPA) and its utility in hydrologic prediction in the La Plata Basin. *Journal of Hydrometeorology, 9*(4), 622-640. doi: 10.1175/2007jhm944.1

Subramanya, K. (2008). *Engineering hydrology.* New Delhi: Tata McGraw-Hill.

SWDP. (2009). How to correct and complete discharge data. *India* Retrieved 30/01/2013, 2013, from http://www.cwc.gov.in/main/HP/download/39%20How%20to%20correct%20and%20complete%20discharge%20data.pdf

Tessema, S. (2011). Hydrological modeling as a tool for sustainable water resources management: a case study of the Awash River basin. [TRITA LWR.LIC 2056].

Wale, A., Rientjes, T. H. M., Gieske, A. S. M., andGetachew, H. A. (2009). Ungauged catchment contributions to Lake Tana's water balance. *JournalHydrological processes : an international journal, 23*(26), 3682-3693.

Wang, J., andWolff, D. B. (2010). Evaluation of TRMM ground-validation radar-rain errors using rain gauge measurements. *Journal of Applied Meteorology and Climatology, 49*(2), 310-324. doi: 10.1175/2009jamc2264.1

Zeweldi, D. A., andGebremichael, M. (2009). Evaluation of CMORPH Precipitation Products at Fine Space–Time Scales. *Journal of Hydrometeorology, 10*(1), 300-307. doi: 10.1175/2008jhm1041.1

ANNEXES

60

Akaki

y = 1.0426x
R² = 0.9942

Raifall current station (mm)

Mean rainfall surrounding Statoin(mm)

Debire Birehan

y = 0.9845x
R² = 0.9973

Raifall current station (mm)

Mean rainfall surrounding Statoin(mm)

Asgori

y = 0.8546x
R² = 0.9979

Raifall current station (mm)

Mean rainfall surrounding Statoin(mm)

Adama

y = 1.0302x
R² = 0.9903

Raifall current station(mm)

Mean rainfall from surrounding
Statoin(mm)

Bishoftu

y = 0.8073x
R² = 0.9975

Raifall current station(mm)

Mean rainfall surrounding Statoin(mm)

Kulumsa

y = 0.9142x
R² = 0.9965

Raifall current station (mm)

Mean rainfall Surrounding Statoin(mm
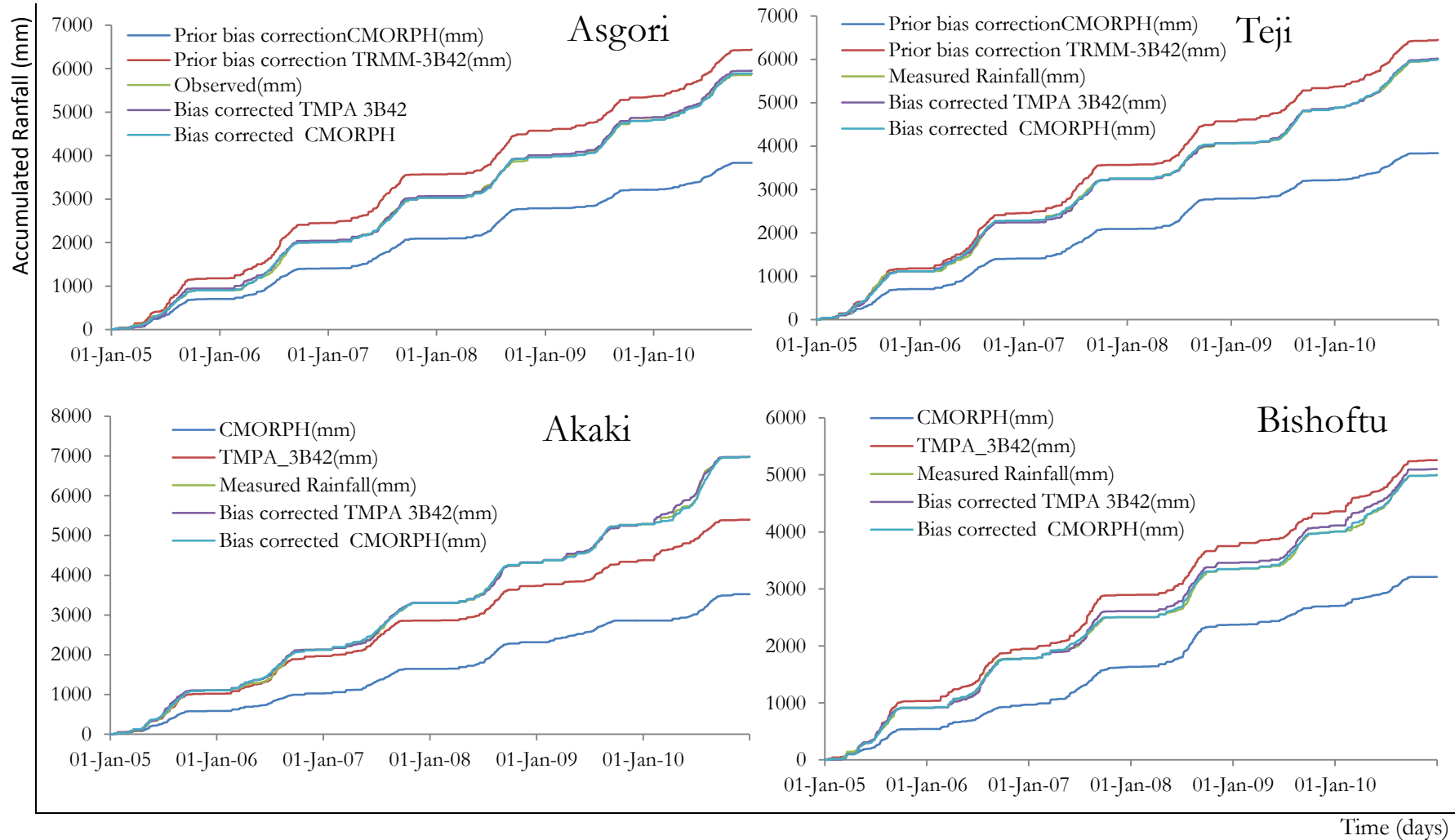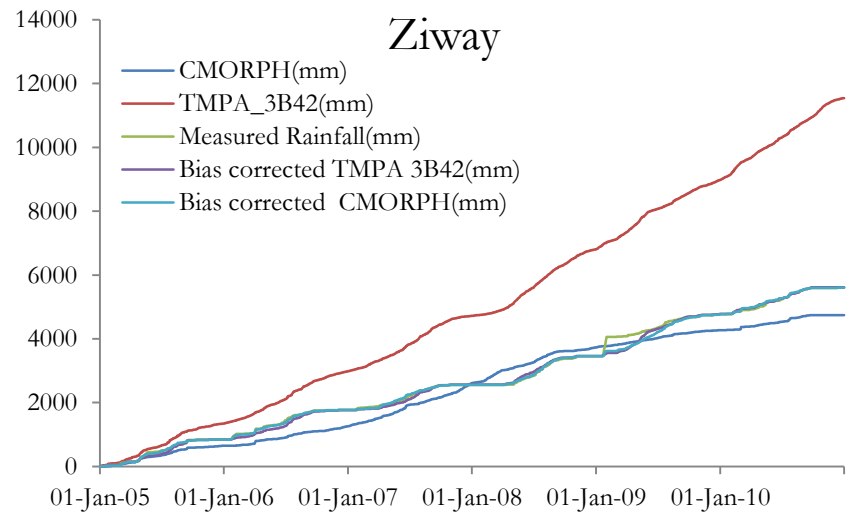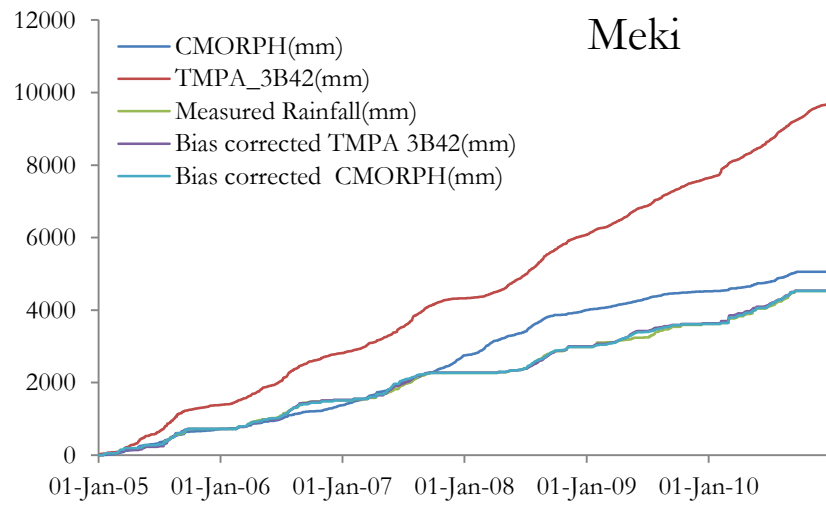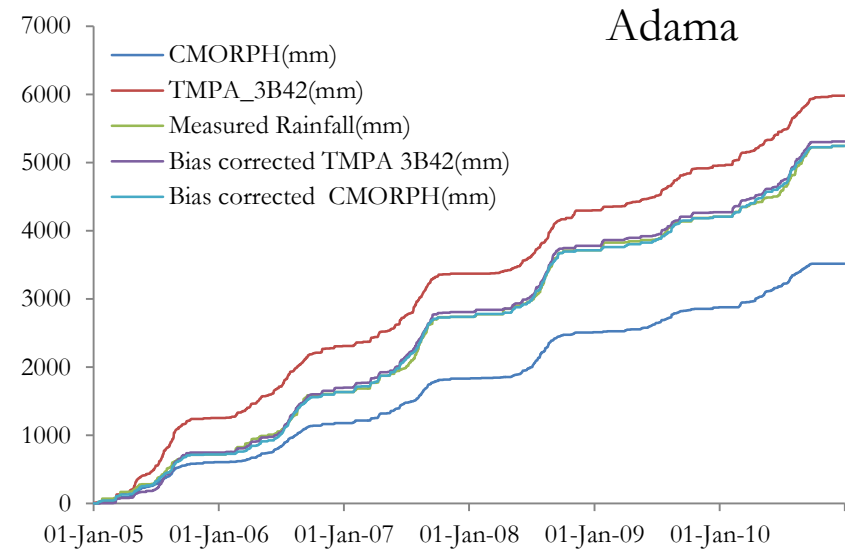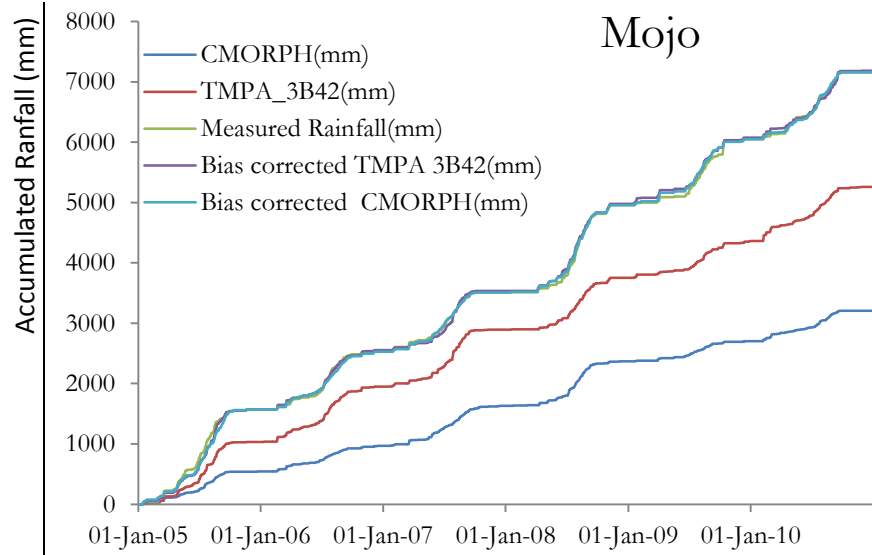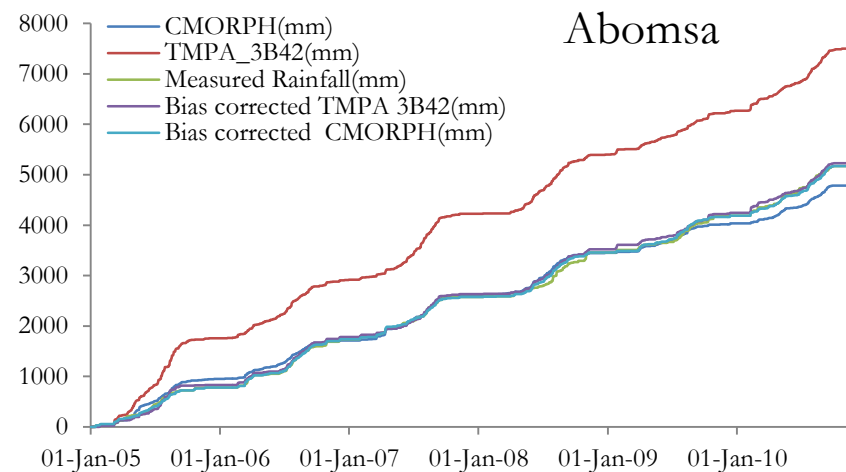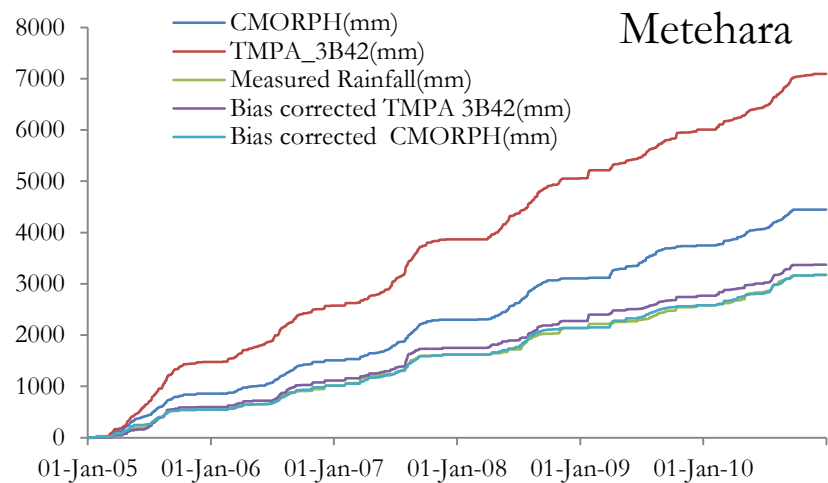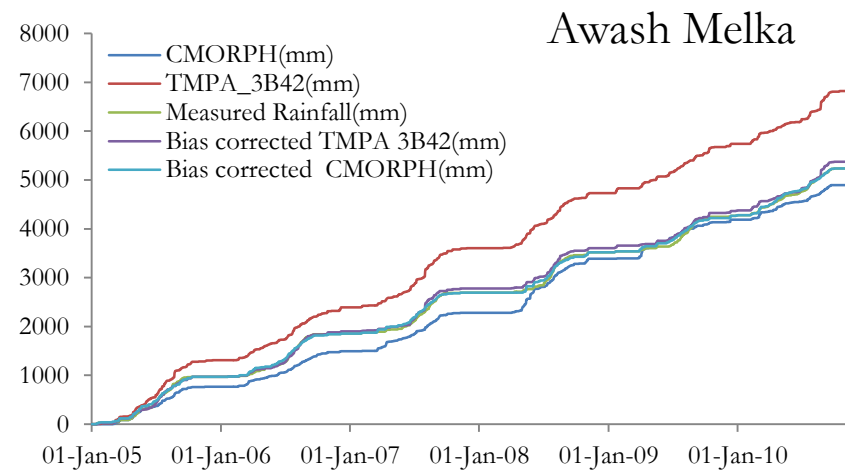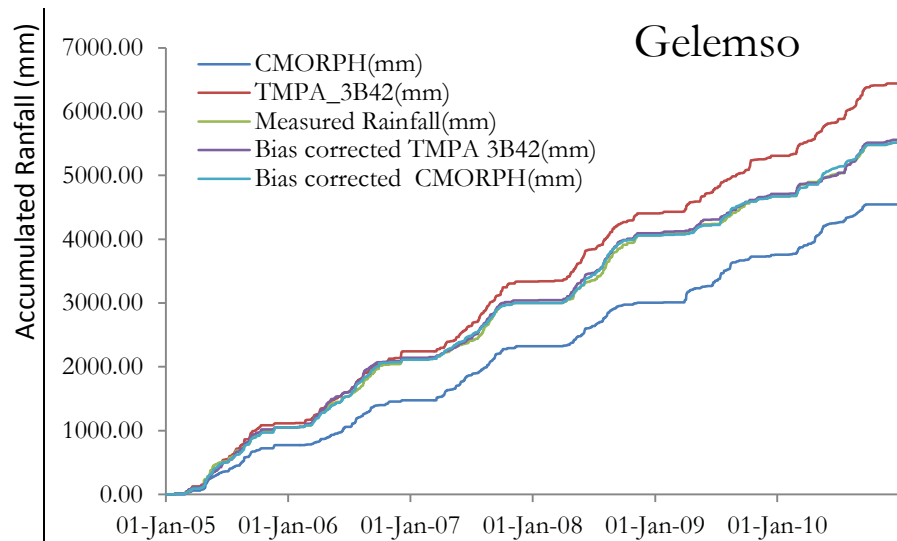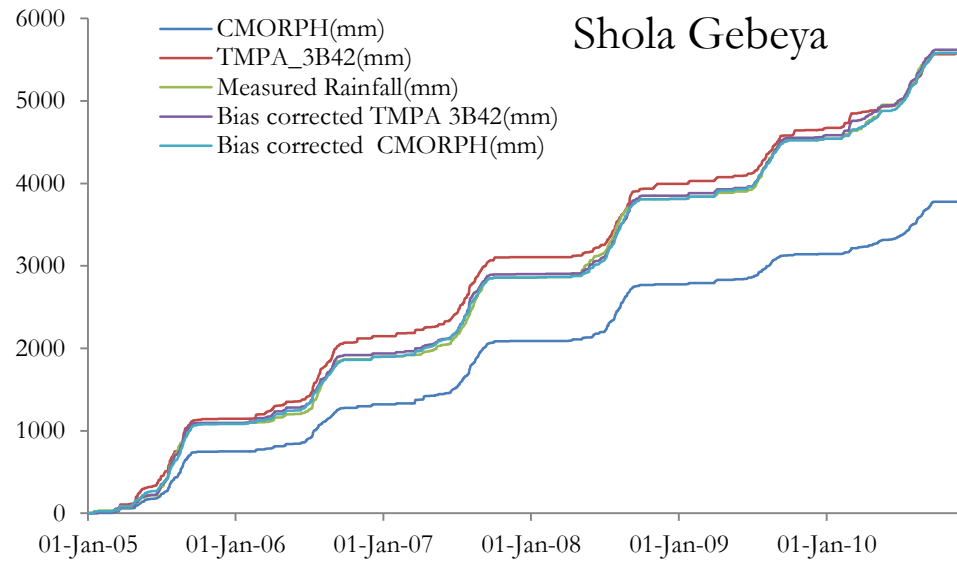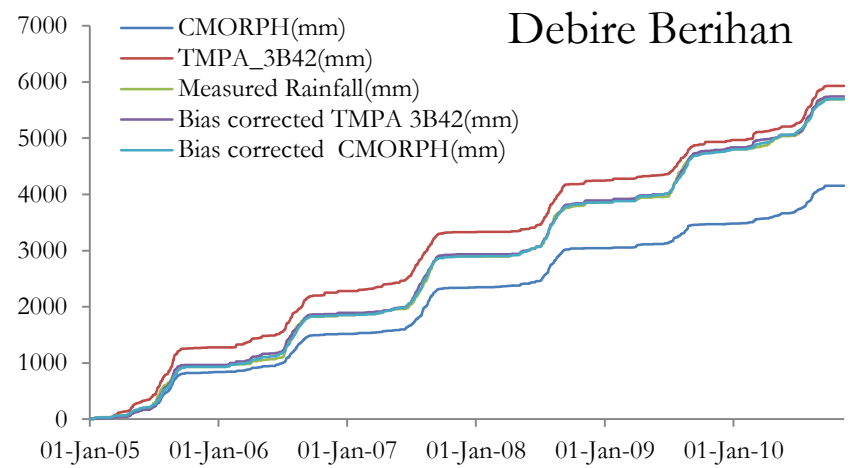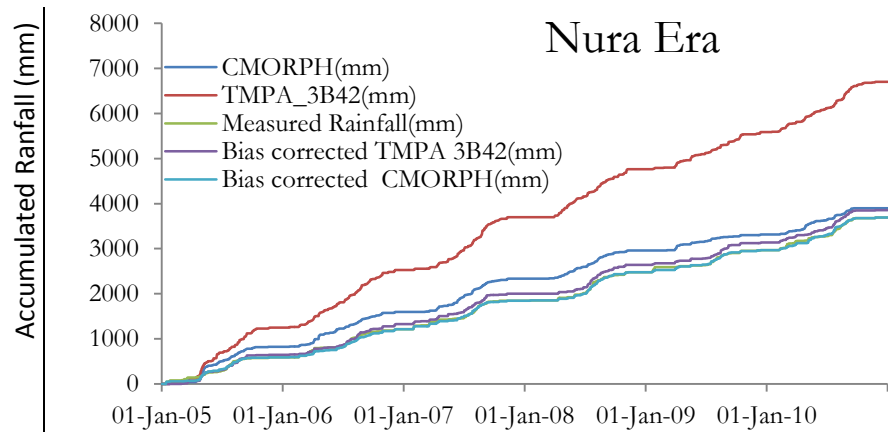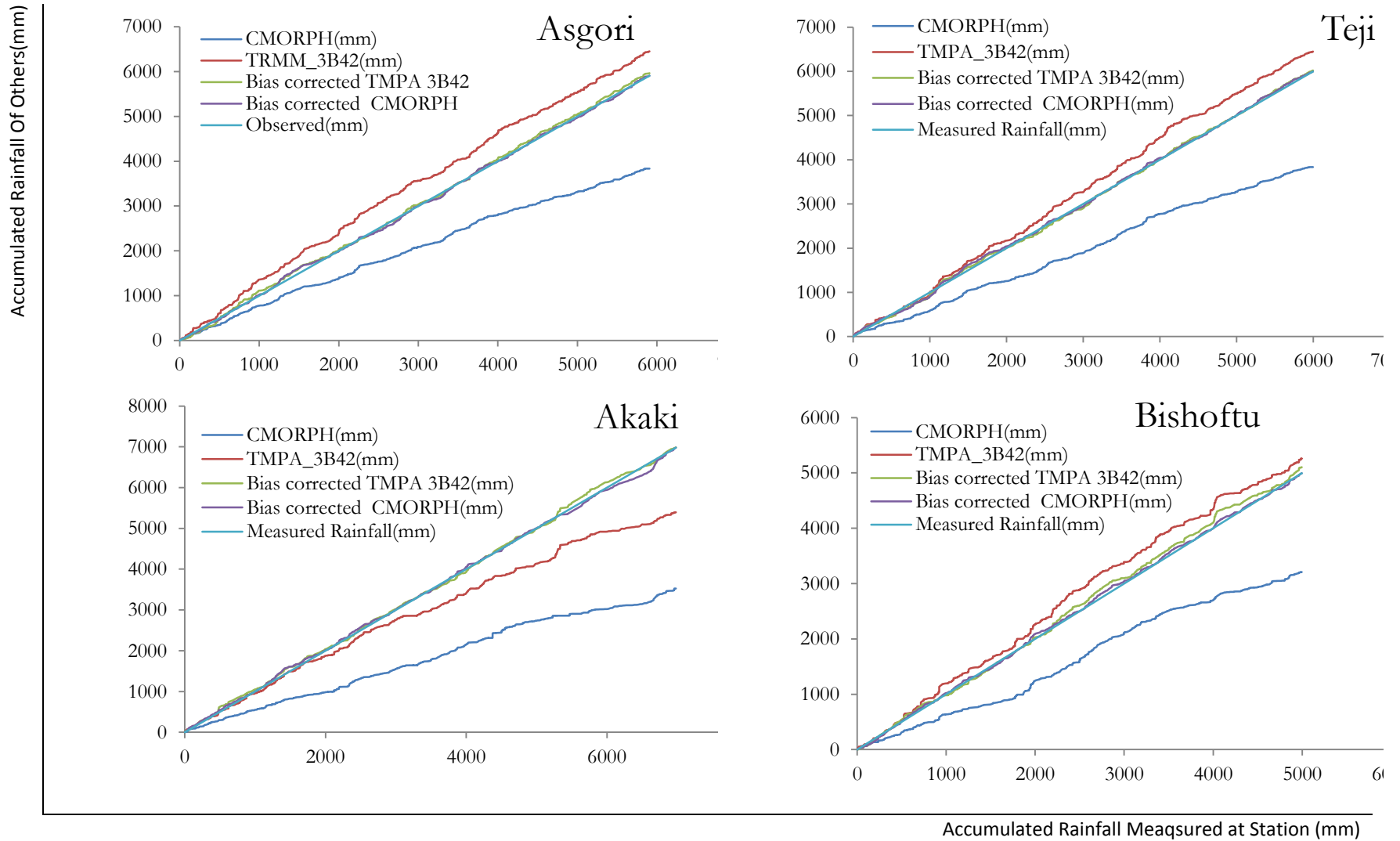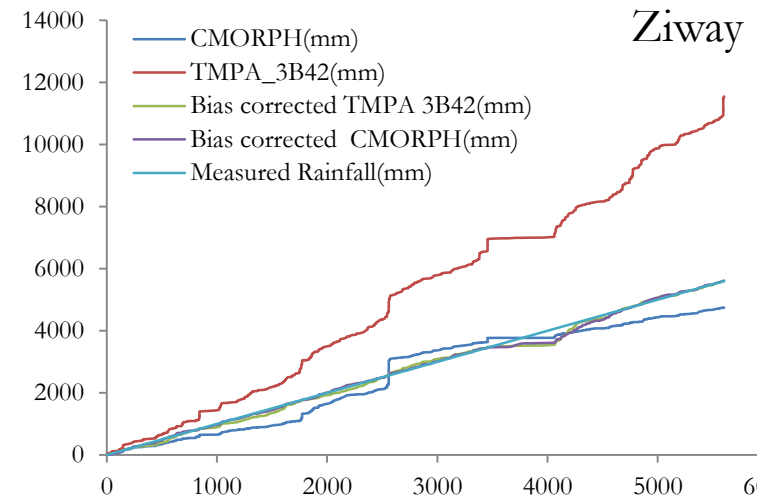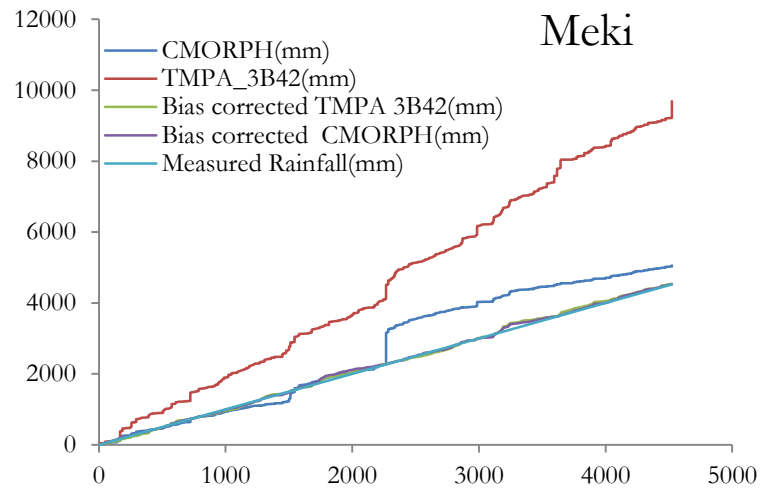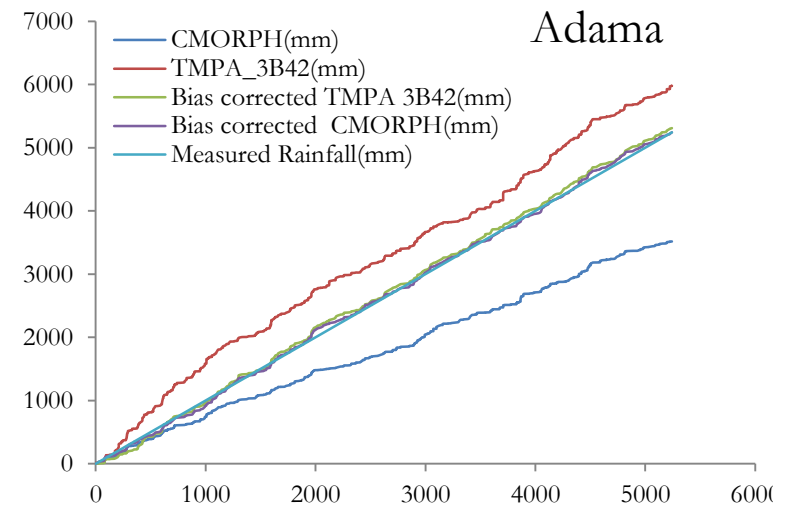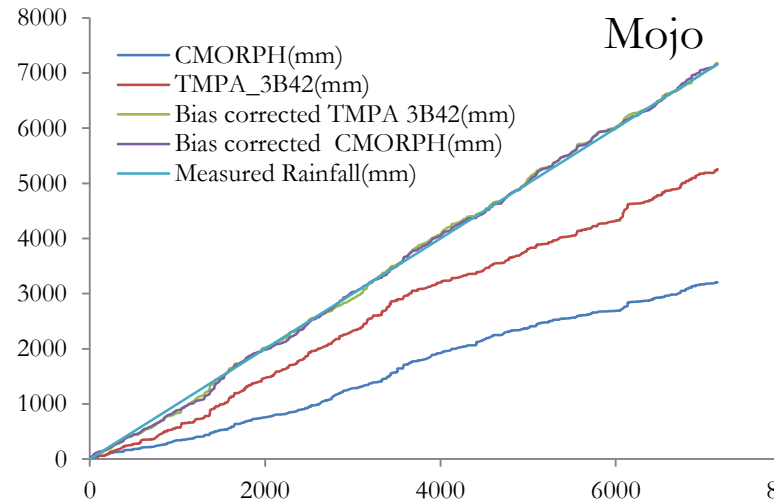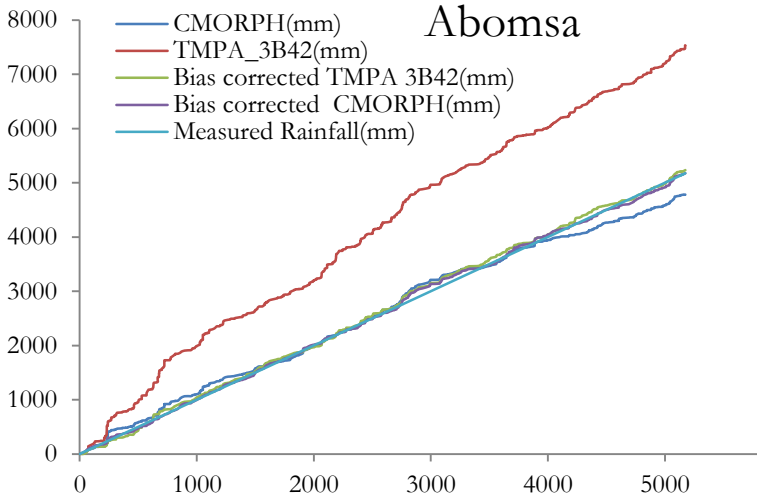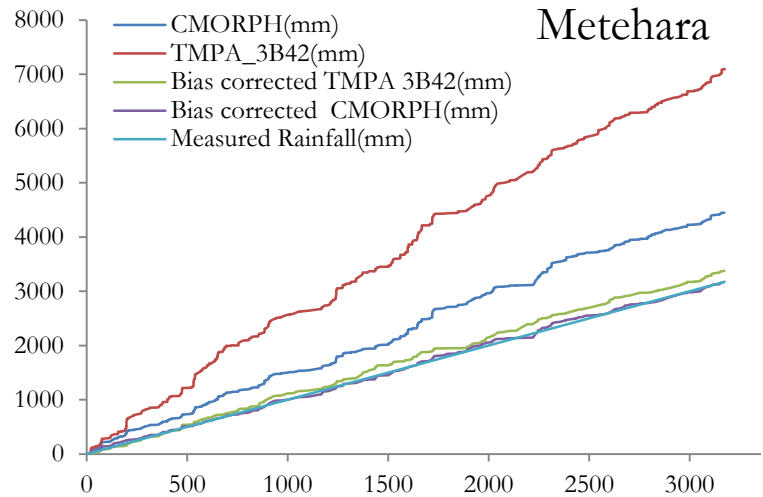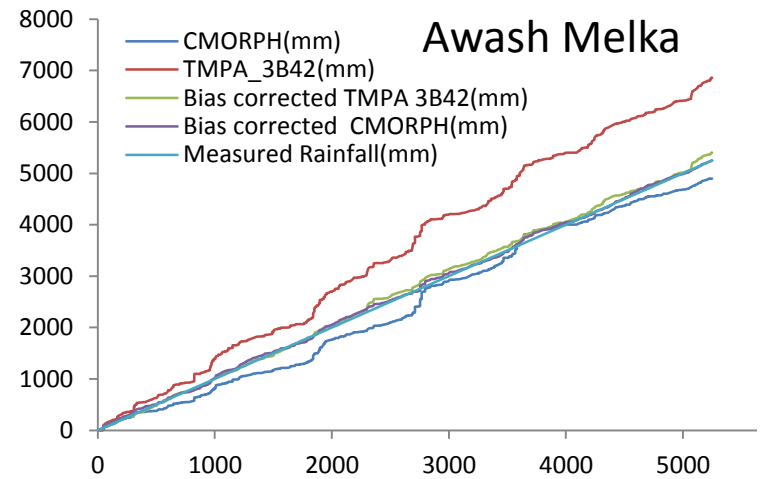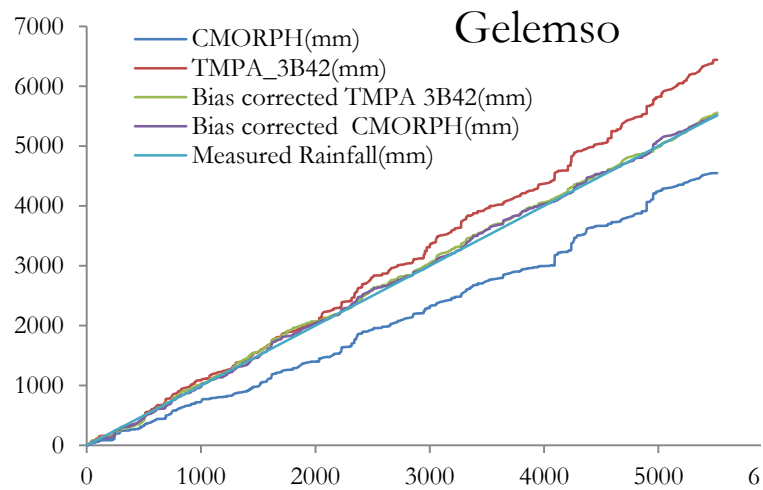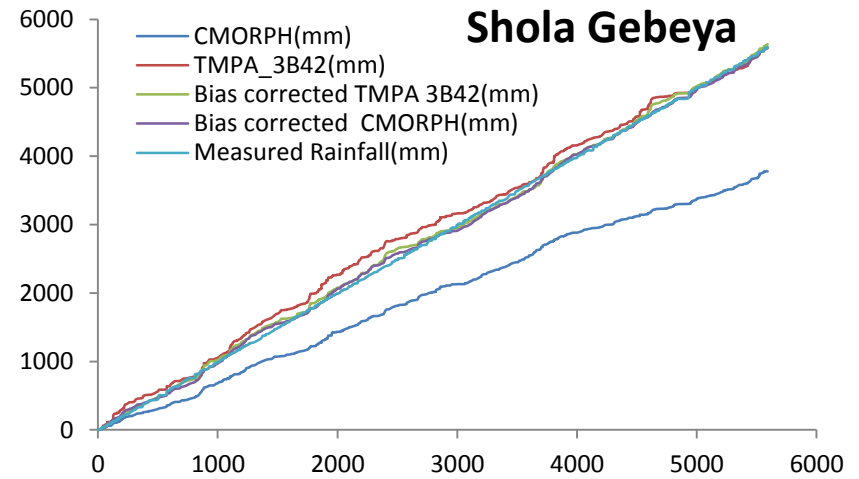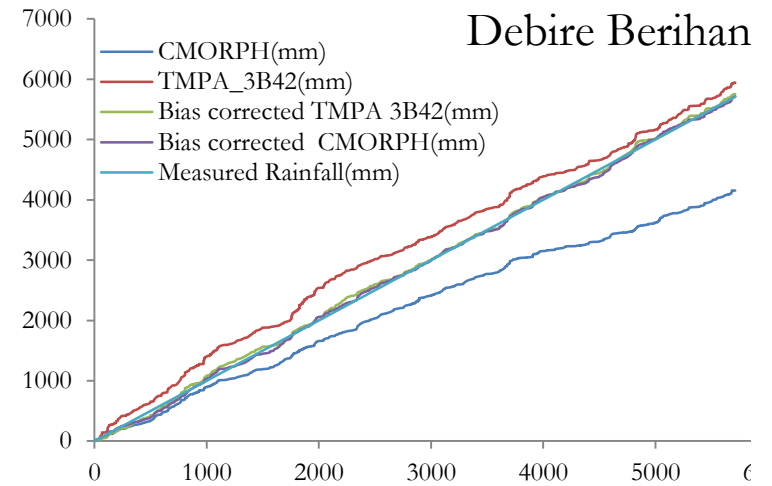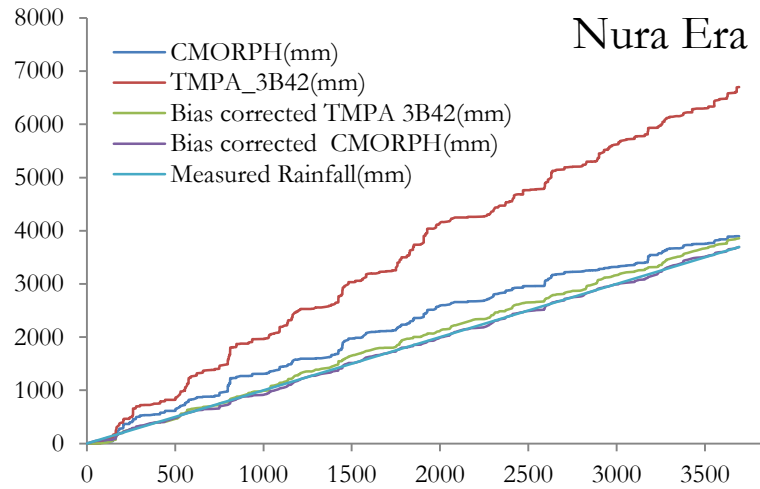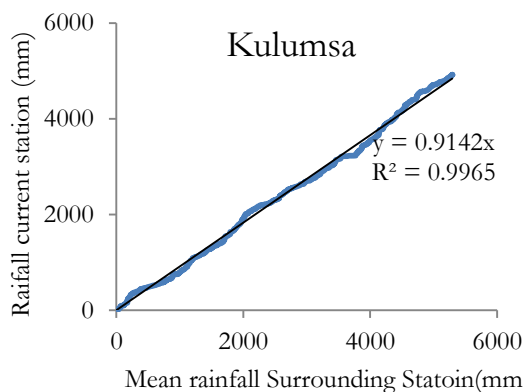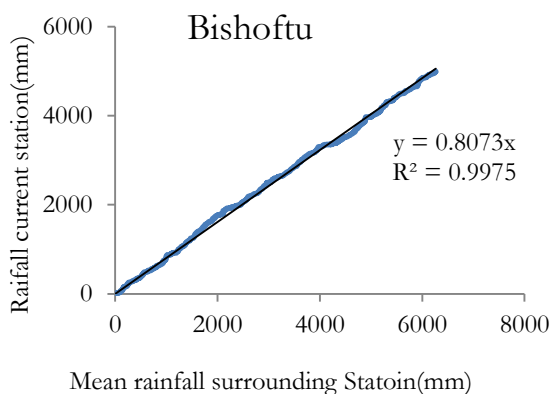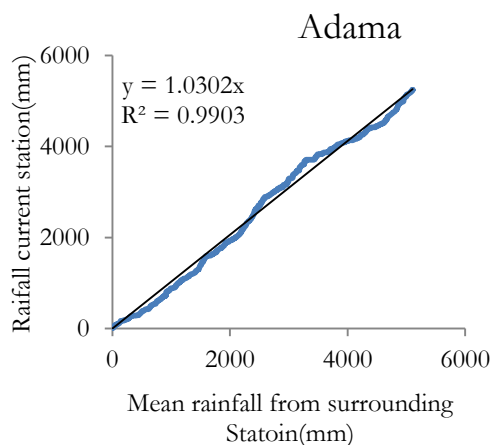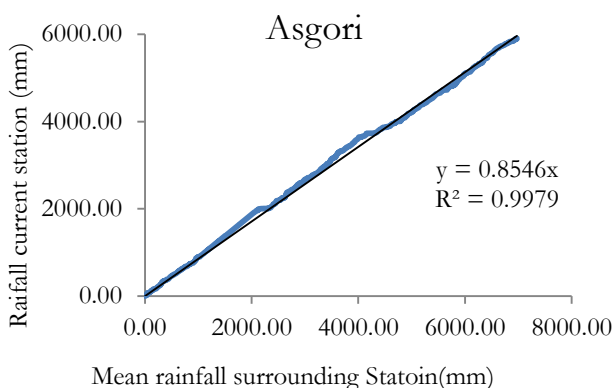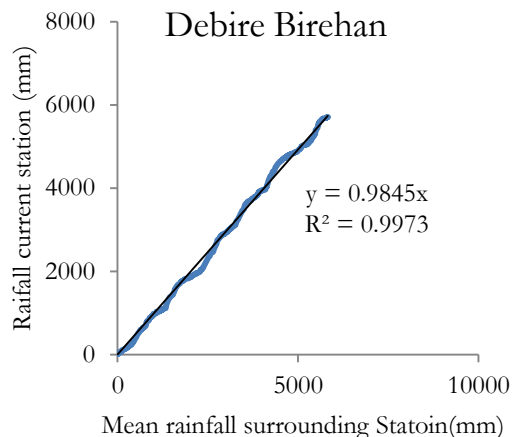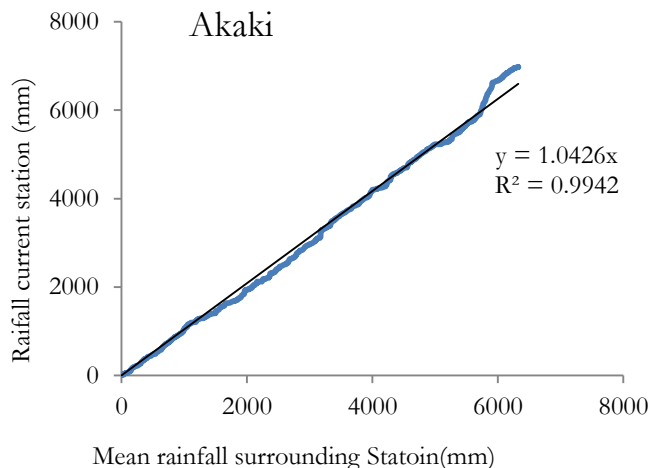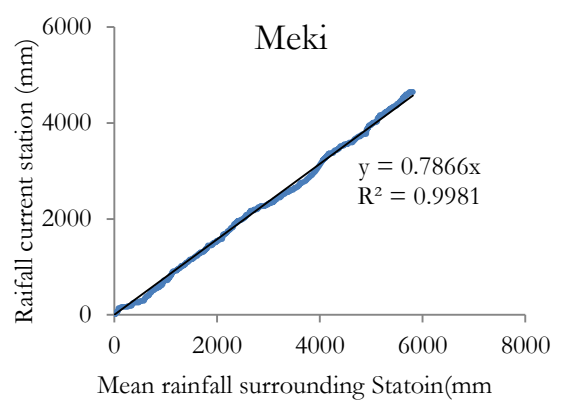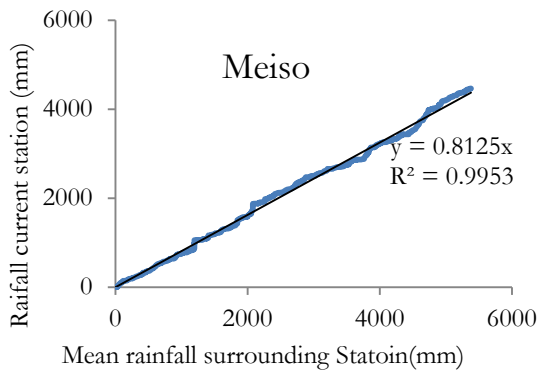
Annex D: Time series plot of ET_O, FEWS NET PET, and bias corrected FEWS NET PET
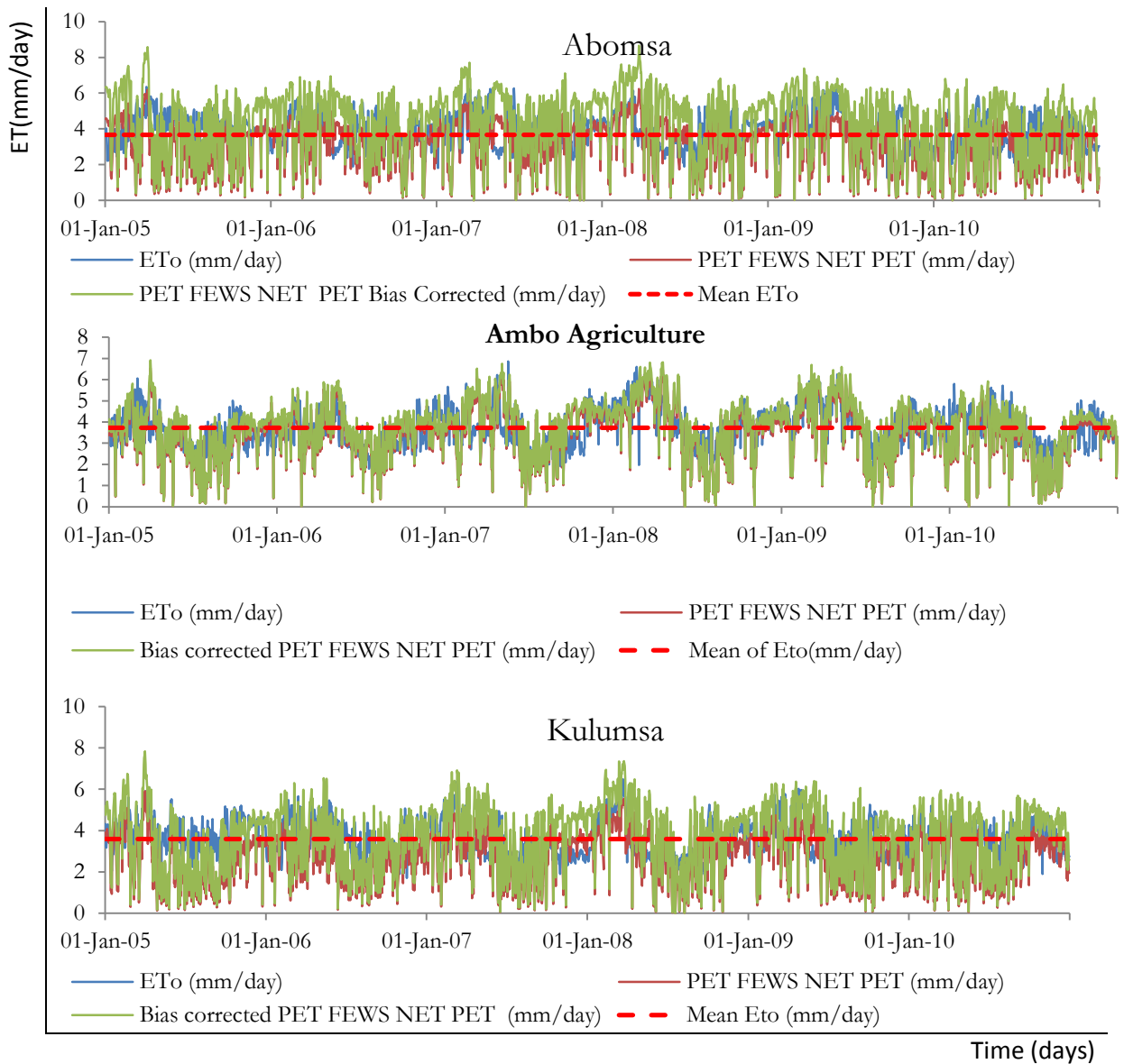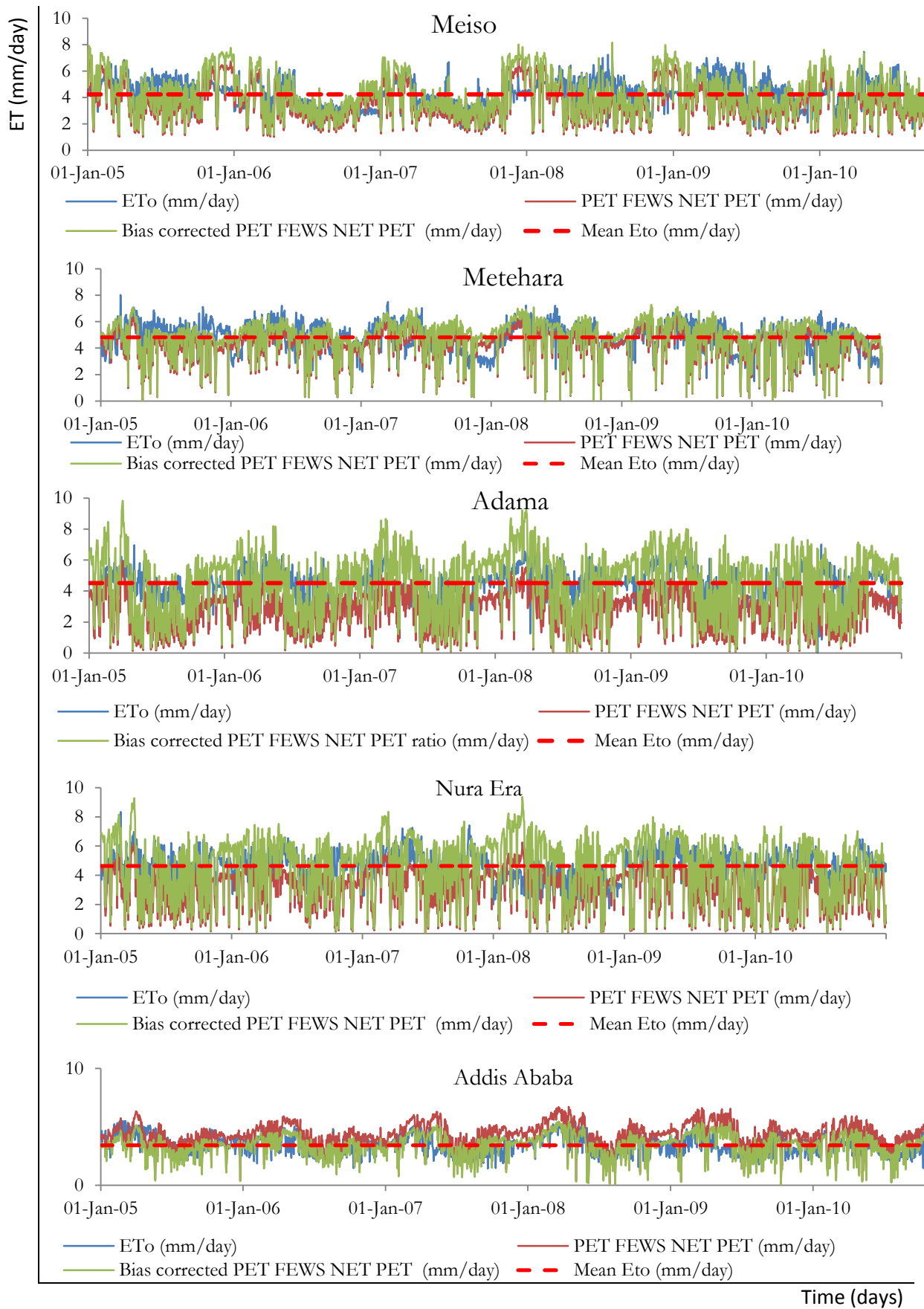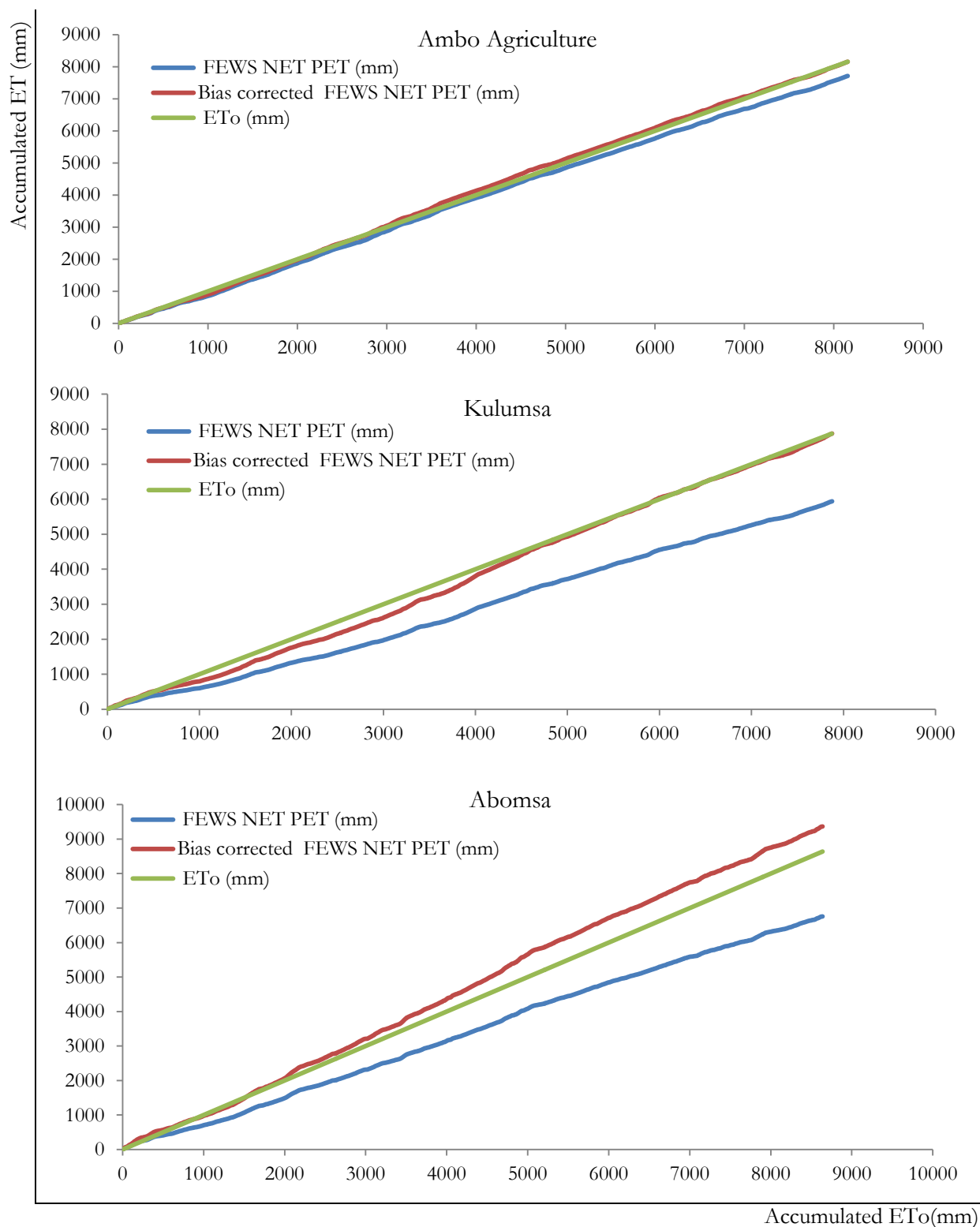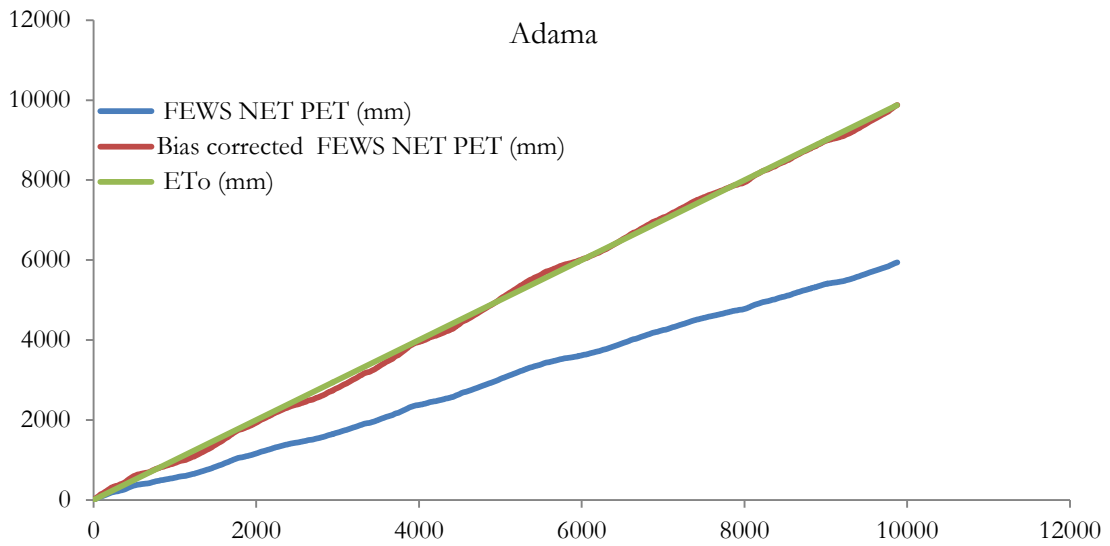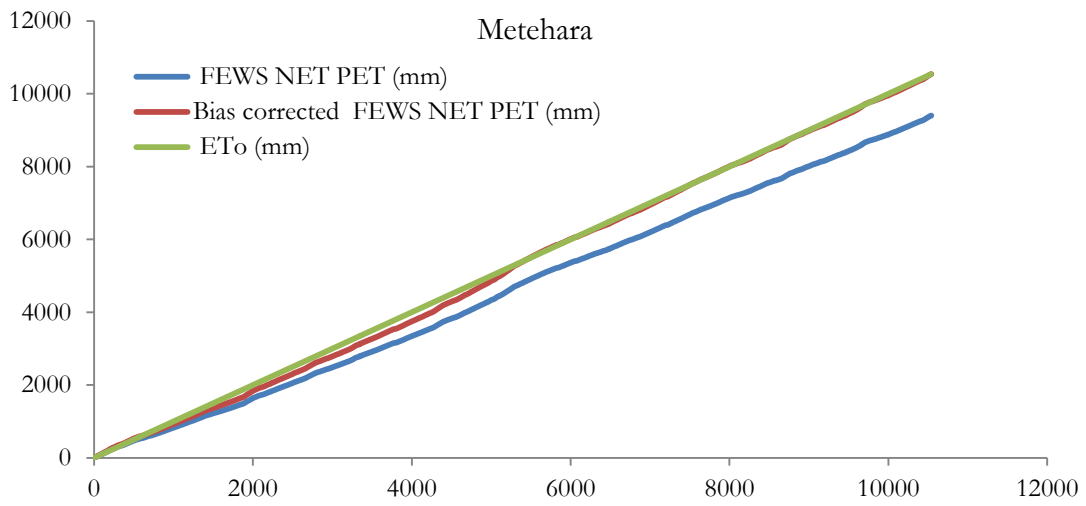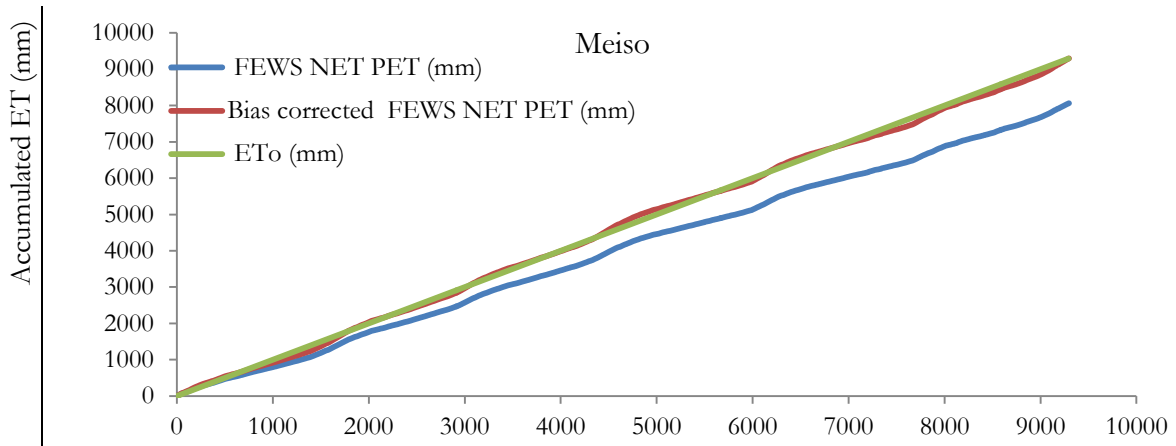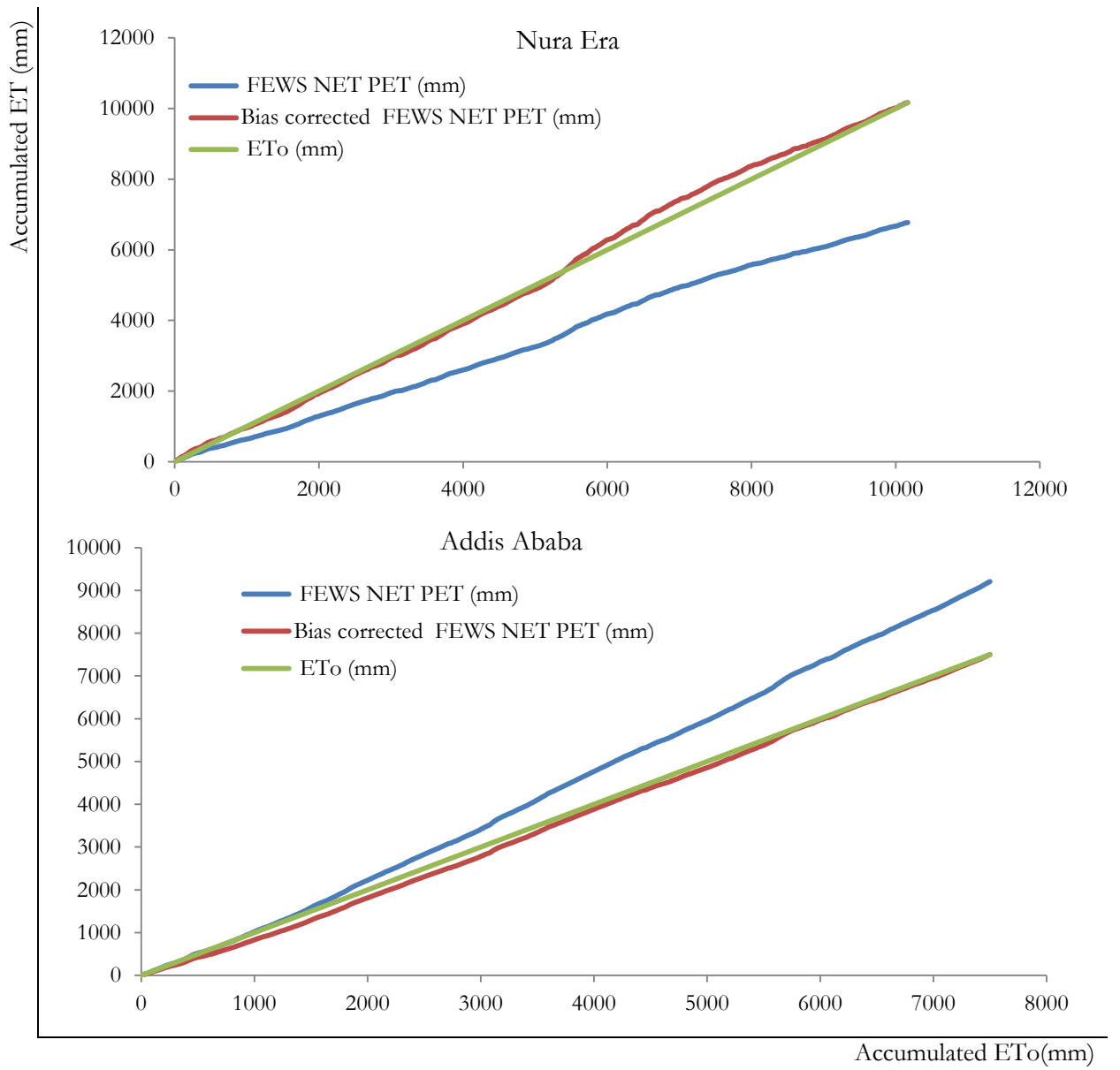
Annex F: Mean annual rainfall of CMORPH, TMPA 3B42, bias corrected TMPA 3B42, bias corrected CMORPH and measured rainfall

Station Name	Elevation (m)	Observed (mm)	CMORPH (mm)	Bias corrected CMORPH (mm)	TMPA 3B42 (mm)	Bias corrected TMPA 3B42 (mm)
Debre Berihan	2750	839	692	952	990	959
Shola Gebeya	2720	833	630	932	930	939
Addis Ababa	2408	1188	738	1332	1063	1324
Kulumsa	2200	740	586	820	997	842
Ambo Agriculture	2130	960	916	1095	1344	1082
Asgori	2130	875	639	984	1075	994
Akaki	2120	1028	588	1163	900	1165
Teji	2100	898	639	999	1075	1003
Gelemso	1940	832	758	919	1073	926
Bishoftu	1900	773	535	832	877	851
Abomsa	1800	784	797	862	1256	872
Mojo	1780	1090	535	1193	877	1197
Ziway	1640	864	791	934	1924	936
Adama	1622	750	586	874	997	885
Meiso	1400	669	816	745	1183	758
Meki	1400	689	843	754	1615	756
Nura Era	1140	571	649	616	1117	643
Metehara	951	488	741	529	1183	562
Awash Melka	916	796	816	875	1143	900
Maximum		**916**	**1924**	**1188**	**1324**	**1332**
Minimum		**535**	**877**	**488**	**562**	**529**

Annex G: Physical Catchment Characteristics of Upper and Middle Awash River Basin

Catchments	Sub-Catchment Code[2]	SAAR	PWET	PDRY	PET	CHR	EUTR	LEPT	VERT
					Gauged Catchments				
Melka Kunture	12	1040.631	6.075	1.293	1408.54	31.01	53.88	1.48	5.87
Akaki	13	994.706	5.657	1.252	1533.75	43.21	46.32	2.11	0.00
Hombole	24	956.178	5.222	1.312	1261.66	15.29	16.05	0.49	28.80
Mojo	11	908.891	5.115	1.171	1533.75	13.78	5.77	21.64	1.05
					Ungauged Catchments				
Jemjem	18	1104.76	6.11	1.48	1277.12	27.46	0.00	29.10	14.34
Wonji	31	919.55	4.96	1.35	1057.58	0.00	47.84	4.68	25.20
Keleta	20	881.03	4.49	1.41	989.56	4.26	68.09	21.31	6.34
Kela	32	905.73	4.69	1.44	1357.26	15.44	67.55	15.41	1.61
Wolenchiti	19	831.84	4.18	1.32	1441.28	0.00	88.51	3.38	5.63
Metehara	33	845.07	4.30	1.32	1422.11	0.00	53.70	22.02	24.28
Abomsa	17	832.71	4.18	1.42	1346.20	0.00	76.72	14.72	7.61
	16	840.84	4.27	1.32	1236.22	7.99	25.20	18.29	41.61
	15	853.50	4.55	1.23	1346.20	44.49	29.53	16.58	0.00
	25	840.84	4.27	1.32	1566.16	0.00	37.84	19.23	42.93
	28	858.50	4.57	1.24	1566.16	39.38	42.28	9.34	9.00
	35	916.64	5.09	1.22	1566.16	17.28	51.02	12.52	20.10
Fentale	34	841.33	4.40	1.25	1566.16	7.27	42.91	4.08	45.74
Arba	10	923.94	5.65	0.97	1566.16	0.00	62.80	8.45	28.74
	29	925.04	5.25	1.17	1566.16	6.44	22.73	22.73	48.10
	6	899.48	5.02	1.18	1618.63	13.35	33.20	18.90	34.56
	36	940.35	5.26	1.23	1566.16	0.00	30.16	11.66	58.19
Melka Werer	37	885.85	4.94	1.16	1566.16	0.00	55.33	11.73	32.95
	38	885.85	4.94	1.16	1566.16	0.00	38.46	10.98	50.86
Kebena	26	889.62	5.01	1.15	1566.16	0.00	55.59	16.64	27.77
	3	889.32	5.22	1.47	1713.79	0.00	88.10	10.71	1.19
	2	889.32	5.22	1.04	1713.79	5.14	64.95	13.90	16.01
	21	884.94	5.12	1.07	1566.16	26.57	51.14	18.63	3.65
	4	884.94	5.12	1.07	1566.16	0.00	59.63	15.29	25.08
Kessem	5	896.72	5.35	1.00	1533.75	20.98	46.83	12.44	19.76
	7	919.58	5.35	1.10	1533.75	14.68	41.76	10.32	33.24
	22	900.84	5.33	1.03	1533.75	0.00	59.20	12.52	0.00
	9	859.27	4.73	1.16	1533.75	0.00	17.16	12.63	70.21
	23	900.84	5.33	1.03	1533.75	0.00	34.42	12.63	52.96
	8	900.84	5.33	1.03	1546.85	0.00	75.93	12.63	11.44
	27	867.40	4.76	1.18	1566.16	1.97	65.64	11.75	20.60

[2] See Figure 6.11

Catchments	Sub-Catchment Code[2]	LUV	DCROP	MCROP	URBAN	FOREST	GRASS	AREA
				Gauged Catchments				
Melka Kunture	12	7.76	82.65	0.152	0	0.109	3.33	4590.50
Akaki	13	8.36	70.42	2.552	7.231	0.182	15.98	1645.8
Hombole	24	39.37	59.84	0	0	2.645	1.94	1701.13
Mojo	11	57.77	93.15	0	0.944	3.821	0.00	2329.5
				Ungauged Catchments				
Jemjem	18	29.10	28.95	0.00	0.00	0.00	71.05	2766.41
Wonji	31	22.50	86.79	0.00	5.00	5.00	0.00	2022.61
Keleta	20	0.00	88.58	0.00	0.00	0.00	0.00	2255.37
Kela	32	0.00	40.33	0.00	10.33	10.33	15.67	1887.11
Wolenchiti	19	2.48	17.44	0.00	0.00	0.00	30.23	2116.42
Metehara	33	0.00	45.19	10.19	3.08	3.08	27.69	2635.27
Abomsa	17	0.00	63.31	0.00	0.00	0.00	14.79	1924.53
	16	0.00	88.48	3.14	5.76	5.76	0.00	2219.69
	15	0.00	54.29	5.14	27.43	27.43	0.00	2381.14
	25	0.00	0.00	6.01	0.00	0.00	93.08	2399.14
	28	0.00	31.75	9.17	44.82	44.82	11.88	589.50
	35	0.00	46.36	0.54	21.31	21.31	29.98	2407.40
Fentale	34	0.00	3.39	29.38	0.00	0.00	67.23	473.50
Arba	10	0.00	65.75	0.00	21.55	21.55	12.71	1901.29
	29	0.00	39.47	0.38	0.00	0.00	48.42	1535.14
	6	0.00	37.22	7.62	4.79	4.79	20.02	1905.04
	36	0.00	26.42	0.00	7.55	7.55	13.21	1826.06
Melka Werer	37	0.00	17.65	0.49	0.98	0.98	56.37	6459.37
	38	0.00	17.55	3.68	6.04	6.04	54.43	6672.14
Kebena	26	0.00	34.58	12.38	0.00	0.00	50.47	6119.84
	3	0.00	80.00	5.26	1.05	1.05	13.68	1861.45
	2	0.00	56.85	6.09	1.52	1.52	32.49	2220.40
	21	0.00	63.08	5.13	3.08	3.08	12.31	2149.44
	4	0.00	65.04	8.85	5.75	5.75	10.62	2000.58
Kessem	5	0.00	68.29	1.22	1.83	1.83	20.12	2468.84
	7	0.00	97.17	1.21	0.20	0.20	0.40	2495.31
	22	28.28	94.79	1.23	0.00	0.00	3.37	2368.67
	9	0.00	91.64	0.00	1.49	1.49	5.67	1770.60
	23	0.00	89.60	2.13	0.00	0.00	1.49	7199.42
	8	0.00	73.60	7.20	0.00	0.00	18.40	7738.39
	27	0.00	53.35	7.12	1.44	1.44	21.88	1877.52

Catchments	Sub-Catchment Code²	EL	DD	SHAPE	CI	HI	AV. SLOPE	LFP	MDEM
				Gauged Catchments					
Melka Kunture	12	1	12	22	26	0.43	3.69	53.385	2488
Akaki	13	2.0	12.0	36.0	30.0	0.4	8.2	19.9	2396.0
Hombole	24	1.00	34.00	8.00	49.00	0.50	4.10	58.21	1398.00
Mojo	11	1.0	31.0	28.0	28.0	0.4	2.5	72.8	2081.0
				Ungauged Catchments					
Jemjem	18	1.63	28.61	28.68	25.75	0.45	4.83	16.66	1911.71
Wonji	31	0.83	40.36	33.05	31.59	0.46	3.18	45.70	1920.09
Keleta	20	0.99	38.29	39.59	24.02	0.48	4.13	33.73	1971.33
Kela	32	0.88	61.28	26.35	35.99	0.44	4.88	26.56	1763.00
Wolenchiti	19	0.78	66.13	29.66	28.54	0.45	4.12	31.31	1772.45
Metehara	33	0.56	55.53	30.60	14.73	0.49	1.78	74.25	1580.25
Abomsa	17	0.92	50.70	25.95	37.83	0.51	6.06	29.38	2124.25
	16	0.98	68.25	33.25	25.49	0.50	11.97	19.49	2270.42
	15	1.11	62.95	17.45	27.57	0.44	12.50	16.49	2038.54
	25	1.18	190.28	15.29	26.99	0.50	1.81	4.83	1397.50
	28	0.81	57.04	32.58	85.81	0.49	6.55	33.63	1891.09
	35	1.03	34.73	22.01	22.14	0.48	7.29	34.80	1771.35
Fentale	34	1.82	28.48	15.99	78.88	0.55	3.16	13.49	1192.40
Arba	10	0.71	104.58	26.12	35.72	0.55	5.23	24.31	1569.33
	29	0.86	80.70	27.01	47.62	0.49	5.37	21.31	1308.27
	6	1.29	26.85	39.94	21.88	0.45	6.64	28.31	1677.07
	36	0.59	249.75	10.90	24.45	0.50	0.64	14.49	796.50
Melka Werer	37	1.30	53.85	25.77	41.71	0.49	4.02	13.90	943.80
	38	1.42	23.64	21.29	36.33	0.49	3.26	26.73	1079.50
Kebena	26	0.58	81.06	19.17	37.47	0.50	3.64	46.46	1435.07
	3	4.29	20.31	23.33	25.36	0.45	52.05	3.41	2199.89
	2	1.68	36.68	22.46	28.21	0.47	12.46	12.31	2257.76
	21	1.33	65.36	39.20	30.52	0.50	18.94	11.07	2189.44
	4	1.82	33.29	22.22	18.93	0.45	23.50	11.49	2301.04
Kessem	5	1.48	37.46	21.09	20.90	0.42	12.45	15.49	2374.15
	7	1.22	40.14	21.02	20.04	0.53	6.70	21.31	2356.87
	22	0.98	54.81	21.33	24.16	0.50	7.66	24.14	2321.00
	9	1.60	38.38	13.80	26.06	0.50	2.34	12.90	1619.50
	23	1.04	74.38	50.07	39.11	0.49	5.46	15.90	1682.63
	8	3.63	21.92	32.07	21.59	0.45	55.91	4.41	2231.86
	27	0.50	62.19	24.83	24.84	0.45	4.29	80.84	1957.96